MODELING, DESIGN, AND CONTROL
of
PARTIAL ICE-STORAGE AIR-CONDITIONING SYSTEMS

by

Mark Stanley Cummings

A thesis submitted in partial fulfillment
of the requirements for the degree of

Master of Science
(Mechanical Engineering)

at the

UNIVERSITY OF WISCONSIN—MADISON

1989

to

THE FAMILY

ABSTRACT

The work documented in this thesis concentrates on the modeling, design, and control of a partial ice-storage air-conditioning system. Mathematical models are presented for each component of an air-conditioning system. These models are useful for simulating the performance of an air-conditioning system over time. An original model of particular interest is the ice-storage model, which is based on fundamental principles. Solution procedures for each model are given, where necessary.

Two air conditioning systems were evaluated: the partial ice-storage system and the conventional system. Both systems were designed to meet the same cooling load requirements. The components of each of these systems were selected based on design-day ambient weather conditions, a design-day space-cooling-load profile, and common design specifications. An outline of the equipment selection procedure is

presented, and detailed design specifications are given for both systems. The fundamental design differences between these two systems are discussed.

These systems were evaluated under various operating conditions. The controlled variables which significantly affect the performance of the ice-storage system during the discharging period and during the charging period are identified. The algorithms necessary to control a model of an air-conditioning system are presented. Methodologies for determining near-optimal control strategies for both the ice-storage system and the conventional system are presented. Static optimization methods are used to determine the near-optimal control strategies for the conventional system. Dynamic optimization methods are used to determine the near-optimal control strategies for the ice-storage system. Several strategies were investigated using system simulation, and the ice-storage system was compared to the conventional system over a typical cooling season, where both systems were operated under near-optimal control.

CHAPTER OUTLINE Chapter 1 describes the various ice and chilled-water storage systems currently in use, presents the basic storage strategies for controlling air-conditioning systems which use either ice or chilled-water storage, and illustrates the economic considerations necessary to begin a detailed design process. Chapter 2 presents the mathematical models for each component in an air-conditioning system. Chapter 3 covers equipment selection, presents detailed design specifications for each system, and discusses the design differences between the two systems. Chapter 4 presents algorithms for controlling a model of an air-conditioning system, develops near-optimal control strategies for each system, and examines the effects of these strategies using system simulation. Chapter 5 summarizes the significant findings and the resulting conclusions and presents recommendations for future work.

ACKNOWLEDGEMENTS

Days End in Madison: Picnic point to the West, Memorial Union to the East, Lake Mendota and a bed of bright orange marigolds to the North greet all with splendor. Scattered ripples, several people in canoes, and three billowing white sails are welcomed by the tranquil blue body below. Two joggers jaunt by, a brown squirrel frolics in the grass, and several people come and go. The sun paints the wisps of white in the western sky as it says good by, for now. Thank you Madison.

Several people have made significant contributions to this work: John W. Mitchell, James E. Braun, Sanford A. Klein, John ("Jack") A. Duffie, and Christine A. Closkey. John and Jim are great men to work for. John has a keen sense of important issues, a lucid train of thought, and a knack for terse writing. His comments, criticisms, ideas, and questions greatly improved this work. I have learned a lot from this man. Jim has a trenchant understanding of all aspects of the research process. He was a constant source of information and ideas. He has been my role model.

Sandy and Jack are also a great pair to work for; however, their style is a bit more intense than that of the aforementioned duo. These two men gave this work purpose in its incipient stages. Sandy is so sharp that it is sometimes painful to be in the same room with him. He piqued my interest and challenged my intellect. His high personal

standards, which are somewhere near mars, gave me something to shoot for. I have tremendous respect for this man. Jack is the nicest man one could hope to meet. He is also a very strong leader: No words said, a simple facial gesture makes one immediately aware that this man means business. He was a significant source of motivation.

Christine has the perfect business touch. She works with speed and alacrity and has a fine sense of what make a piece of paper sing. She has been a constant source of motivation. Her many comments, criticisms, and corrections have greatly enhanced this work. In addition, special thanks goes to Diane for her careful corrections of Chapter 1 and to Florian for his careful corrections of Chapter 3.

Several companies made significant contributions to this work: Johnson Controls, Inc., The Trane Company, The Marley Cooling Tower Company, The Allen-Bradley Drives Division, The Electric Power Research Institute, The Scot Division of the Ardox Corporation, and The Baldor Electric Company. Several individuals gave noteworthy advice: Clay G. Nesler, Donald Eppelheimer, Neil W. Yohnk, Daniel R. Crum, and Michael J. Fairchild.

Many people made Madison a great place to go to school: Frank D. Drake (tennis animal, and cultural guru), Florian L. F. Pape (jack-of-all trades), Doug T. Reindl (barefoot beast, and Johnny driver), Tim U. Townsend (cycling king, and Johnny of all Johnnies), Diane L. Kozlowski (mom) and her husband Ken (party animal), Ken Ramczyk (curling king), Blake V. Minnerly (all-around frisbee-throwing jocular dude), Mohammed Asfour (fashion tycoon), Manfred C. Wirsum (connoisseur of fine German beer), and Harold Klein (style guru). In addition, special thanks goes to Bill Beckman and his wife Sylvia for their generosity and friendly hospitality; their gatherings have always been memorable.

OVERVIEW

Chapter One

Chapter Two

Chapter Three

Chapter Four

CONTENTS

Chapter One

INTRODUCTION TO COOL STORAGE SYSTEMS

Chapter One (continued)

Chapter Two

COMPONENT MODELING AND CHARACTERISTICS

Chapter Two (continued)

Chapter Two (continued)

Chapter Three

SYSTEM DESIGN

Chapter Three (continued)

Chapter Four

SYSTEM SIMULATION AND CONTROL

Chapter Four (continued)

Chapter Four (continued)

Chapter Five

CONCLUSIONS AND RECOMMENDATIONS

VII. APPENDICES

TABLES

Chapter One

Chapter Two

Chapter Three

FIGURES

Chapter One

Chapter One (continued)

Chapter Two

Chapter Two (continued)

Chapter Two (continued)

Chapter Two (continued)

Chapter Two (continued)

Chapter Two (continued)

Chapter Three

Chapter Four

Chapter Four (continued)

Chapter Four (continued)

Chapter Four (continued)

NOMENCLATURE

Roman Symbols

Symbol	Definition
A	amplitude
A	surface area
A	constituent
A_{cs}	cross-sectional area
a_f	finned surface area per unit length
a_H	surface area per unit packed-height available for heat transfer
a_M	surface area per unit packed-height available for mass transfer
B	constituent
C_E	energy charge
C_P	demand charge
C_p	specific heat at constant pressure
C_S	specific heat of the gas-vapor mixture per unit mass of dry gas

Roman Symbols (continued)

Symbol	Definition
$C_S^{'}$	average saturation specific heat
C_{Q_v}	coefficient of discharge
$C_{\Delta H}$	coefficient of head
C_{P_s}	coefficient of power
C_v	specific heat at constant volume
CFA	cooling-coil face area
CFV	coil face velocity
COP	coefficient of performance
D	diameter
D	molecular diffusivity
d	differential
F	mass-transfer coefficient
F_o	fraction of outdoor air
f	frequency
f	function
H	head
H	height
h	convection coefficient
h	enthalpy
$h^{'}$	heat-transfer coefficient which includes the effects of mass transfer
h_{if}	latent heat of fusion

Roman Symbols (continued)

Symbol	Definition
h_{fg}	latent heat of vaporization
h	enthalpy per unit mass
Δh_{lm}	log-mean enthalpy difference
I_T	solar radiation per unit area fall on a tilted surface
i	inflation rate
J	error sum of squares function
K	constant
k	thermal conductivity
k_ω	gas-phase mass-transfer coefficient
L	length
$\overline{L}$	mean value of the daily utility load
Le	Lewis number
M	molecular weight
$\dot{m}$	mass flow rate
m	mass
N	absolute molecular flux across the phase interface
N	economic life
N	speed
N	number
NEMA	National Electrical Manufacturers Association

Roman Symbols (continued)

Symbol	Definition
Ntu	number of transfer units
ODP	open drip proof
P	power
P	pressure
P_A	partial pressure of constituent A
P_s	shaft power
p	number of pairs of poles
$\dot{Q}$	load
$\dot{Q}$	heat transfer rate
$\dot{Q}_{cool}$	amount of heat and moisture removed from the zone
$\dot{Q}_{gain}$	overall latent and sensible gain for the building
$\dot{Q}_{loss}$	storage losses
Q_v	volume flow rate
R	cooling-tower range
R	heat-capacity-rate ratio
R	demand ratchet
Re	Reynolds number
r	market discount rate
r'	market discount rate which includes the effects of inflation
r	radius
SHR	sensible heat ratio

Roman Symbols (continued)

Symbol	Definition
S^*	superficial half-length
S	actual half-length
T	temperature
T_{BO}	blended outlet temperature
T_b	cooling degree-day base temperature
T	period of the day
$T_{sol\text{-}air}$	sol-air temperature of the surrounding atmosphere
t	ice thickness
TEFC	totally enclosed fan cooled
TRNSYS	A Transient Simulation Program
U	overall conductance
$(UA)_z$	overall conductance and area product of the zone
$\dot{W}$	rate at which mechanical or electrical work is performed
x	dimensional coordinate
Z	packed-volume per unit cross-sectional area
~	varies as

Greek Symbols

Symbol	Definition
α	solar absorptivity of the material of the outer surface of the zone
α	thermal diffusivity
γ	relative speed
ε	surface roughness
ε_a	air-side effectiveness
Δ	change
η	efficiency
η_f	fin efficiency
η_o	temperature effectiveness of a fin
θ	time
ρ	density
ρ_a	density of standard air
τ	period of time
ω	absolute humidity ratio
∂	partial differential

Subscripts

Symbol	Definition
A	constituent
a	air
act	actual
amb	ambient
b	base
b	brine
BO	blended outlet
c	condenser
c	cooling coil
char	charging period
ch	chiller
chw	chilled water (pure water or 25% ethylene glycol solution)
circ	circuit
cool	cool
cs	cross-sectional area
dischar	discharge
e	evaporator
eq	equivalent
f	fan
G	bulk gas phase

Subscripts (continued)

Symbol	Definition
G	pure, or dry, gas
gain	gain
i	inlet condition
i	interface phase
ice	ice
in	input
inf	infiltration
int	internal
L	liquid
lat	latent
lm	log-mean
lw	leaving water
M	gas-vapor mixture
m	motor
m	month
max	maximum
min	minimum
mwl	main water-loop
nom	nominal
o	environment
o	outlet condition

Subscripts (continued)

Symbol	Definition
o	reference
out	output
p	pump
req	required
s	season
sens	sensible
sol	solar
sol-air	sol-air
stor	storage
sys	system
t	tank
t	tower
tot	total
twl	tower water loop
v	vapor
w	water
wb	wet-bulb
z	conditioned-space air
z	zone or conditioned space within the conditioned space
1	inlet condition
2	outlet condition

Superscripts

Symbol	Definition
SAT	saturation
*	superficial quantity
'	modified value

Miscellaneous

Symbol	Definition
.	rate of change
–	mean value
^	fitted value

CHAPTER
ONE

INTRODUCTION TO COOL STORAGE SYSTEMS

As an introduction to the concept of comfort cooling using ice storage and chilled-water storage, the importance and nature of the American ice harvests are first discussed followed by two interesting accounts of the development of mechanical refrigeration and the birth of commercial comfort cooling. Two men were instrumental in these developments: Dr. John Gorrie, the father of both air conditioning and commercial ice manufacturing [1], and Dr. Willis Carrier, the definitive leader in the development of air conditioning [2].

These first applications of cool storage (a general term embodying ice storage, chilled water storage, and eutectic storage) are then related to current applications with emphasis placed on the utilities' role in the advancement of these systems. This is followed by a general description of the various types of cool storage techniques currently in use. Next, the utilities are shown to play a significant role in the promotion

of cool-storage systems and also to significantly influence the manner in which these systems operate. The chapter concludes by demonstrating the economic link between the electric utility and the process of selecting a cool-storage system.

1.1 HISTORICAL BACKGROUND

Although ice storage and chilled-water storage systems are currently burgeoning in the air conditioning industry, the basic technologies were developed long ago. From a historical perspective, this section introduces the concept of comfort cooling using either ice storage or chilled-water storage.

1.1.1 The American Ice Harvests

The use of natural ice, or ice made without the aid of mechanical refrigeration, goes back to far distant times; however, it began to be used extensively in the early years of the nineteenth century. In the winter months, ice was harvested from a number of sources—such as rivers, lakes, ponds, and mountains—in the colder regions of the United States [1].

This process was quite elaborate. Ice was first cut into a manageable size, usually by a manually-operated ice saw, which sometimes took three men to operate if the ice was sufficiently thick, or by a horse-drawn cutting mechanism; then, the ice-block was lifted to a horse-drawn sleigh and, subsequently, transported to the ice house for storage. There, ice-blocks were laid on 8 inches of saw dust and stacked several blocks high with a layer of saw dust between each adjacent block; a thick layer of

sawdust (typically 1 to 2 feet) covered the top and perimeter of the resulting stack of ice blocks.

Ice was essential for preserving especially perishable foods, such as butter, milk, and meats, and it was also used to chill drinks and aid in the manufacture of high quality beers. Most farmers throughout the country made their own ice houses. On the other hand, people from large urban areas—such as New York, Chicago, and New Orleans—had to rely on local ice factories. These factories stored large quantities of ice and distributed it to neighboring customers via horse drawn ice-wagons.

1.1.2 The Development of Mechanical Refrigeration

Besides preserving man's goods, ice was also used for other reasons. In the middle of the nineteenth century, ice storage, in its most primitive form, made its fledgling debut. Dr. John Gorrie, an American physician, hung buckets filled with ice in hospital rooms and directed an air stream over the ice to cool malaria and yellow fever patients.

Gorrie's Invention In 1844, Dr. Gorrie, director of the U.S. Marine Hospital in Apalachicola, Florida, recognized the need for a continuous supply of ice to cool his patients. In those days, natural ice was supplied, via steamship, from ice factories in the northern states, such as Maine and New York; in summer months the ice would often arrive irregularly. Accordingly, the ingenious Dr. Gorrie, aware that a sudden expansion of compressed air cooled itself, invented and subsequently patented the first compressed-air ice making machine [1]. This was the first commercial machine in the world built and used for refrigeration and air conditioning and the forerunner to today's compressed-air refrigerating machine [3].

Gorrie's machine and the ammonia absorption refrigerating machine invented in 1851 by Ferdinand P. E. Carre of France gave America the power to do, as described in the words of the time, "only what God Almighty could": make perfectly clear ice. (An interesting depiction of the times may be noted from Gorrie's apprehension to publicly ascribe his invention to himself. After just completing his air cycle refrigerating machine, Gorrie published an account of his work in a local newspaper under the pseudonym *Jenner* since he was circumspect with regard to the religious ramifications of his undertakings. His fears were indeed well founded as a well-known newspaper in New York *The Globe* wrote, "there is a crank, down in Apalachicola, Florida, that thinks that he can make ice by his machine as good as God Almighty." [1].)

The Need for Refrigeration Natural ice was easily obtained in the northern and central states; however, it was more difficult to obtain in the southern states because transportation costs and losses—by ship, by horse-draw wagon, or by rail—were high. Consequently, in several southern states, ice making plants were established.

By 1869, six *artificial-ice* making plants were operating in America—all in the southern states, such as Louisiana, Texas, and Tennessee. Most ice manufacturers used Carre's ammonia absorption refrigeration machines for which 30 tons was considered to be a large-capacity unit at that time. By 1899, the number of artificial ice plants in operation was 790, and by 1915, when the annual production of artificial ice surpassed that of natural ice, the number of plants was 5000 [1].

Additionally, during the period from 1860 to 1900, mechanical refrigeration began to be applied to more than just ice making. In fact, the primary driving forces behind

the development of mechanical refrigeration were a) the need for artificial ice, b) the need for brewing and storing beer at low temperatures, c) the need to preserve meat over extended periods of time by chilling or freezing, d) the need to preserve milk and dairy produce, fruits and vegetables, and other foodstuffs (such as, ice cream, eggs, poultry, fish, chocolate, margarine and fats, wines, gassy drinks and fruit juices, and baked goods), and e) the need to satisfy the requirements of industrial process applications, such as those experienced in the slaughter and subsequent treatment of meat by packers, and those experienced in the immediate cooling of fresh milk after pasteurization by dairymen [1].

1.1.3 The Birth of Modern Air Conditioning

Although mechanical refrigeration was firmly established as a means to preserve goods, it was not until after 1890 that the first practical applications of industrial air conditioning emerged. This type of air conditioning was directed toward facilitating process applications or controlling the environment for certain materials or equipment. It was to these applications which mechanical refrigeration was primarily applied for the next thirty years. And it was ice that would lead America into the age of comfort-cooling air conditioning.

Cooling Theaters Using Ice Theaters were among the first applications to use air conditioning. In 1914, many theaters in the United States were cooled using ice. Figure 1.1 shows the means by which this was done. Before the silent picture was to begin (talking movies date back to 1927), ice was delivered by a horse-drawn ice wagon (deliveries by motor-van did not begin until 1915) and then loaded into the vessel shown in schematic form in Figure 1.1. Water was then circulated through the

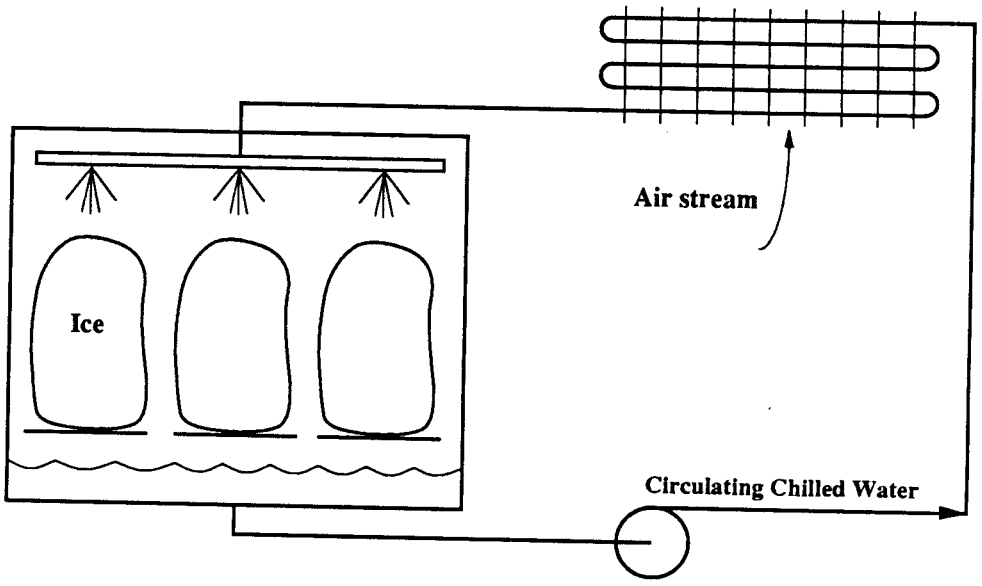

Figure 1.1 Air cooling by circulating ice-cooled water.

coils, over which air was blown, and then sprayed uniformly over the blocks of ice from a header located above them. In this manner sensible and latent heat from the air was transferred to the ice [1].

It was not until 1923 that mechanical refrigeration became viable for commercial comfort cooling applications. In this year two important developments were realized. The first development, pioneered by William Carrier, was the advent of the modern centrifugal compressor which utilized new refrigerants and new technology to simplify the refrigeration process. Carrier developed the philosophy that making chilled water should be, in practice, no more difficult than making hot water. He envisioned, in prior years, a device into which went warm water and out of which came chilled water

without the necessity of having a skilled operator to supervise the process. The second development was the need to cool large spaces where a great number of people gathered; these spaces were typically department stores, movie theaters, churches, and meeting halls [2].

Cooling Theaters Using Chilled Water An interesting illustration of these two developments is the story of one of Carrier's first commercial air-conditioning installations in a large movie-theater complex in Houston, Texas. During the hottest summer months of July and August, movie attendance frequently was discouragingly low. In order to avoid this and to boost summer sales, the owner desired to cool the theater by mechanical refrigeration. Carrier's design employed the use of chilled water storage, whereby the large short-duration cooling load of the theater could be met

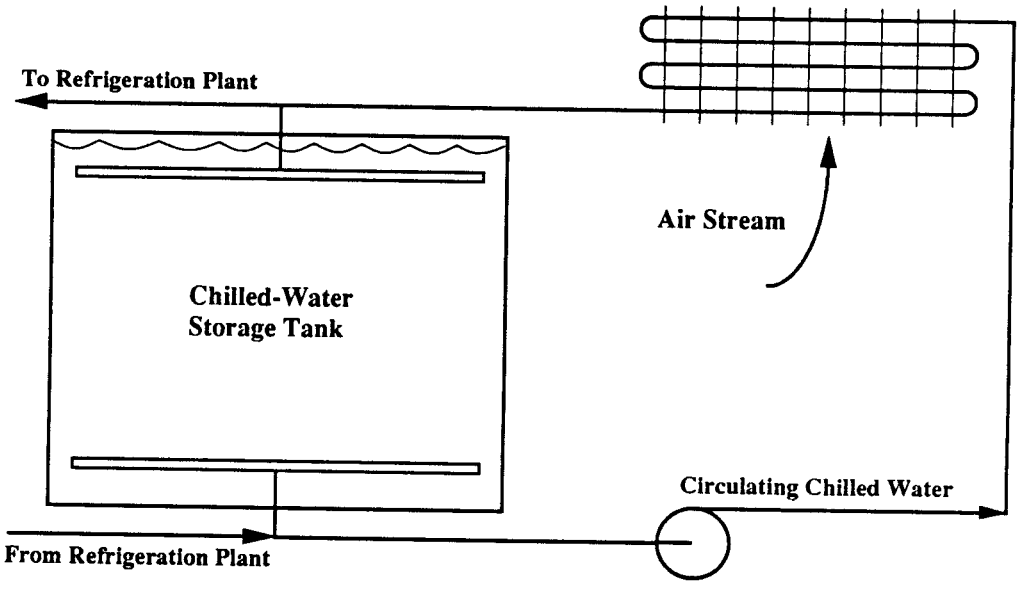

Figure 1.2 Air cooling by circulating stored chilled water.

economically by the limited capacity refrigeration machines of the day. Figure 1.2 shows this design technique.

On opening day, a great crowd gathered before the theater armed with fans, which they waived fervently in the summer heat, as they were sceptical about the efficacy of the new technology. The crowd entered the building, filled all the seats, and also filled the remaining standing room in the rear, while Carrier and his team scrambled to effect repairs to the system which had incurred problems just prior to the grand opening. The room was hot; people groaned, and they fanned furiously. Then almost imperceptibly, as the air conditioning system became operational, the room began to cool; people became comfortable and stopped fanning. And the age of commercial comfort cooling was born.

1.1.4 Cool Storage and the Electric Utility

The early applications of cool storage were limited to buildings with infrequent, short-term cooling loads, such as those experienced by theaters, churches, meeting halls, dairies, and breweries.

Suitable Building Loads for Cool Storage Applications The goal of these applications was to significantly down-size the capacity of the air conditioning or refrigeration equipment and, thus, ultimately reduce the first cost of the system. This was possible since the extra capital required to purchase the storage equipment was outweighed by the savings obtained in selecting a relatively smaller chiller. (For example, a system with a 25-ton chiller and 4 hours of stored cooling has the same capacity as a conventional system with a 125-ton chiller, when the cooling load lasts for

1 hour.) Thus, the selection of a cool storage system was limited to special cases involving long periods between loads to allow for storage.

Today, however, the selection of a cool storage system is not as stringently dependent on the length of time between loads; accordingly, other building load profiles have become amenable to cool storage. The new candidates for cool storage applications are office buildings, school and college buildings, laboratories, large retail stores, libraries, and museums. The reason for this increase in the number of application opportunities is not due to any inherent change in the technology itself; rather, it is driven by new electric rate structures.

The electric rate structures, as determined by the utility, are strongly dependent upon the utility's *baseload* (the minimum power demand on a utility's generation system over a specified period) capacity and its *load factor* (the quotient formed by dividing the utility's average load by its peak load, or more precisely, the integrated load over a period divided by the product of the maximum demand during that period and the length of time of the period). The load factor of American utilities, on average, has been steadily declining since the 1960's where the average load factor was approximately 67 percent. Currently, the average load factor is approximately 62 percent [4].

The Ideal Utility Load Ideally the utilities would like a load factor of unity: a perfectly flat load profile where the average load is at all times equal to the peak load. This maximizes the effective use of generating capacity where the plant baseload capacity is, ideally, at all times greater than or equal to the instantaneous demand on the plant. Accordingly, the utility would have no need to invest in or operate peaking units which are designed to meet demands that are in excess of the utility's baseload

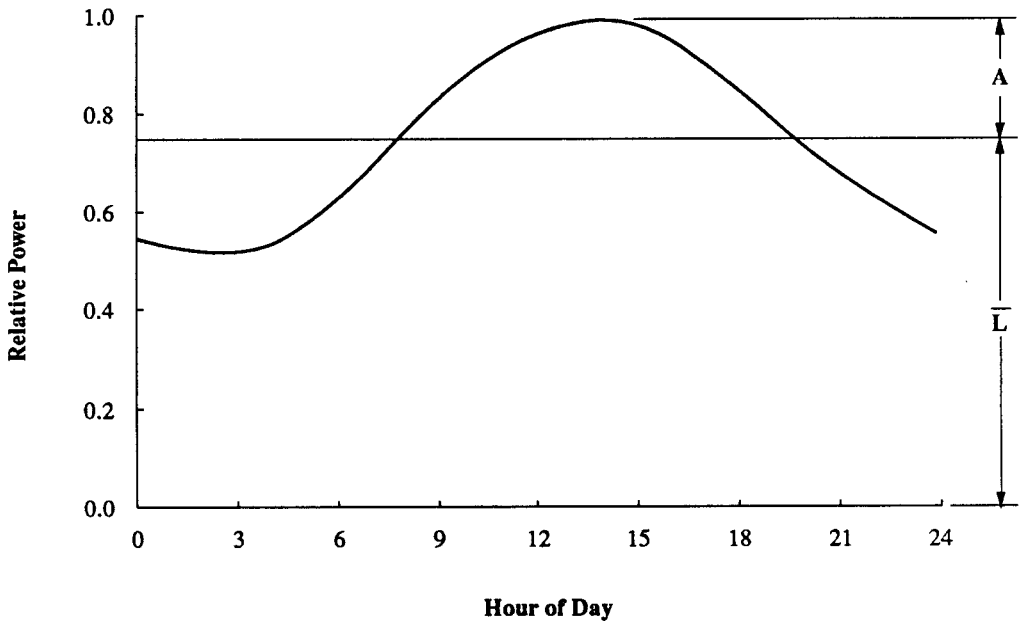

Figure 1.3 Typical daily utility load profile.

generating capacity. Typically, the operational cost per generated kilowatt for baseload electricity generation is only a small fraction of that for electricity generated by peaking units. Thus, utilities would like to avoid unnecessary use of the peaking units.

The Actual Utility Load A typical daily utility load profile (shown in Figure 1.3) is approximately sinusoidal in nature, reaches a maximum at approximately 3:00 p.m. and a minimum at approximately 4:00 a.m., has a mean value $\overline{L}$ about which the sinusoid varies, and has an amplitude A [5]. From the utility's perspective three cases regarding Figure 1.3 are of interest. Case 1, if the maximum daily load is greater than the baseload generating capacity then peaking units must be employed to meet the demand. Case 2, if the maximum daily load is only slightly less than the baseload

capacity then the utility must consider one of several options in the near future to avoid a brownout. If the electrical distribution network is adequate then the utility must invest in either peaking units or additional baseload capacity or both. If the network is not of adequate capacity then the utility must invest in one of the above choices plus the necessary additional electrical distribution network. Case 3, if the maximum daily load is substantially less than the utility's baseload capacity then the cycling of baseload equipment or the part load operation of this equipment with demand variation may concern the utility.

In all of the above cases, especially the first and second, an improvement in the utility's load factor would lead to more efficient operation. For case 1, the utility's reliance on less efficient peaking units could be reduced; for case B, the utility could

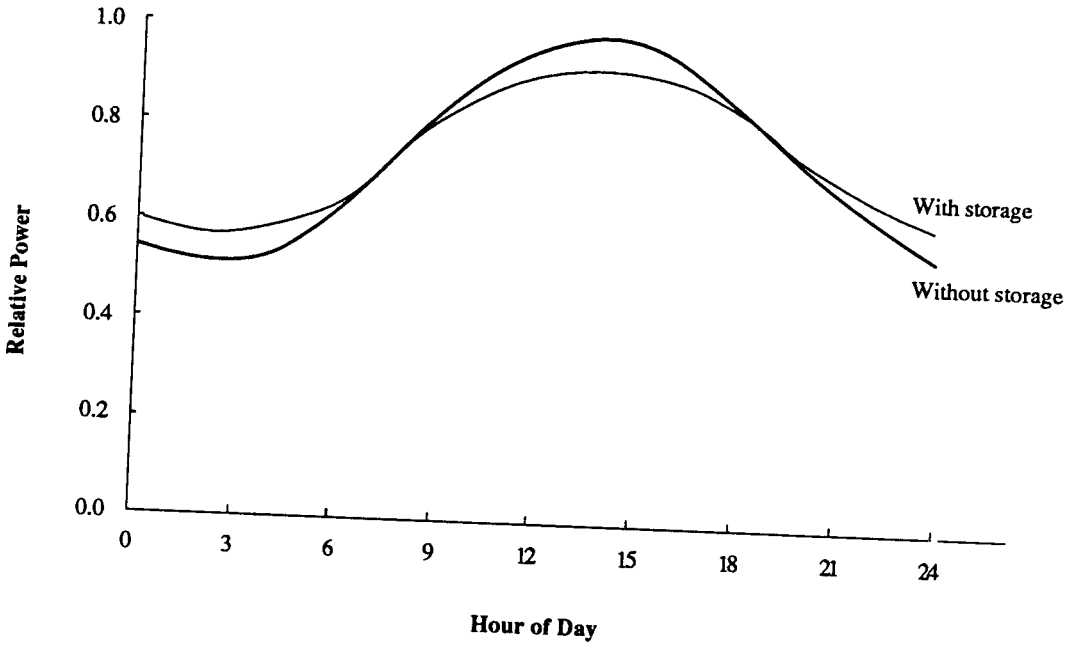

Figure 1.4 Typical daily utility load profile with cool storage and without cool storage.

avoid or delay a potentially considerable capital expenditure; and for case C, the performance of large baseload generators could benefit from operating at constant load. How can the load factor be improved?

Cool Storage Aids the Utility Cool storage offers a mechanism by which the utility can improve its load factor. Because of the large demand for commercial comfort cooling, the most severe seasonal demand occurs, for most utilities, during the hottest summer months. Of the total electrical demand by the commercial sector, approximately 44 percent is related to comfort cooling during a summer peak [4]. Accordingly, cool storage applications have the potential to enhance the utility's load profile by decreasing the demand for electricity during the peak period of the day and shifting it to the late evening and early morning hours. This effect is demonstrated in Figure 1.4 [6].

1.2 THE FUNDAMENTALS OF COOL STORAGE

Cool storage is a general term embodying ice storage, chilled-water storage, and eutectic storage. A cool storage system acts as either a *heat sink,* a region into which heat—from a building or a process—may be transferred, or a *heat source,* a region from which heat—from the storage media—may be transferred. (In general, for cooling operations, the term cooling load, or just load, is defined as the rate of heat transfer into a heat sink; thus, for example, a storage tank experiences a load when heat is flowing into the tank.) Accordingly, a path for heat transfer must exist to allow for communication between the storage system and its intended surroundings. Currently, there are several means by which to effect this process. This section discusses the

common types of ice storage systems and chilled-water storage systems, the various storage strategies, the promotional incentives given by utilities, and the basic cool-storage system control techniques.

1.2.1 Chilled-Water Storage Systems

Chilled-water storage systems all have one feature in common: to prevent warm and cool regions of water from mixing. This section discusses the three common designs that have been developed to efficiently store chilled water: the naturally-stratified, single-tank storage system; the physically-stratified, single-tank storage system; and the physically-stratified, multiple-tank storage system.

Naturally Stratified Storage The simplest cool-storage system is the naturally-stratified chilled-water storage tank; that is, a thermally stratified tank in which no artificial means are employed to separate regions of disparate temperature. This system and its operation are shown in Figure 1.5 (typical temperatures are shown in °F). The primary components of interest are the chiller, the storage tank, and the air handling system, or load. Observe that the chiller, storage tank, and load are linked together in a parallel configuration. This is typical for chilled-water storage systems and it allows the system to conduct charging and discharging simultaneously.

The operation is quite simple: in order to charge the tank, water is pumped from the top section of the tank, cooled by the chiller, and then returned to the bottom section of the tank. Similarly, in order to discharge the tank—after it has been charged—the process is reversed; that is, water is pumped from the cooler bottom section of the tank, heated by the load, and the returned to the warmer top section of the tank. The words

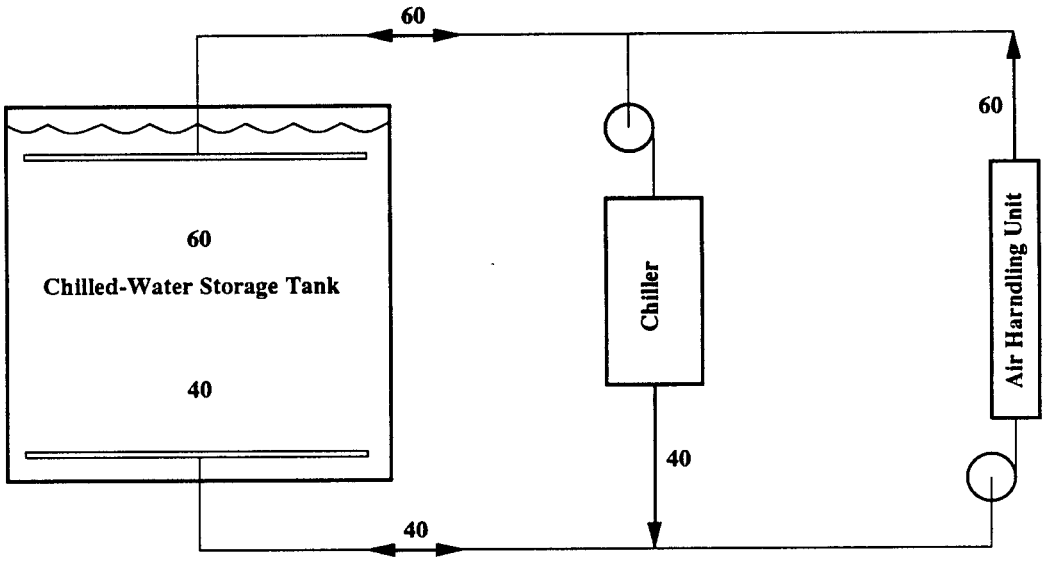

a) Naturally stratified chilled-water storage system.

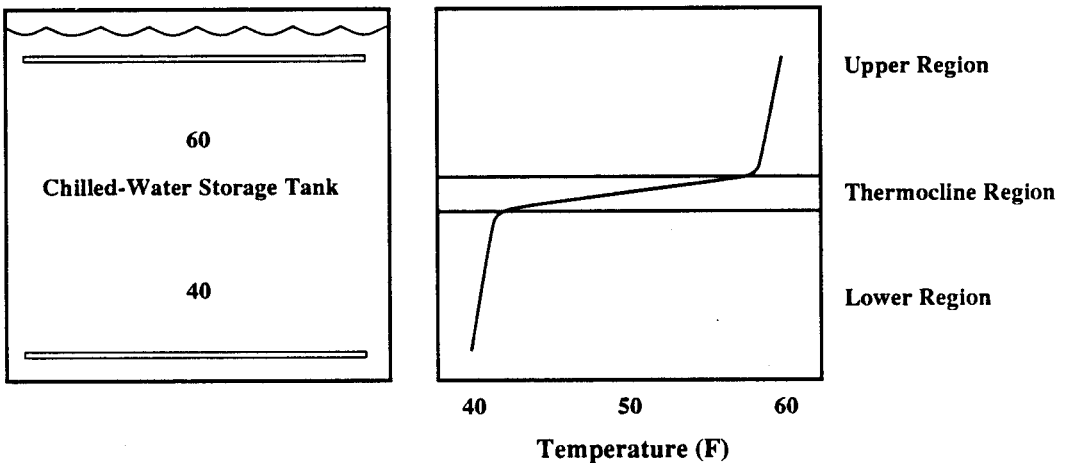

b) Temerature variation with tank height.

Figure 1.5 Naturally stratified chilled-water storage system (a), and the temperature variation with tank height (b).

charge and *discharge* are general terms that are frequently applied to cool storage systems; to charge the storage system is by definition to remove heat from the storage system and, conversely, to discharge is to add heat.

The region of the tank separating the warm upper section from the cool lower section is called the *thermocline region,* or mixed region. The water within the tank maintains these three discrete regions because of thermal stratification, the separation of warm and cold regions of a fluid caused by differences in density. The upper and lower regions are nearly uniform with respect to temperature, unlike the mixed region where the temperature profile varies considerably. These regions and the temperature variation with tank height are shown in Figure 1.5. The major temperature changes occur within the mixed region. The design objective is to maintain a very thin mixed region over the range of mass flow rates encountered in operation. Typically, this region is very thin for well designed tanks which employ the use of elaborate manifolds and diffusers to uniformly distribute the flow as it enters the tank and avoid turbulence and the generation of convective currents as the flow exits the tank.

The density variation of water with temperature is very slight between 40 and 60°F; therefore the driving force for thermal stratification is, indeed, very small. Hence, alternative chilled-water storage systems have been developed to combat this problem.

Physically Stratified Storage: Single Tank One alternative to allowing warm and cool regions to remain stratified naturally is to physically separate these regions using a diaphragm, or membrane. The operation is the same as that of the naturally-stratified storage system. However, the mixture region is no longer present, instead a flexible rubberized cloth separates the two remaining regions. Although there exists a

physical separation, this separation does not prevent the transfer of heat across the membrane between the two regions.

Tanks employing this technique are typically more costly and require more maintenance. Additionally, membranes have been known to tear and to clog inlet and outlet ports. Moreover, a recent study conducted by researchers in New Mexico revealed that the thin mixture region in naturally stratified systems was, in fact, more effective in maintaining thermal separation between the warm and cool regions than was the membrane in physically stratified systems [7].

Physically Stratified Storage: Multiple Tanks To prevent the thermal mixing inherent in either of the aforementioned single tank methods, a second method to physically separate the two regions is to use several tanks linked in parallel with each other and the load and in *reverse-return* with the chiller (Figure 1.6). One of these tanks is empty when the system is either fully charged or discharged; fittingly, the method is called the *empty tank* method.

The operation of this system is more complex than that of the previously mentioned systems. In order to charge the tanks—assuming they are fully discharged initially and arranged from left to right, such that the left-most tank is the empty tank—warm water is drawn from the bottom of the first full tank to the right of the empty tank (the middle tank in Figure 1.6), cooled by the chiller, and then issued into the empty tank (the first tank in Figure 1.6). When the "empty tank" is eventually filled, a new empty tank (the middle tank in Figure 1.6) is ready to be charged. Warm water is then taken from the first full tank to the right of the new empty tank, and the process is repeated until all tanks are charged. Tank discharging is conducted in the inverse order of the charging

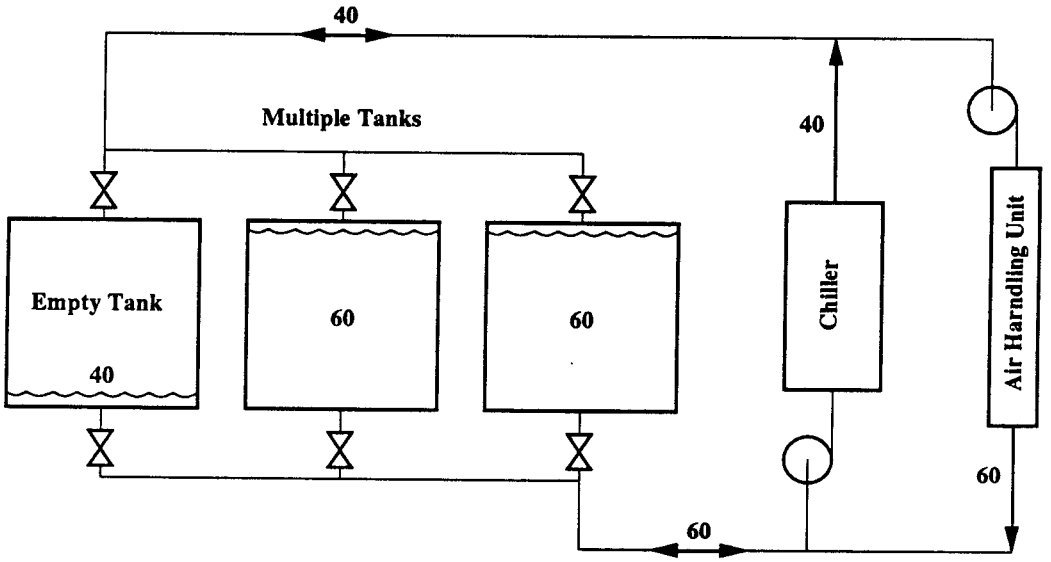

Figure 1.6 Physically stratified chilled-water storage system: multiple tanks. Tanks are fully discharged.

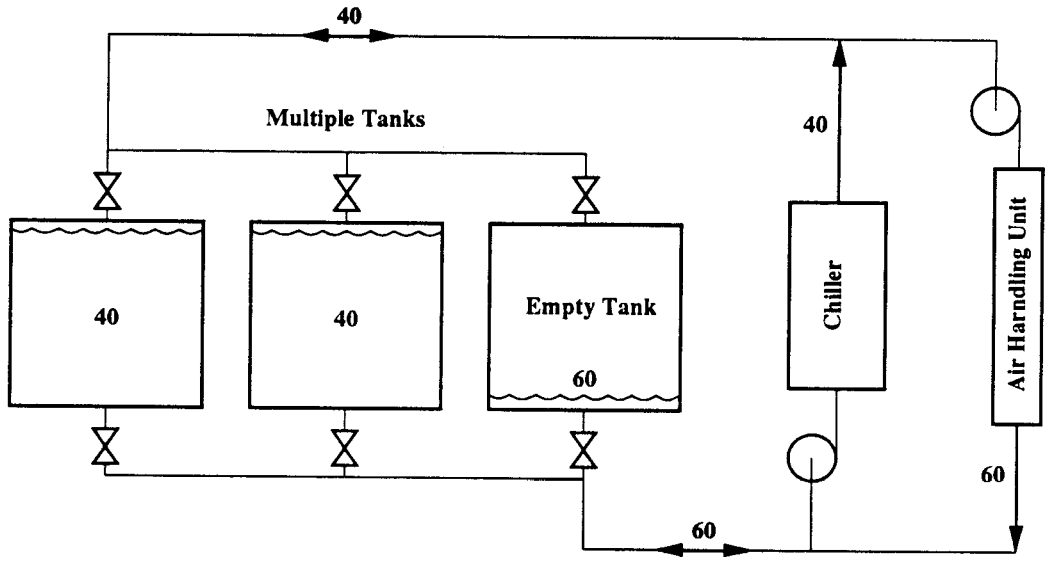

Figure 1.7 Physically stratified chilled-water storage system: multiple tanks. Tanks are fully charged.

process with the load replacing the chiller (Figure 1.7). As with all typical chilled water systems, charging and discharging occur simultaneously; this is not, however, the case with many ice storage systems.

Since this system is more complex in its operation, it requires more elaborate controls than single tank systems. Additionally, since multiple tanks are used the surface area to volume ratio is high and, consequently, unfavorable to storage losses. Moreover, because one tank is empty when the system is fully charged, the effective capacity of the system is always one tank less than the installed capacity, which results in tank costs that are higher than those of other systems. When space limitations must be considered, the modular nature of the multiple-tank system may be advantageous.

1.2.2 Ice Storage Systems

This section discusses the three common designs that have been developed to efficiently store ice: the static ice-on-coil storage system, the static constrained-area storage system, the dynamic ice-harvester storage system. Whereas the various chilled-water storage systems all have the common goal to prevent warm and cool regions of water from mixing, ice storage systems have the common goal to prevent ice from becoming too thick.

The Static Ice-On-Coil Storage System

The oldest and most traditional design of the four common designs is the static ice-on-coil storage system. This system and its manner of operation are shown in Figure 1.8. The primary components of interest are the refrigeration plant, the storage tank, and the

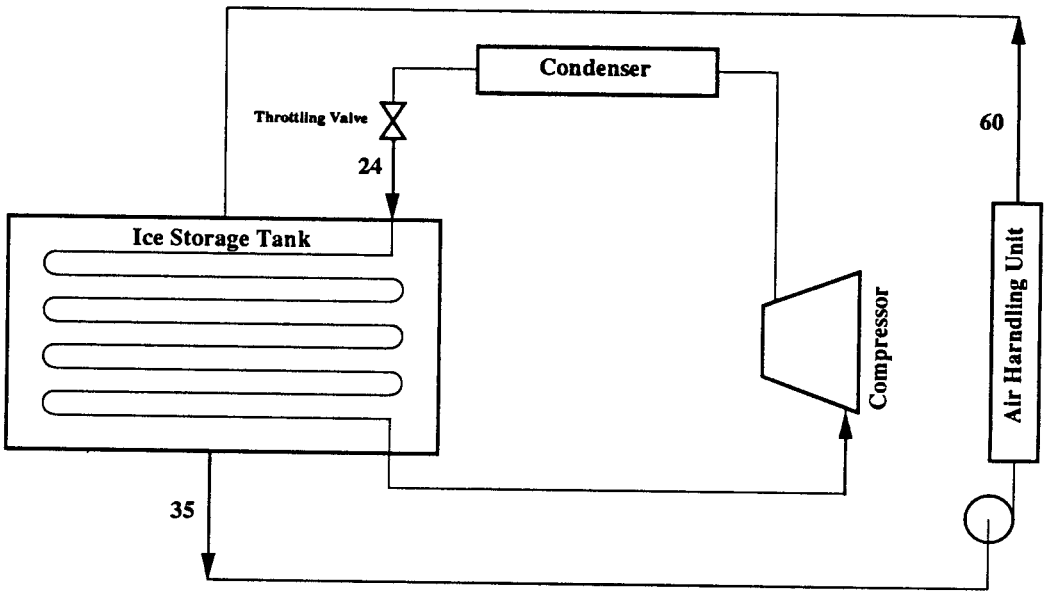

Figure 1.8 Static ice-on-coil storage system.

load. Observe that the evaporator coils of the refrigeration plant are located directly within the storage tank.

Charging Cycle During the charging cycle—assuming that the storage tank is completely uncharged initially—high-pressure, high-temperature refrigerant condensate is expanded through the throttling valve into the low-pressure region of the evaporator coils. The condensate flashes into a two phase mixture comprising mostly liquid, the remainder being vapor. The energy, in the form of latent heat, required to effect this change in thermodynamic state is surrendered by the fluid in the form of sensible heat; accordingly, the fluid temperature is decreased. Consequently, the evaporator is thus capable of functioning as a heat sink with respect to the surrounding storage medium. Additionally, since the condensate is directly expanded into the evaporator coils that are

located in the storage tank, the system is often referred to as a *direct expansion* system.

As sensible heat from the storage medium is transferred to the evaporator, the temperature of the medium decreases; moreover, in order to maintain a relatively constant flow of heat into the evaporator, the temperature within the evaporator must also correspondingly decrease. Since the thermal performance of the refrigeration plant degrades significantly as the evaporating temperature decreases, this type of system—as well as all other ice-storage systems—experiences a severe performance penalty as charging progresses.

Furthermore, as the charging process continues, ice begins to form on the surface of the evaporator coil. Ice is approximately 30 times less conductive than the tubes of the evaporator (which are typically made from hot-dipped galvanized schedule 40 steel pipe, $1\frac{1}{4}$ inch outside diameter) upon which it forms and typically reaches a thickness between 1 and 3 inches by the end of the charging period; as a result, a significant thermal resistance progressively builds through the charging period which, in turn, leads to still lower evaporator temperatures and further reduces the thermal performance of this system.

By the end of the charging cycle, the storage tank contains approximately 50 percent water and 50 percent ice. The final ice formations on the surface of the tubes are not—as would be intuitively expected—cylindrical in nature; rather, they are sheet-like in nature. Figure 1.8 shows a single row of coils stacked in a vertical plane; not shown are the other rows located behind the first row. It is these rows that become vertical sheets of solid ice by the end of the charging period, and typically they reach a thickness of up to 7 inches and are nearly as long and high as the storage container [10].

The storage system is designed to prevent horizontal *ice-bridging* between adjacent rows, but not within rows. This is achieved by spacing tubes farther apart between rows than within rows and by using one of several mechanisms, such as compressed air or secondary pumping, to achieve proper internal water flow patterns. In this manner, a suitable surface area is maintained to facilitate heat transfer during the discharge period, while the available storage capacity is effectively utilized.

Discharging Cycle During the discharging cycle, ice-cold water is drawn from the bottom of the storage tank, warmed by the load, and issued back into the top of the tank. Within the tank, again, physical agitation takes place to assure that the ice sheets are melted, or *burned*, in a uniform manner. Like the chilled-water storage systems, the storage tank and the load are connected in a open loop circuit. This creates a big splash when these systems are used with tall buildings where the location of the load is elevated far above the storage tank. In order to avoid this splash caused by falling water, the tank inlet must be throttled or—a more economical method from an operational standpoint—a hydraulic recovery turbine must be used. The turbine recovers some (typically 40 to 60 percent) of the pumping energy required to lift the stream of water to the elevation of the load by capturing the kinetic energy of the falling-water stream and transmitting it to the water pump. This problem can be circumvented altogether, at a price, by isolating the storage system through the use of a heat exchanger.

The Static Constrained-Area Storage System

The problems encountered in selecting an open-loop storage system can be circumvented by employing the static constrained-area storage system. This system

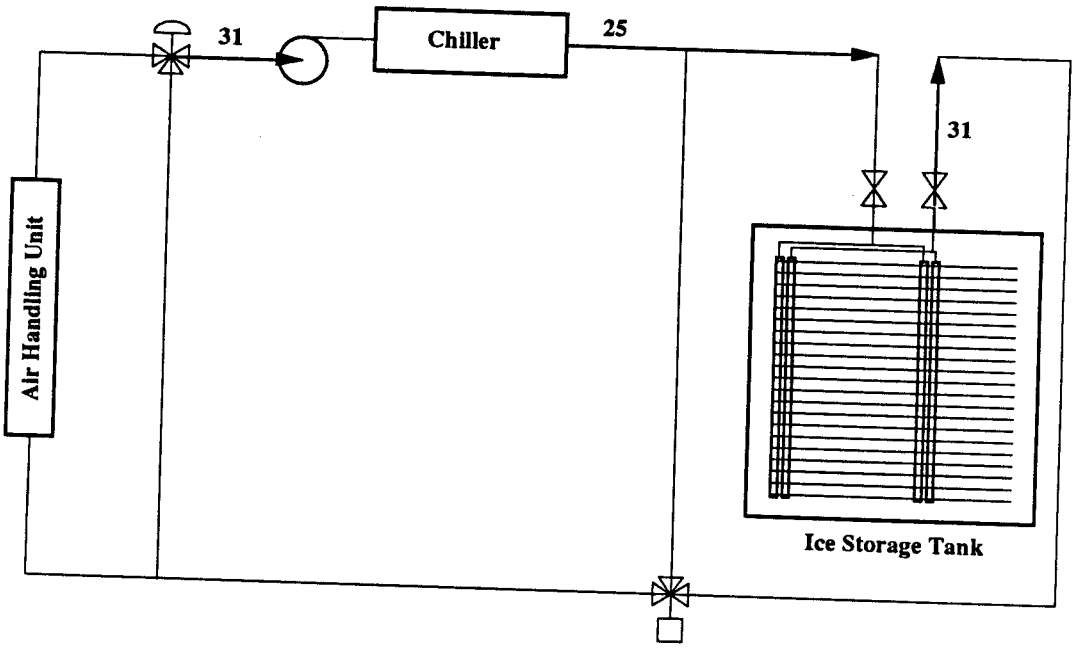

a) The charging cycle.

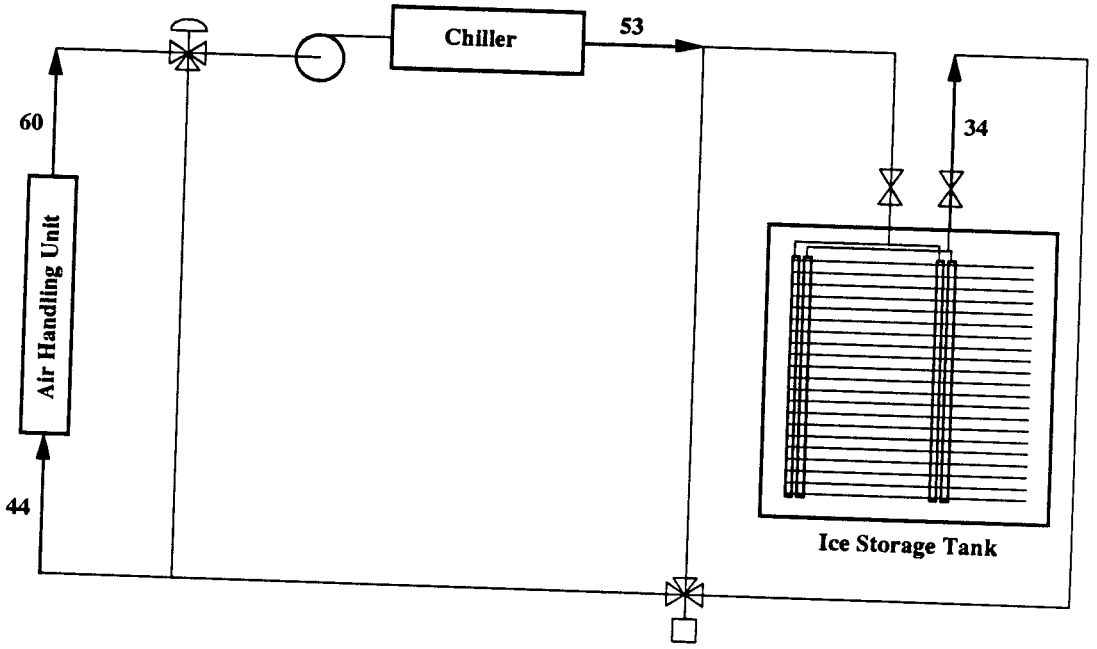

b) The discharging cycle.

Figure 1.9 Static constrained-area storage system charging (a) and discharging (b).

and its manner of operation, which is quite different than the static ice-on-coil storage system previously discussed, are depicted in Figure 1.9. The primary components of interest are the storage tank, the chiller, and the load. The tank is located remotely from the refrigeration plant, a packaged chiller in this case.

Charging Cycle During the charging cycle (Figure 1.9 a)—assuming that the storage tank is completely uncharged initially—chilled brine is issued from the chiller, extracts heat from the storage tank, and is then returned to the chiller. The brine is typically an aqueous ethylene-glycol solution; the concentration of ethylene glycol is specified such that freezing in the chiller's evaporator bundle is avoided, usually 25 percent-by-weight ethylene glycol is sufficient for ice-making applications. As the charging process continues, the temperature of the storage medium decreases—and, correspondingly, so does the chiller's evaporator temperature which results in a degradation of thermal performance—until it reaches its freezing point. At that time ice begins to form on the surface of the tubes contained within the storage tank.

Unlike the static ice-on-coil system, the tube density in this system is very high; that is, the spacing between adjacent tubes (approximately $\frac{6}{10}$ of an inch) is much smaller than in the static ice-on-coil system (approximately 6 inches in the vertical direction). As a result, the penalty associated with the thermal resistance caused by ice thickness is not a problem—and this is widely promulgated. However, these systems are not free from the penalties associated with ice building.

Whereas the static ice-on-coil storage-system design seeks to prevent ice-bridging between rows of coils to provide an adequate amount of surface area to effect heat transfer during the discharge period, the static constrained-area storage-system design

does not. Because of the high tube density and, therefore, large surface area available for heat-transfer associated with these systems, adequate surface area for the transfer of heat from the storage medium immediately adjacent to the outer surface of the tubes—in the liquid or solid phase—to the brine carried within these tubes is always ample. Thus, no penalties are associated with this system experiencing ice-bridging during the discharging period.

On the contrary, there exists a significant penalty due to ice-bridging during the charging period because the surface area available for the transfer of heat from the remaining liquid in the tank to the brine carried within the tubes is not always adequate. Because the distance between adjacent tubes is relatively small, as charging progresses the advancing ice formations on one tube eventually intersect the formations of all other adjacent tubes. As soon as this occurs the surface area available for heat transfer between the remaining liquid in the storage tank and the brine decreases at a drastic rate as the formations continue to advance. Thus, constrained-area storage systems encounter a considerable problem with ice-bridging during the charging cycle which is generally not the case for the static ice-on-coil storage system.

Discharging Cycle During the discharging cycle (Figure 1.9 b), warm brine is pumped from the outlet terminals of the cooling coil (contained within the air handling unit shown in Figure 1.9), partially cooled by the chiller, and then split into two streams, one of which is diverted to the inlet terminal of the storage tank and the other of which is issued to the three-way mixing valve.

The stream entering the storage tank is subsequently split into two streams, one of which is diverted to a header located near the center of the storage tank, the other of which is issued to a header located near the perimeter of the storage tank (these headers

are shown in Figure 1.9). From the headers the streams are further subdivided into a number (typically fifty) *circuits* (a circuit is an independent path for fluid flow). This serves two purposes: a) since this system contains great lengths of tubing (several miles of tubing is typical for commercially available modular systems), dividing the flow stream into several circuits reduces the head loss experienced by the brine as it passes through the storage tank; b) it allows the ice to build uniformly and melt uniformly.

Two spirally-wound planer circuits are contained within each row shown in Figure 1.9. The plan view of this arrangement is shown in Figure 1.10. One of the circuits begins at the header located at the perimeter of the storage tank, it is spirally wound in a counterclockwise fashion, and it terminates at the header located at the center of the storage tank. The other circuit is wound in a manner exactly opposite of the first one; that is, it begins at the central header, it is wound clockwise, and ends at the perimetral

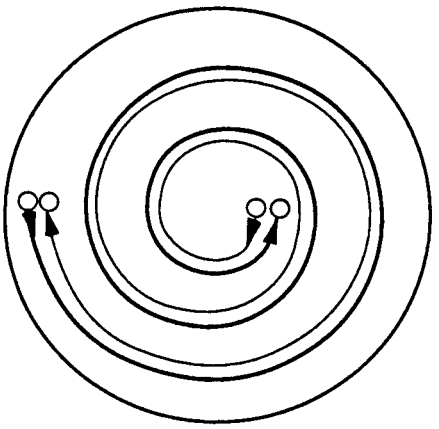

Figure 1.10 Plan view of the countercurrent circuits located within the static constrained-area storage tank .

header (see Figure 1.10). Nearly uniform building and melting occur from the counter-current flow of brine through these circuits.

In this process, the brine passing through the storage tank transfers heat to the storage medium and approaches the freezing point of the water which separates the ice from the tube surface within the storage tank. The temperature of the brine approaches the freezing point of water quite closely near the beginning of the discharging cycle and less closely near the end of this cycle because of the insulating effect of the water (which is caused by its poor conductive properties and its poor convective properties at temperatures near its freezing point; namely, the coefficient of thermal expansion which is identically zero at 4°C, 39.2°F). The two brine streams recombine at the mixing valve where the outlet temperature from this valve is maintained at a specified value. Finally, the combined stream enters the inlet terminals of the cooling coil and is then warmed by the load.

Although this system benefits from a closed-loop pumping circuit, the storage media is not in direct contact with the evaporating surface; as such, there is a thermal penalty associated with employing an intermediary transport fluid to link the refrigerant within the evaporator and the storage medium.

Dynamic Ice-Harvesting Systems

The thermal performance degradation caused by the formation of thick ice layers around the evaporator tubes of the static ice-on-coil storage system and the thermal performance degradation due to ice-bridging between the tubes of the static constrained-area storage system can be avoided by employing dynamic ice-harvesting storage systems. The two commercially available systems, distinguished by the

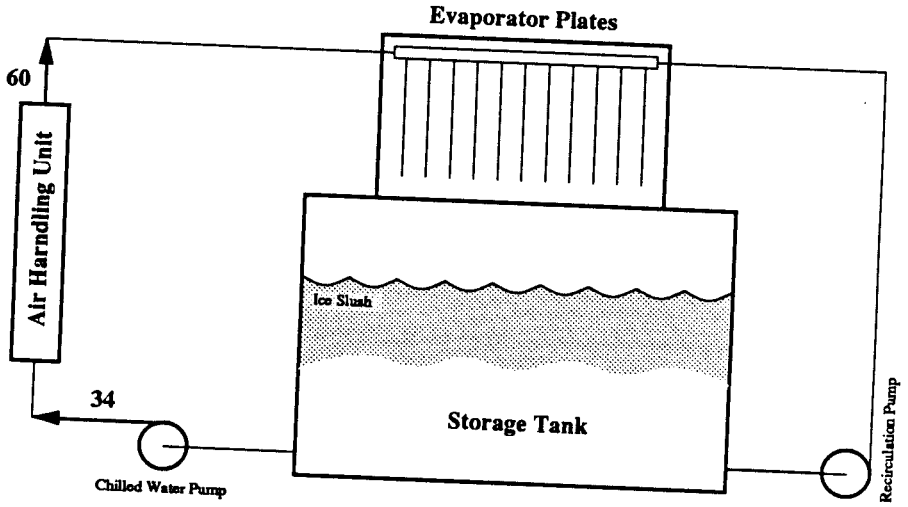

Figure 1.11 Dynamic ice-harvesting storage system: plate-ice machine.

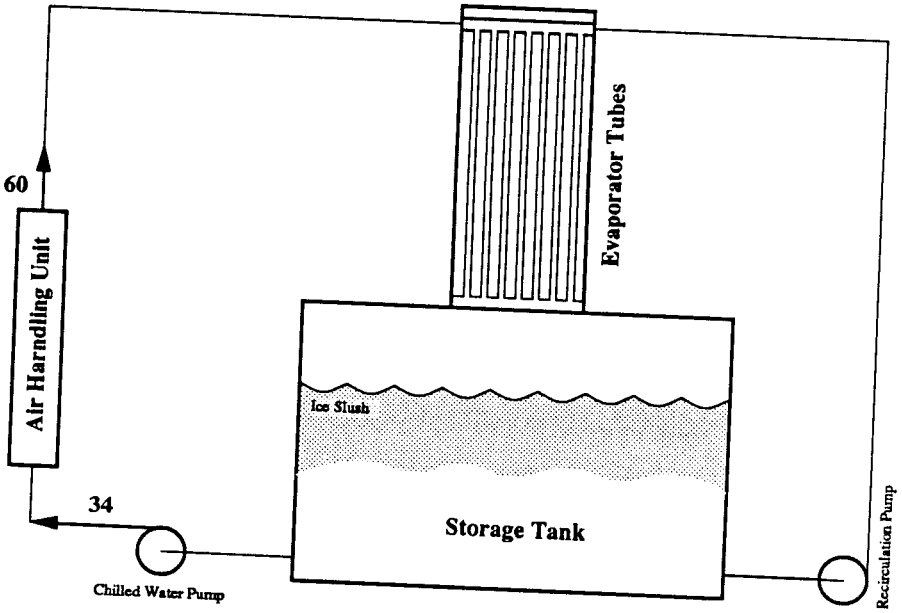

Figure 1.12 Dynamic ice-harvesting storage system: tube-ice machine.

method by which ice is formed, are the dynamic ice-harvesting plate-ice machine and the dynamic ice-harvesting tube-ice machine. These systems and their manner of operation, which is very similar, are shown in Figures 1.11 and 1.12. The primary components of interest are the storage tank, the evaporator of the refrigeration plant (the condenser, compressor, and expansion valve of the refrigeration plant are omitted for clarity, but may be viewed in the figure representing the static ice-on-coil system, Figure 1.8), and the load. The evaporator in both of these systems is suspended above the storage medium and the plates and tubes of the evaporators are arranged vertically.

Charging Cycle During the charging cycle, warm water is pumped from the bottom of the tank, cooled by the evaporator, and then issued back into the tank. As this process continues, some of the circulating water begins to solidify on the evaporator surface, which forms ice sheets on the plates of the plate-ice machine and ice cylinders within the tubes of the tube-ice machine. The plates (usually made of stainless steel) are corrugated on the outer surface to promote the adhesion and formation of ice and to create space for internal passages through which refrigerant passes. The tubes of the tube-ice machine (also usually made of stainless steel) are surrounded by refrigerant which is contained within the shell of the evaporator, and the tubes' inner surfaces are used to form ice. Within the evaporator in the plate-ice machine, water is sprayed over the plates of the evaporator surface. The disadvantage associated with this is that the ice formations obtained tend to have only half the density of solid ice—due to aeration of the water prior to freezing [15]. On the other hand, this is not the case with the tube ice machine where water is allowed to cascade freely down through the suspended evaporator tubes—thus clear solid ice is formed.

After a desired thickness is attained (typically $\frac{1}{4}$ of an inch for ice sheets and approximately $\frac{1}{2}$ of an inch for ice cylinders), the ice is *harvested*, or removed from the evaporator surface, by displacing the refrigerant inside the evaporator with hot refrigerant vapor which is by-passed directly from the compressor discharge to the evaporator. Subsequently, the layer of ice immediately adjacent to the evaporator surface liquefies, which allows the remaining solid ice to slide down the evaporator surface and into the storage container. When the plate-ice machine is used, the ensuing impact with the water and ice-slush surface is sufficient to break the ice formations into a number of smaller fragments—which is desired to promote an adequate surface area for heat transfer during the discharging period. In contrast, the tube-ice machine typically requires a cutter plate to cut the ice cylinders before they are issued into the storage tank.

Thus, for these systems the performance penalty caused by a thick layer of ice forming on the evaporator surface or ice-bridging between adjacent tubes of the storage tank is avoided; hence, the compressor operates at an approximately constant *suction temperature* (the temperature of the refrigerant as it just enters the suction port, or inlet, of the compressor) during the latent charging portion of the charging cycle (the period of the charging cycle beginning when ice first begins to form on the evaporator surface). This is a very important advantage that these systems have over the static systems previously discussed. However, the harvesting cycle associated with the dynamic systems not only requires additional controls but it also degrades the thermal performance of these machines because of capacitance effects within the evaporator and the additional compressor load resulting from the hot-gas by-pass.

Discharging Cycle During the discharging cycle, warm water is pumped from the outlet terminals of the cooling coil, partially cooled by the evaporator, and then reissued into the storage tank. Since the evaporator surface is located remotely from the storage medium, the refrigeration plant can be reset to operate in a water-chilling mode and thereby substantially increase its operating efficiency; the static constrained-area storage system shares this beneficial characteristic, whereas the static ice-on-coil storage system does not. Note also that these dynamic systems are linked in an open loop with the load and, thus, are subject to the same pumping problems as the static ice-on-coil storage system.

The most important points discussed in this subsection are the following: a) static storage systems generally experience excessive ice-thickness or ice-bridging problems during the later portion of the charging period and thus are thermally penalized from a performance standpoint, whereas the dynamic systems do not experience these problems, b) the evaporator surface of the static ice-on-coil storage system is immersed directly into the storage medium; therefore, it does not permit the refrigeration plant to benefit from being reset to operate in the water-chilling mode during the discharging cycle, whereas all the other ice-storage systems previously discussed are able to benefit from this rest process and c) the static constrained-area storage system is connected in a closed loop; hence, it does not encounter the pumping problems inherent in the open-loop circuits of the other ice-storage systems.

1.2.3 The Four Fundamental Storage Strategies

Now that a solid foundation has been established with regard to the physical and operational characteristics of the various cool-storage systems, it is possible to readily

comprehend the manner in which these systems can be used to achieve their ultimate goal: to save money.

As a basis for comparison of the basic storage strategies, this section begins with a discussion of the power and load characteristics of the conventional air conditioning system. Next, the four common fundamental storage strategies employed in the design and operation of cool storage systems are discussed; they are the full storage strategy, the partial storage strategy, the demand-limited storage strategy, and the modified demand-limited storage strategy. Although a particular storage system is typically designed using one of the fundamental storage strategies, the actual storage system operation on an arbitrary day during the cooling season may be significantly different than the intended design day operation.

This freedom of operation allows more complex control strategies to be developed for system operation during periods of lighter loads; the crux of these strategies is not to minimize the amount of energy consumed in general, but the amount of energy consumed during periods of high energy cost and high power cost, or equivalently high utility *energy charges* or high utility *demand charges*. These more complex strategies serve to bring additional savings to the owner after one of the basic storage strategies has already been employed in the storage system design; these strategies are the topic of future chapters. For comparative purposes, the utility's on-peak period is assumed to be from 11:00 a.m. to 6:00 p.m. (which is typical for many utilities today).

The Conventional Air Conditioning System By definition the phrase *conventional air-conditioning system* refers to any air conditioning system that does not employ thermal storage (either cool storage or otherwise). The operational strategy of these systems is such that the instantaneous *air-conditioning load,* or *cooling load,*

is always transferred directly to the refrigeration plant. Note that the term instantaneous air-conditioning load refers to the amount of heat that must be removed from the conditioned space to maintain that space at a specified temperature; it does not, however, refer to the instantaneous overall building load—which comprises several sub-loads: solar load, ambient latent and sensible load, internal latent and sensible load, and infiltration latent and sensible load—that may in fact be quite larger or smaller than the instantaneous air-conditioning load because of capacitance effects associated with the building structure.

Power-based viewpoint From a power-based viewpoint, the most important economic figure of merit is the total instantaneous power demand of the building, which may be divided into two general categories: the power demanded by equipment specifically assigned to aid in cooling the building, or the *cooling load* (in its mechanical equivalent form) and the power demanded by equipment not assigned to help cool the building, or the *noncooling load.*

The cooling load, from this power-based viewpoint, is the amount of power required by the refrigeration plant and all of its associated distribution mechanisms (fans, pumps, controls) to transfer the heat generated from or accrued by the building load, the fan load (heat generated by distributing air and by fan inefficiencies), the ventilation load (heat accrued by cooling warm and moist air to the climatic conditions within the building), and the pumping load (heat generated by distributing water) to the surrounding atmosphere. The noncooling load is composed of several sub-loads, such as those caused by lights, electric motors, machines, copiers, computers, elevators, and other mechanical and electrical equipment. Since the noncooling load is relatively uniform throughout the year, it can be used as a *datum* for the power demand; that is,

the maximum noncooling-load power demand is the minimum total building demand attainable if the cooling load could be shifted, or moved, to periods of low noncooling-load power demand.

Energy-based viewpoint Similarly from a energy-based viewpoint, the most important economic figure of merit is the total amount of energy consumed during the utility's on-peak period, which also may be divided into cooling and noncooling components. Again, since the noncooling load is relatively uniform throughout the year, it can be used as a datum for the total energy consumption during the on-peak period. These two loads are displayed in Figure 1.13 which shows a typical hourly

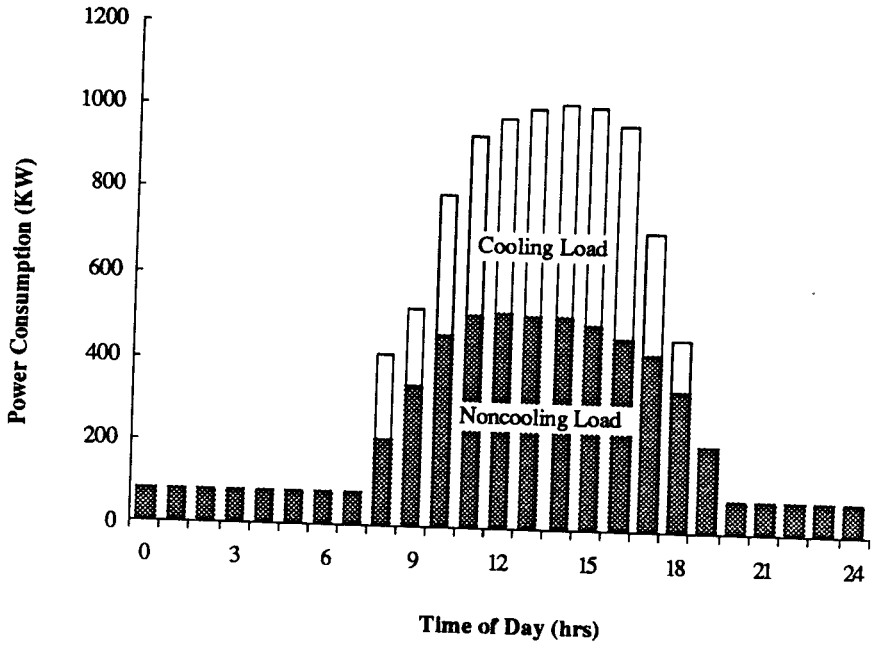

Figure 1.13 Conventional-system hourly power consumption on the design day.

building load profile on the *design day,* or hottest weather day. In Figure 1.13, the cooling and noncooling loads are shown stacked upon each other; thus, the cooling load may be determined from the total load and the noncooling load.

The salient features of Figure 1.13 are that the cooling load exists from 8:00 a.m. to 6:00 p.m. (which is typical of a modern commercial office building, although many buildings do in fact experience low nighttime cooling loads), reaches its peak demand at approximately 3:00 p.m., and experiences a local peak in the first hour of operation (this is more evident from Figure 1.18) due to a morning building *pull-down period* (a period in which the heat gained by the building during the previous night is extracted from its structure). The relative magnitude of this local morning peak varies considerably with local climate and the type of building construction. In addition, the noncooling load peaks early and remains relatively flat throughout the day; during the night it is approximately uniform and weak in relative magnitude.

If a nighttime cooling load were present, it may be handled by a separate cooling system or handled by the main cooling plant operating at part load or operating a fraction of the total number of chillers if the system is large. Furthermore, with regard to the design of ice storage systems, these nighttime loads may indeed seriously affect the amount of refrigeration capacity required, since the refrigeration plant will be operating in the ice making mode when these nighttime loads occur. This is not, however, a concern with chilled-water storage systems.

The characteristics of these loads combine to form a large energy demand between 10:00 a.m. and 5:00 p.m.. For economic reasons, both the utility and the building owner would like to avoid this. With the aid of cool storage, the characteristics of the noncooling load profile are ideally suited to effect their desires.

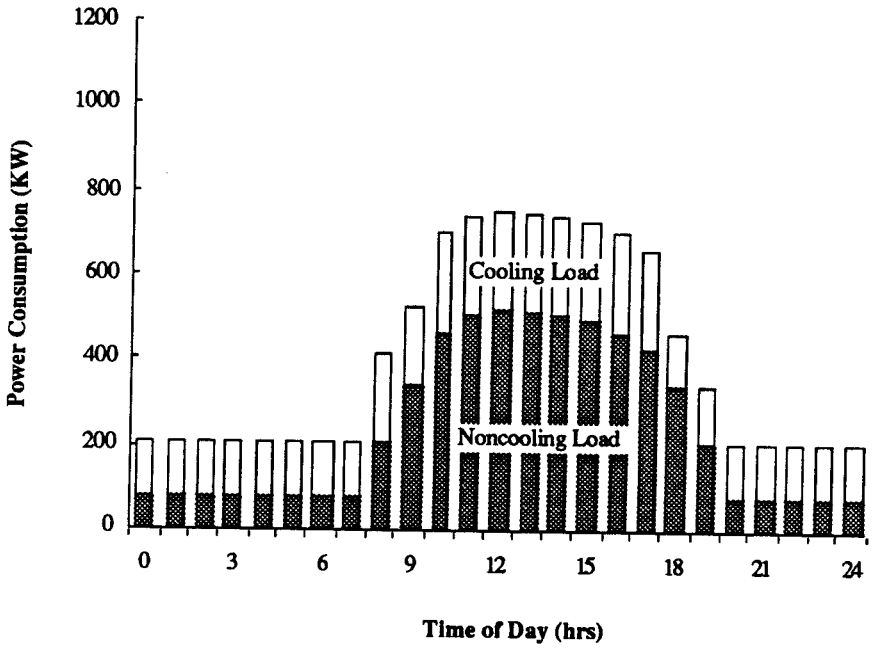

Figure 1.14 Partial-storage-system hourly power consumption on the design day.

The Partial Storage Strategy The objective of any cool-storage strategy is to reduce the maximum power demand during the utility's on-peak period and to shift the cooling load toward the off-peak periods. The most popular method from an economic standpoint to accomplish this goal is the partial storage strategy. This method approximately distributes the cooling load evenly over every hour of the design day by allowing the refrigeration plant to operate continuously over the 24 hr period.

The resulting load profile is shown in Figure 1.14. With respect to the conventional system's load profile, the two most important aspects to note from the partial storage system's load profile are, first, that the maximum on-peak demand has be reduced from 1020 kW to 747 kW and, second, that the total on-peak energy

consumption has, similarly, been reduced from 7138 kW hr to 5506 kW hr (assuming, as previously stated, an on-peak period from 11:00 a.m. to 6:00 p.m.).

The primary advantage of this strategy is that the refrigeration plant is allowed to unrestrictedly aid the storage medium in meeting the daily cooling load.

The Full Storage Strategy An alternative method is the full storage strategy. This method shifts the entire cooling load to either off-peak hours or non-occupied hours (the period of time in which the building is generally not occupied) by allowing the refrigeration plant to operate only during these hours.

Figure 1.15 shows the resulting load profile for the latter case. The salient facts are that the on-peak demand has been reduced from 1020 kW to 521 kW which corresponds to the demand datum of the noncooling load and that the total on-peak

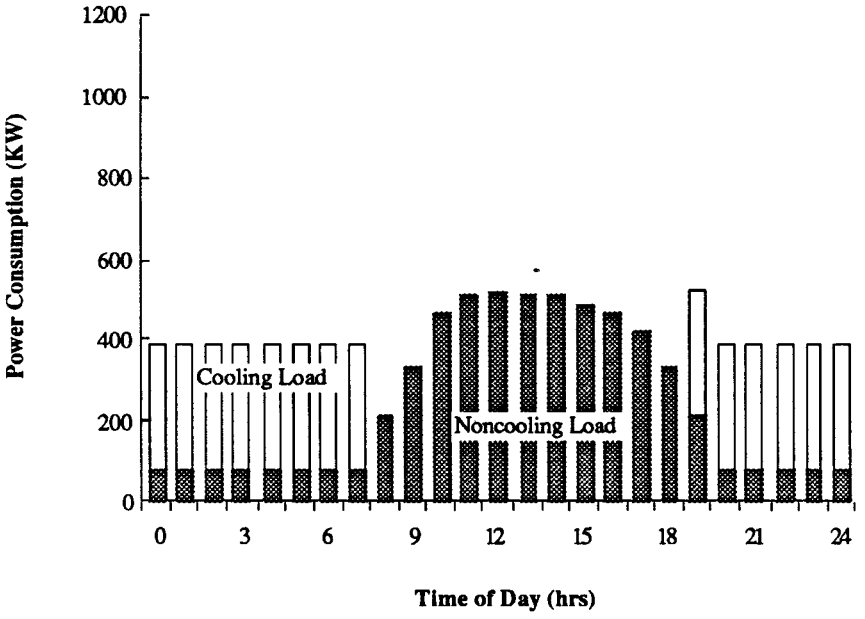

Figure 1.15 Full-storage-system hourly power consumption on the design day.

energy consumption has been reduced from 7138 kW hr to 3798 kW hr which corresponds to the energy-consumption datum of the noncooling load. Thus, both the monthly demand bill and the monthly on-peak energy bill are reduced to minimum level with this storage strategy; this is the only strategy which is capable of minimizing both the demand and on-peak energy bills.

The disadvantage with this method is that the chiller is *locked-out*, or not allowed to operate, during the occupied period; therefore, the amount of storage must be sufficient to meet the entire daily cooling load and, furthermore, the capacity of the chiller must be sufficient to effect the entire charging process within the non-occupied period (13 hours in Figure 1.15). Thus, this strategy requires both larger storage capacities and larger refrigerating capacities than the partial storage strategy.

The Demand-Limited Storage Strategy Lying somewhere between the two aforementioned strategies is the demand-limited storage strategy which is a rather complex modification of the full storage strategy. Like the full storage strategy, one of the goals of the demand-limited storage strategy is to reduce the monthly demand bill to zero. However, its other goal, which is more like that of the partial storage strategy, is to maximize the use of available chiller capacity throughout the day.

These two contradictory goals are reconciled by *demand limiting* the operation of the chiller; this means that the chiller is allowed to supply direct cooling to the load so long as the total power demand is less than or equal to the demand datum set by the noncooling load. Thus two cases, or rules, exist. First, if the difference between the demand datum and the noncooling load is greater than the power drawn by the chiller at its full capacity and if the cooling load is also greater than the chiller capacity, then and

only then is the chiller allowed to operate at its maximum capacity—the rest of the load is met by storage. Otherwise, the chiller operates to meet the entire cooling load.

Second, if the difference between the demand datum and the noncooling load is less than the power drawn by the chiller at its full capacity and if the cooling load (expressed in its mechanical equivalent form) is smaller than this difference, then the chiller operates to meet the entire cooling load. Otherwise, the chiller operates to supply as much of the cooling load as is permissible under the restriction that it cannot draw any more power than that power defined by the difference between the demand datum and the noncooling load—the remaining load is met by storage.

To clarify this exposition, Figure 1.16 has been constructed using these exact rules. (Note: In order to fully trace the above procedure Figure 1.16 must be used in

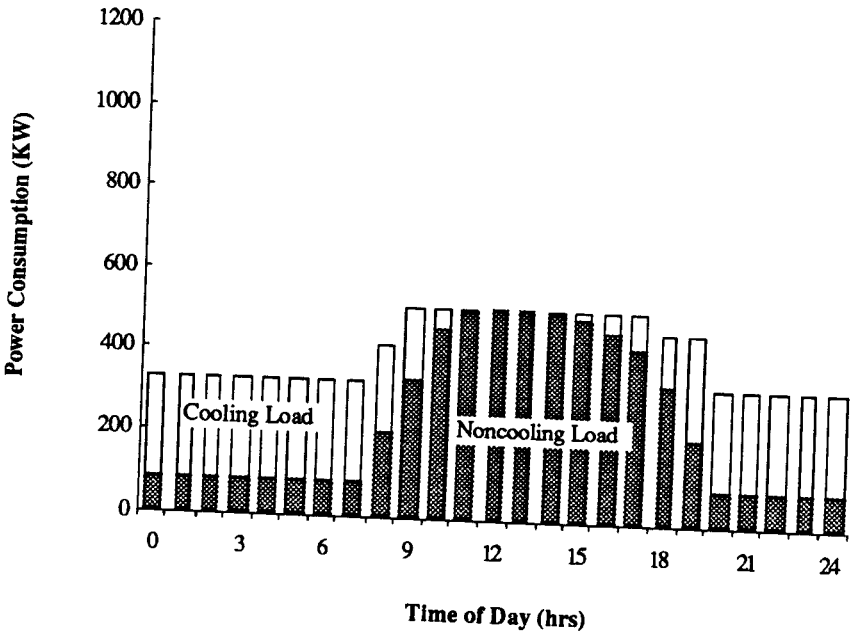

Figure 1.16 Demand-limited-storage-system hourly power consumption on the design day.

conjunction with Figure 1.20.) The points of interest to be gleaned from this figure are that the on-peak demand has been reduced from 1020 kW of the conventional system to 521 kW which, like the full storage strategy, corresponds to the demand datum of the noncooling load and that the total on-peak energy consumption has been reduced from 7138 kW hr to 4155 kW hr which is very close to the energy consumption datum of the noncooling load; that is, nearly all of the cooling load is met by off-peak energy.

The advantage of this method over the full-storage method is that the refrigeration plant is allowed to operate, although in a restricted fashion, during the occupied period. Thus, this strategy requires both smaller storage capacities and smaller refrigerating capacities than that of the full storage strategy. However, since the chiller operation is restricted, this strategy requires both larger storage capacities and larger refrigerating capacities than those of the partial storage strategy.

The Modified Demand-Limited Storage Strategy The final fundamental storage strategy to be discussed is one that is very attractive from the utility's perspective. It is a practical modification of the demand-limited storage strategy and incorporates some of the benefits associated with the partial storage strategy.

The characteristic load profile for this strategy is shown in Figure 1.17. The profile has components which are characteristic of the demand-limited storage strategy—the restricted chiller operation—and the partial storage strategy—the unrestricted chiller operation. Specifically, this strategy allows unrestricted chiller operation at all times except the on-peak period.

This method has the same on-peak demand and the same on-peak energy consumption as the demand-limited storage strategy and, therefore, offers no advantage

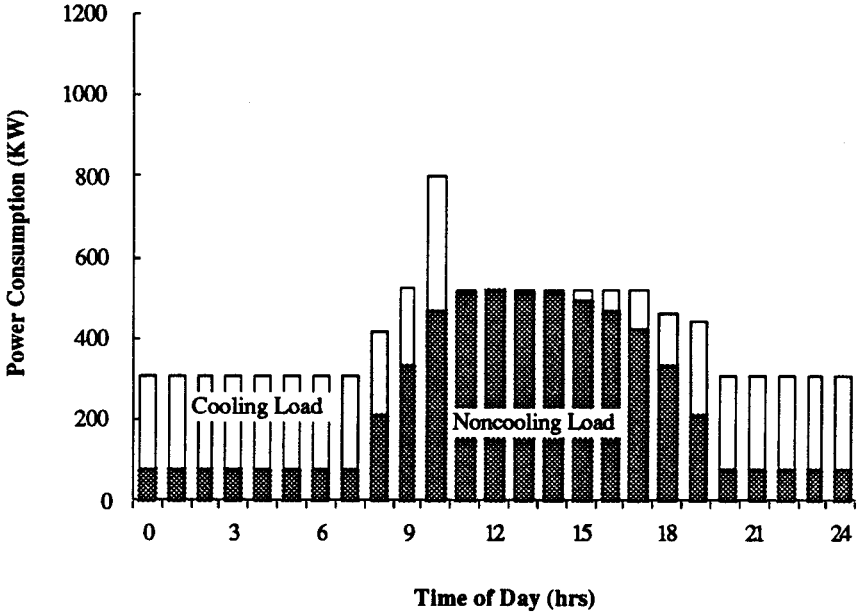

Figure 1.17 Modified demand-limited-storage-system hourly power consumption on the design day.

in this regard; however, it does have a advantage from a design standpoint. That is, since the chiller is allowed to operate unrestrictedly during the off-peak period, the required storage capacity and the required refrigeration capacity are reduced. Because this strategy achieves a maximum reduction in on-peak demand and also requires less storage capacity and less refrigeration capacity than that of either the full storage strategy or the demand-limited storage strategy, it benefits both the utility and the potential cool storage customer. For these reasons some utilities are currently advocating this strategy. However, if the utility was not able to influence the customer through monetary incentives, then the demand charges or the time-of-day rates would necessarily have to be high for the customer not to choose the partial storage strategy,

since this strategy has the benefits of the smallest required storage and refrigeration capacity and also some additional benefits resulting from demand reduction and load shifting.

1.2.4 Utilities' Role in Promoting Cool Storage

As previously discussed in Section 1.1.4, many utilities throughout the United States are experiencing declining load factors; to counter this decline and thus enhance their operational efficiency, they are advising their customers to participate in *load management strategies.*

Load management strategies are designed to reduce on-peak demand by shifting energy consumption from on-peak to off-peak periods. In general, the objective of these strategies is to reduce the need for additional generation, transmission, and distribution capacity; to conserve scarce resources by efficiently utilizing existing resources; and to provide electricity and services to customers at a reasonable price.

The load management program most applicable to cool storage applications is the *time-of-use* load management program. This program is designed to encourage customers to use energy when it is least expensive for the utility to generate. Time-of-use rate structures are the primary incentives used in this program to induce the customer to conform to the utility's desires.

These rate structures are designed to reflect the actual cost incurred by the utility to supply power to the customer. Specifically, both the average cost of electricity generation and the incremental cost (the change in total cost caused by a specified change in electricity generation) of electricity generation rise as the total demand rises above the baseload level because the utility must bring on-line, or operate, *peaking*

since this strategy has the benefits of the smallest required storage and refrigeration capacity and also some additional benefits resulting from demand reduction and load shifting.

1.2.4 Utilities' Role in Promoting Cool Storage

As previously discussed in Section 1.1.4, many utilities throughout the United States are experiencing declining load factors; to counter this decline and thus enhance their operational efficiency, they are advising their customers to participate in *load management strategies.*

Load management strategies are designed to reduce on-peak demand by shifting energy consumption from on-peak to off-peak periods. In general, the objective of these strategies is to reduce the need for additional generation, transmission, and distribution capacity; to conserve scarce resources by efficiently utilizing existing resources; and to provide electricity and services to customers at a reasonable price.

The load management program most applicable to cool storage applications is the *time-of-use* load management program. This program is designed to encourage customers to use energy when it is least expensive for the utility to generate. Time-of-use rate structures are the primary incentives used in this program to induce the customer to conform to the utility's desires.

These rate structures are designed to reflect the actual cost incurred by the utility to supply power to the customer. Specifically, both the average cost of electricity generation and the incremental cost (the change in total cost caused by a specified change in electricity generation) of electricity generation rise as the total demand rises above the baseload level because the utility must bring on-line, or operate, *peaking*

units (typically fast response oil- or gas-fired gas turbines), purchase electricity from other neighboring utilities, or invest in new construction to expand its baseload capacity. Hence, when the demand for energy is high the cost of energy is correspondingly high, and this is reflected in the rate structure.

The utility charges the customer for the total amount of energy used, the *energy charge*, and the maximum amount of power used, the *demand charge*. The energy charge, or commodity charge, is issued to recover operating costs and fuel costs incurred by the utility in generating and supplying power. The demand charge is issued to recover a portion of the capital costs and operating costs—which are associated with installing and maintaining the necessary generation, transmission, and distribution equipment—incurred by the utility for providing sufficient operating capacity to meet the power requirements of the customer. When these charges are a function of time, they are called *time-of-use rate structures.*

An additional utility rate structure germane to cool storage economics is a *demand ratchet*, or a ratchet clause. This clause states that the monthly demand charge levied against the customer will be the greater of the actual monthly demand billing or R percent of the maximum monthly demand billing over a specified period, where R is called the *ratchet.* It is designed to stabilize the utility's revenue and cover capacity costs; it also discourages large daily load fluctuations within seasons.

Table 1.1 shows typical time-of-use demand and energy charges as well as a typical demand ratchet. Also shown in Table 1.1 is a common utility incentive: the up-front *cash rebate*. Most utilities will make a single payment to the cool-storage customer of a specified amount of cash per kilowatt of on-peak demand reduced. This payment, or rebate, helps reduce the additional capital cost incurred by the customer for installing a

Typical Time-of-Use Rates:

	Demand Charge	Energy Charge
on-peak	$5 to $ 20 per kW per month	$.04 to $.10 per kW hr
off-peak	$0 per kW per month	$.02 to $.05 per kW hr

Typical Demand Ratchet: 50% to 100% over the previous year

Typical Rebates for Peak Demand Reduction: $115 to $550 per kW of peak demand reduced

Typical Summer On-Peak and Off-Peak Periods:

on-peak	11:00 a.m. to 6:00 p.m.
length of peak	6 to 12 hr duration typically includes hours from noon to 6:00 p.m.

Table 1.1 Typical utility rate structures, incentives, and peak periods.

cool-storage system. For the utilities, it is potentially more economical to invest in the cool storage systems of a great number of customers—enough such that a significant on-peak demand reduction may be realized—than to absorb the high capital costs required to build new generating plants (which typically cost from $1200 to $4000 per

kW of additional capacity [8]). The last important piece of information given in Table 1.1 is the typical length and most common times of the on-peak period.

All other things being equal, a relatively short on-peak period is highly advantageous to cool-storage systems based on the full storage strategy (where the full storage system is allowed to operate during the off-peak portions of the occupied period) or either of the demand-limited-storage strategies because this allows more time for the refrigeration plant to meet the cooling load directly which therefore decreases both the required storage capacity and the required refrigeration capacity. In general, cool storage becomes more economically attractive when on-peak demand charges are high, off-peak demand charges are low, the demand ratchet is high, and the differential between on- and off-peak energy charges are high. In addition, without time-of-use rates cool storage is seldom feasible [4].

1.3 ICE-STORAGE STRATEGIES

This section is designed to show the manner in which the most suitable fundamental storage strategy is selected based on 1) the characteristics of the cooling and non-cooling load profiles, 2) the performance characteristics of the constituents of the system, and 3) the prevailing economic conditions.

1.3.1 Ice-Storage System Operation on the Design Day

The purpose of this subsection is to demonstrate the manner in which each of the four basic ice-storage systems (designed based on the four fundamental storage strategies previously discussed) operate and to show quantitatively how the storage capacity and

the refrigeration capacity depend on the selected fundamental storage strategy. All of the systems are sized using ice as the storage medium; the assumptions made in the analysis are given in the problem statement below.

Finally, the sizing procedure conducted in this introductory chapter is limited in scope and, therefore, is not of the rigorous standard set forth in Chapter 3: System Design; however, the results are indeed accurate enough to determine the fundamental economic figures of merit necessary to determine the ultimate fundamental storage strategy upon which the system design should be based.

Problem Statement The utility rate structure to be considered has an on-peak period from 11:00 a.m. to 6:00 p.m., an off-peak period from 6:00 p.m. to 11:00 a.m., and thus no *shoulder periods* (periods between on- and off-peak periods which have, correspondingly, intermediate demand charges and energy charges). Furthermore, since this utility desires to improve its load factor, it imposes a substantial demand charge (for example, $10/kW per month) which is applied only during the on-peak period. As a further incentive for customers to shift their load, the utility offers time-of-use rates where the difference between on- and off-peak energy charges are significant (for example, $.08/kW hr on-peak and $.04/kW hr off-peak). Moreover, because this utility desires that its load not be subject to large daily fluctuations within seasons, it invokes a ratchet clause (Section 1.2.4) which is also significant (for example, an 85 percent ratchet over the previous 12 months of billing).

The system is to be designed to service a typical commercial office building, of new construction, with a floor area of 100,000 square feet and a daily cooling load requirement which has the following characteristics on the design day: 521-ton peak load, 4060-ton-hr total daily load, and a 71-percent load *diversity* (the quotient formed

by dividing the average daily load by the peak load); furthermore, the cooling load begins at 8:00 a.m. with a brief morning pull-down period and ends by 6:00 p.m.—no significant nighttime cooling loads exist (Figure 1.18). Additionally, the noncooling load is that given in Figure 1.13.

The possibility of using chilled-water as the storage medium has been ruled out, since based on design experience it is known that ice-storage systems are generally more cost-effective for buildings with less than 500,000 square feet of floor area (conversely, for building with floor area greater than 500,000 square feet, chilled-water storage may be more cost-effective than ice storage since the cost per storage-volume decreases significantly as the size of the chilled-water storage system increases, whereas ice storage systems which tend to be modular in nature do not experience this substantial benefit) [4]. Lastly, because the owner desires that the system control be simple in nature, the closed-loop static constrained-area storage system is selected.

The Partial Ice-Storage System The first option investigated is the partial storage system. Figure 1.18 shows the overall building cooling load together with the load on the refrigeration plant on the design day. This system operates under the fundamental partial storage strategy discussed in Section 1.2.4.

The charging cycle begins at 7:00 p.m. At this time the chiller is set, or controlled, to produce a 25°F *set-temperature* brine solution which is circulated through the ice banks. Since the chiller must produce a very low temperature solution its capacity is reduced by approximately 35 percent as compared to its nominal, or rated, capacity (which is based on a 45°F chilled-water set temperature). The chiller operates in this ice-making mode throughout the night until 8:00 a.m. when its is reset to produce a 53°F brine solution (actually the set temperature is allowed to float, but the temperature

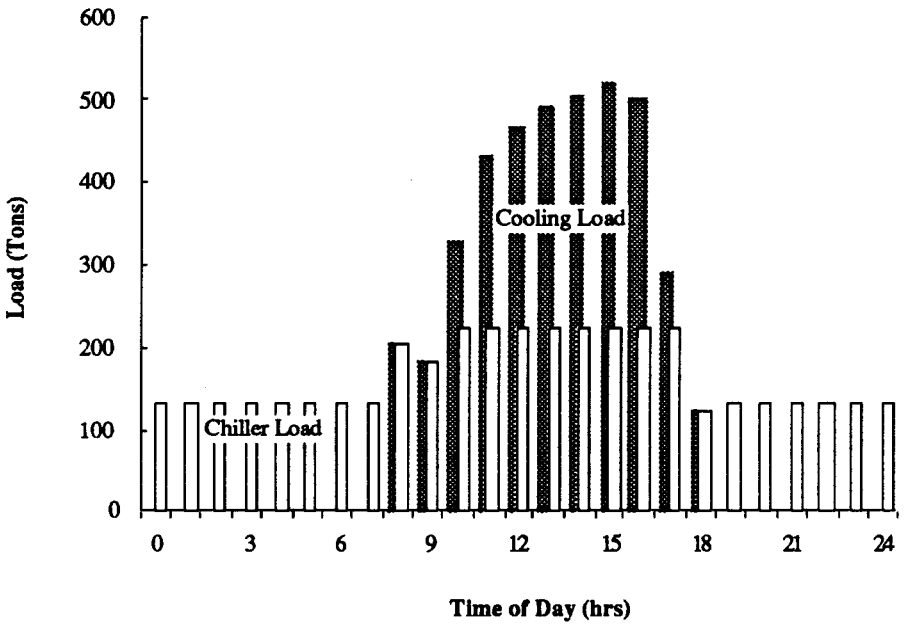

Figure 1.18 Partial-storage-system hourly load profile on the design day.

typically averages approximately 53°F). Since the chiller now produces a relatively high temperature solution, its capacity is enhanced by approximately 10 percent relative to its nominal capacity. This mode is called the *direct cooling mode* since the chiller operates to meet the cooling load directly with chilled water, or without first producing ice. (The capacity reductions and enhancements given are typical of reciprocating compressors; however, they are not greatly in error for other forms of compression.)

From 8:00 a.m. to 6:00 p.m. the chiller operates to meet as much of the cooling load as it possibly can; the remainder of the load which is greater than the chiller's capacity is met by storage. At 8:00 and 9:00 a.m. and at 6:00 p.m. the chiller does not operate at its maximum capacity. One might postulate that the excess capacity during

these hours be could used to make ice. However, since the capacity of the chiller is significantly reduced during ice-making conditions, the only available hour for which this is possible is 6:00 p.m. and even in this case the amount of cooling that could be stored is very small and the energy penalties are great. Hence, in general, it is very inefficient to operate the refrigeration plant in the ice making mode when any substantial cooling load exists which could be met by operating the plant in the direct mode.

The important facts to be noted from Figure 1.18 are that the required chiller capacity is 206 nominal tons and the required amount of storage is 1736 ton hours (which is simply the difference between the cooling load and the chiller load over the period during which the cooling load exists).

The Full Ice-Storage System The second option investigated is the full storage system. Figure 1.19 shows the overall building cooling load together with the load on the refrigeration plant on the design day. This system operates under the fundamental full storage strategy discussed in Section 1.2.4.

Like the partial storage system, the charging cycle begins a 7:00 p.m. where the chiller is set to produce 25°F brine, and the chiller operates in the ice-making mode throughout the night. Unlike the partial storage system, the refrigeration plant of the full storage system is shut down at 7:00 a.m.—just prior to the beginning of the morning pull-down period. And it remains off for the duration of the cooling-load period.

The required chiller capacity is 481 nominal tons and the required storage capacity is 4061 ton hours (Figure 1.19).

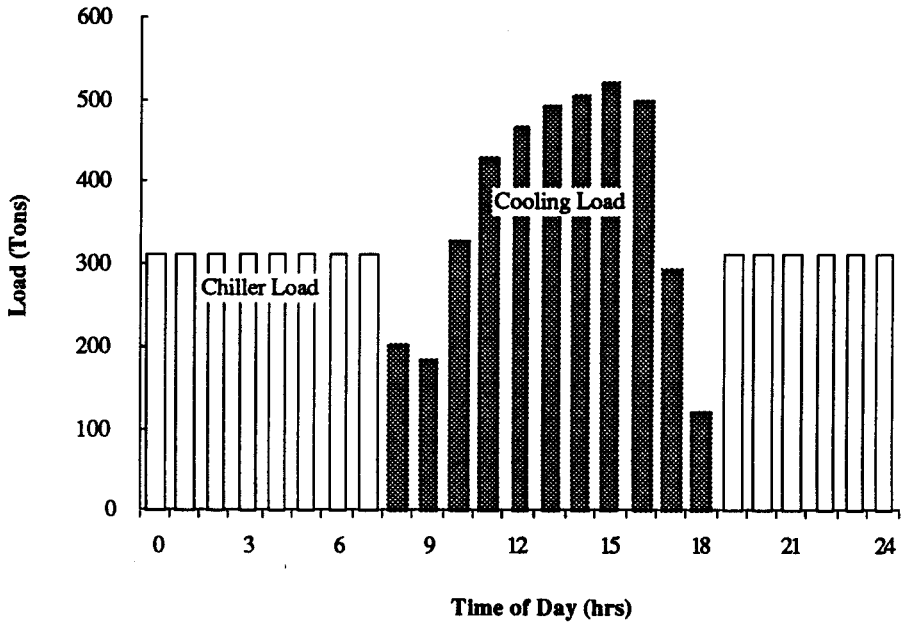

Figure 1.19 Full-storage-system hourly load profile on the design day.

The Demand-Limited Ice-Storage System The third option investigated is the demand-limited storage system. Figure 1.20 shows the overall building cooling load together with the load on the refrigeration plant on the design day. This system operates under the fundamental demand-limited storage strategy discussed in Section 1.2.4.

The charging cycle is similar to both of the aforementioned systems, but the discharging cycle is not. At 8:00 a.m. the chiller operates to meet the load directly. By 9:00 a.m. the noncooling load (shown in Figures 1.13 through 1.17) has become large enough such that it is necessary to begin demand limiting the operation of the chiller which is reflected in the cooling load profile of Figure 1.20 where it is observed that a

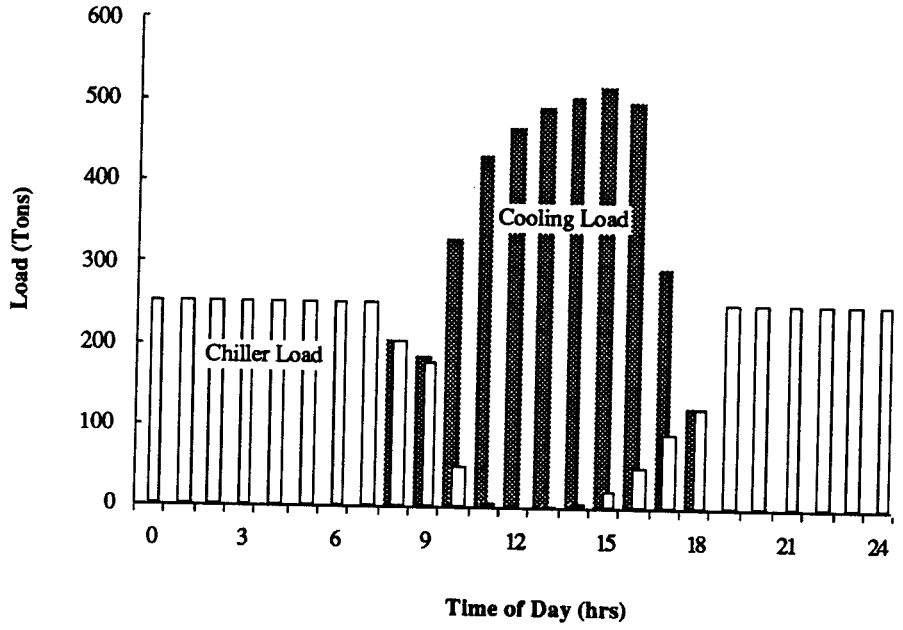

Figure 1.20 Demand-limited-storage-system hourly load profile on the design day.

very small portion of the overall cooling load is met by storage. From 10:00 a.m. to 5:00 p.m. the cooling load is primarily met by storage.

In practice, operating the chiller below 20 percent of is nominal capacity is very inefficient—since the chiller is typically cycled or operated using a hot-gas bypass (in which hot refrigerant vapors from the discharge port of the compressor bypass the condenser and are reissued into the evaporator) to stabilize the compressor operation—and can lead to operating problems, such as surging with centrifugal compressors and hot valves with reciprocating compressors; therefore, in practice the chiller would be shut down from 10:00 a.m. to 4:00 p.m., and to account for this, the system design would be slightly altered.

The required chiller capacity for this system is 392 nominal tons and the required storage capacity is 3308 ton hours (Figure 1.20).

The Modified Demand-Limited Ice-Storage System The fourth option investigated is the modified demand-limited storage system. Figure 1.21 shows the overall building cooling load together with the load on the refrigeration plant on the design day. This system operates under the fundamental modified demand-limited storage strategy discussed in Section 1.2.4.

Its operation is identical to that of the demand-limited storage system except that the chiller is allowed to operate unrestrictedly during the off-peak period. Thus, this system is capable of meeting the entire cooling load directly at 9:00 and 10:00 a.m.

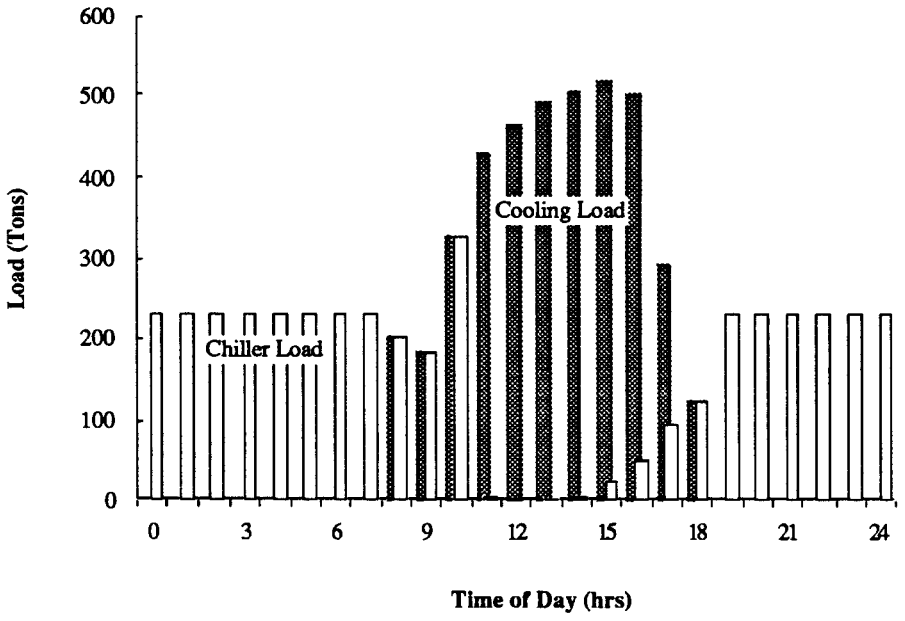

Figure 1.21 Modified demand-limited-storage-system hourly load profile on the design day.

The required chiller capacity for this system is 358 nominal tons and the required storage capacity is 3023 ton hours (Figure 1.20).

1.3.2 Comparative Numerical Summary

Table 1.2 summarizes the important results obtained from the analysis of the four storage systems previously discussed in Sections 1.2.3 and 1.2.5. The results presented in the table are based on the design-day hourly power-consumption profiles of Figures 1.13 through 1.17 and the design-day hourly cooling load profiles of Figures 1.18 through 1.21. All systems are thus compared based on the same design-day cooling load requirements. The energy consumption and maximum demand for the design day are based on a constant overall system coefficient of performance of 3.5 (which corresponds approximately to 1 kW/ton) for all of the systems considered (that is, the effect of performance degradation during ice making conditions is not included; it effects are addressed in the following section on economics).

Table 1.2 also gives the important results of this analysis on a percentage basis to facilitate comparisons. From a first cost standpoint, the partial storage system with a required refrigeration capacity which is only 40 percent of the conventional system's capacity and a required storage capacity which is only 43 percent of the full storage system's capacity maintains a clear advantage over the other systems. On the other hand, from an operational cost standpoint, the full storage system with a peak demand which is only 51 percent of the conventional system's peak demand and an on-peak energy-use of only 53 percent of the conventional system's on-peak energy-use based on the design day maintains a clear advantage over the other systems. But more importantly, which system is best overall?

	Conventional System	Partial Storage System	Full Storage System	Demand Limited Storage System	Modified Demand Limited Storage System
Nominal Chiller Capacity (Tons)	521	**206**	481	392	358
Required Storage Capacity (Ton hrs)	0	**1736**	4061	3308	3023
Maximum On-Peak Demand (KW)	1020	747	**521**	**521**	**521**
On-Peak Energy Use (KW hr)	7138	5506	**3798**	4115	4115
Maximum Off-Peak Demand (KW)	801	696	526	**521**	801
On-peak period is from 11:00 a.m. to 6:00 p.m.; off-peak is from 6:00 p.m. to 11:00 a.m.; no shoulder periods.					
Important results on a percenteage basis					
Percent of Conventional Chiller Capacity	100	**40**	92	75	69
Percent of Full-Storage Storage Capacity	0	**43**	100	81	74
Percent of Conventional On-Peak Demand	100	73	**51**	**51**	**51**
Percent Conventional On-Peak Energy Use	100	77	**53**	58	58

Table 1.2 Comparison of the fundamental storage strategies.

1.3.3 Basic Economic Analyses

In the previous sections, many important economic figures of merit were generated by analyzing the four fundamental storage systems and their operating strategies. With these economic figures of merit (summarized in Table 1.2), local utility rate structures, and equipment prices, the most economical fundamental storage strategy, under which the system will ultimately be designed, can be straightforwardly determined.

Simple Economic Analysis To help answer the question which of the four ice-storage systems is the best overall, several cases of interest were studied using the economic figures given in the problem statement of Section 1.2.5. It was also assumed that the system studied operated an average of 20 days per month for 5 months of the cooling season. The design day load profile was used for all days of operation, which yields the maximum amount of savings obtainable over a specified time period by employing a cool-storage system rather than a conventional system. Hence, this analysis favors those storage strategies with large operational savings. Lastly, the effects of load profile variation over the days and months of the cooling season is a subject to be addressed in subsequent chapters.

From the owners perspective, a very important economic parameter is the *simple payback* period (the number of years required for the operational savings of an alternative system to accrue to a value equal to the incremental first cost between the *alternative* system and the system it is compared to; the time value of money is not included when evaluating this parameter); typically, a simple payback between 2 and 4 years is attractive to most owners as long as the reliability of the alternative system is

approximately the same for all systems involved. The cost of the chiller and its associated equipment and the cost of storage were assumed to be $550/ton and $60/ton-hr respectively (which are typical 1989 values for centrifugal chillers and constrained-area ice banks) [16, 11].

Regarding the air-side equipment, ice storage systems typically require the selection of a cooling coil with a greater number of rows than the cooling coil of a conventional chilled-water system to effect the same heat transfer under the same conditions since the transport properties of brine are not as efficacious as those of water. On the other hand, ice-storage systems enable the air-side system to be designed using low temperature brine which can compensate for the brine's poor transport properties.

Referring to Tables 1.3 and 1.4, the first case of interest is the called the ideal comparison since it is the case most favorable to the alternative systems. It is based on identical system coefficients of performance of 3.5 for all of the systems investigated, including the conventional system, under all operating conditions—which is indeed not a good assumption; however, it serves as an indicator of the maximum possible performance attainable by any of the storage systems.

A more realistic case is listed next. It accounts for the thermal performance degradation encountered by the refrigeration plant when it operates under ice-making conditions by assuming a 25 percent reduction in the overall system coefficient of performance. Tables 1.3 and 1.4 demonstrate that the full storage system is most adversely affected by this reduction in the coefficient of performance since it operates continuously in the ice-making mode and, conversely, the partial storage system is least affected since it operates in the direct mode for a significant amount of time.

The ideal storage capacity, or nominal storage capacity, is usually insufficient to reliably meet the peak cooling load because of constraints on the storage system discharge rate (the tank outlet temperature rises significantly above the freezing point of the storage medium near the end of the discharging period, Section 1.2.2) or because of problems involved in achieving the maximum level of charge caused by the significant thermal penalty encountered near the end of charging with the constrained-area storage system. Therefore, the actual storage capacity required is typically 25 percent greater than the nominal storage capacity. The first cost of all of the storage systems are greatly affected by this necessary increase in storage capacity (Table 1.4). Again, the partial storage system is least affected since it requires the smallest amount of storage and, conversely, the full-storage is most affected.

The cost of a chiller and its associated equipment strongly influence the simple payback period of a partial storage system, but does not, however, strongly influence the payback period of a full storage system. This is because the partial storage system derives most of its savings benefit from the reduction in chiller capacity, whereas the full storage system does not—it relies on large operational savings. Although it is difficult to see this from Table 1.3, it may be inferred by comparing the simple payback periods of the full- and modified demand-limited storage systems.

The last case of interest involves a utility inducement which is highly advantageous to the modified demand-limited storage system as previously discussed in Section 1.2.4. Even with a very moderate utility incentive of $150 per reduced on-peak kW, the modified demand-limited storage system with a simple payback period of 2.4 years becomes economically attractive (Table 1.3). The ultimate choice between the partial storage system and the modified demand-limited storage system entails a more detailed

economic analysis which includes the time value of money, such as a life-cycle savings analysis.

Life Cycle Savings Analysis A life-cycle savings analysis of the last case illustrated in Tables 1.3 and 1.4 was performed where the objective was to determine whether the partial storage system or the modified demand-limited storage system should be selected based on an *economic life* of N years and a *market discount rate* of r percent. The other alternatives were screened-out since they both have a higher first cost and a lower operational savings than the modified demand-limited storage system. Furthermore, based on design experience, the economic life of ice-storage systems was assumed to be approximately 20 years [15].

In the life cycle savings analysis, the yearly savings over N years (the conventional system's yearly electric bill minus the alternative's bill) are each discounted to their *present worth* and then summed; the *incremental cost* of the alternative investment (the first cost of the conventional system minus the first cost of the alternative) is then subtracted from this sum; the result is the net present worth of the savings obtained by selecting the alternative investment, or the *life cycle savings* (which can be positive, indicating savings, or negative, indicating loss).

The savings obtained in year n is discounted to its present worth by multiplying it by the *discount factor* (or more precisely, the single-payment present-worth factor): $1/(1+r)^n$. The analysis is performed in real dollars; thus, the yearly savings are assumed to increase at the rate of inflation, and the discount rate represents the real cost of money exclusive of all inflationary effects (or alternatively an inflation rate i could

be assumed and inflationary effects could be incorporated into the new market discount rate r' in which case the discount factor becomes $(1+i)^n/(1+r')^n$ where the relationship between r and r' is $r' = r + f + rf$; the results, in either case, are exactly the same).

This method was used to determine the net present value of each alternative for two cases. The first case assumes a low value of the discount rate: 5 percent, whereas the second case assumes a high value: 15 percent. For a discount rate of 5 percent the clear choice is the demand-limited storage system, since the operational savings associated with this system are substantially greater than for the partial storage system (Table 1.4). Because the discount factor is relatively small, the benefits of operational savings are realized even as the system nears the end of its economic life. On the other hand, for a discount rate of 15 percent the clear choice is the partial storage system, since the first cost of this system is substantially less than the full storage system. Because the discount factor is now relatively large, the benefits of operational savings are not as significant as the benefits of first cost savings. The numbers which evince these assertions are these: for case one at a market discount rate of 5 percent, the modified demand-limited storage system saves 120 percent more than the partial storage system; for case two at a discount rate of 15 percent, the partial storage system saves 128 percent more than the modified demand-limited storage system.

The overall savings is significantly better with either alternative at lower discount rates; for example, the partial storage system saves 117 percent and 70 percent of the first cost of the conventional system for the 5 and 15 percent market discount rates respectively.

1.4 CHAPTER SUMMARY

The purposes of this chapter were to introduce the concept of comfort cooling using cool-storage, to demonstrate that many American utilities are eager to lend support to the installation and operation of cool-storage strategies, to give the reader valuable insight into the physical and operational characteristics of cool-storage systems, to show the common strategies employed in controlling these systems on the design day (variations of which are used for non-design days), to demonstrate the operational characteristics of a typical ice storage system used for air conditioning while operating under the four fundamental storage strategies on the design day, and to show how one of the four fundamental cool-storage systems is selected based on the building's cooling and noncooling loads, the utility's rate structure and inducements, the equipment's first cost, the system's economic life, and the market discount rate. In short, this chapter provides a firm foundation upon which more rigorous material of future chapters may be built.

The conclusion of this chapter is that for a typical commercial comfort cooling application in a moderately sized building, an ice-storage system will generally be selected, and it will be designed to operate under either the partial storage strategy or the modified demand-limited storage strategy on the design day. Therefore, there is a need to conduct a detailed analysis of the operating characteristics of these ice-storage systems to determine if in fact the results of a simplified analysis, such as the one conducted in this chapter, actually lead to the correct conclusions about the benefits of cool-storage systems.

The work documented in this thesis concentrates specifically on the detailed synthesis, modeling, and analysis of a partial ice-storage air-conditioning system. The

synthesis aspect of this work entails the design of the ice-storage system based on specified design day conditions and a typical commercial-office-building design-day load profile; the design procedure is rigorous: manufacturer's data is used to size and iteratively balance every component in the system. Additionally, for comparative purposes, a conventional system is also designed to meet the same design day criteria.

The modeling portion of this work involves the mathematical formulation of equations which accurately describe the operation of the components within the designed system; the models are modular in nature and, as such, they may be linked together to form a set of independent equations which may be solved numerically.

The analysis part of this work involves the determination of the actual operating characteristics of the partial ice-storage system and also the conventional system under a variety of loads and ambient conditions. These characteristics are then used to determine the control strategies that lead to the most thermally efficient operation of these systems based on the cooling load and ambient conditions. For the conventional system, this is the optimal control strategy; but, for the partial storage system, the thermal and economic optima do not necessarily coincide because of variable utility rate structures. Accordingly, control strategies of the partial storage system are modified to account for this. With these control strategies, a fair comparison of the partial storage system and the conventional system can be conducted based on the requirement that they meet the same cooling load.

REFERENCES 1

1. Thevenot, R., *A History of Refrigeration Throughout the World,* International Institute of Refrigeration, Paris, France, 1979.

2. Ingles, M., *Father of Air Conditioning,* Country Life Press, Garden City, Michigan, 1952.

3. Woolrich, W. R., "The History of Refrigeration; 220 Years of Mechanical and Chemical Cold: 1748-1968," *ASHRAE Journal,* pp. 31-39, July 1969.

4. *Commercial Cool Storage: Reduced Cooling Costs with Off-Peak Electricity,* Electric Power Research Institute, Palo Alto, California.

5. *A Guide to Ice Storage System Design,* Baltimore Aircoil Company, Incorporated, Baltimore, Maryland, February 1985.

6. *Thermal Energy Storage Inducement Program for Commercial Space Cooling,* First Revision, San Diego Gas and Electric Company, San Diego, California, April 1984.

7. Wildin, M. W., and C. R. Truman, *Evaluation of Stratified Chilled-Water Storage Techniques,* Electric Power Research Institute, Palo Alto , California, EPRI EM-4352, December 1985.

8. Elliot, T. C., "Cool Storage: Special Report," *Power,* pp.9-15, January 1989.

9. *Strata-Therm: Stratified Chilled-Water Storage System,* CBI Industries, Incorporated, Oak Brook, Illinois.

10. Stamm, R. H., "Thermal Storage Systems," *Heat/Piping/Air Conditioning,* pp. 133-137, 144-151, January 1985.

11. *An Introduction to Ice Bank Stored Cooling Systems for Commercial Air Conditioning Applications,* Calmac Manufacturing Corporation, Englewood, New Jersey, April 1988.

12. *Thermal Storage Ice Harvesting for Air Conditioning and Process Cooling,* Turbo Refrigerating Company, Denton, Texas, 1986.

13. *Ice Harvesting Thermal Energy Storage for Commercial Air Conditioning and Process Cooling,* Henry Vogt Machine Company, Louisville, Kentucky.

14. *Vogt Tube-Ice Machines: The "Hole" Story About the Finest Ice Making Units Ever Made,* Henry Vogt Machine Company, Louisville, Kentucky.

15. Electric Power Research Institute, *Commercial Cool Storage Design Guide,* Hemisphere Publishing Corporation, New York, 1987.

16. *ASHRAE Handbook, Systems and Applications Volume,* American Society of Heating, Refrigerating and Air Conditioning Engineers, Incorporated, Atlanta, Georgia, 1987.

17. *Resource: An Encyclopedia of Utility Industry Terms,* Pacific Gas and Electric Company, San Francisco, California, January 1985.

18. Blank, L. T., and A. J. Tarquin, *Engineering Economy,* Second Edition, McGraw-Hill Book Company, Incorporated, New York, 1983.

CHAPTER

TWO

COMPONENT MODELING AND CHARACTERISTICS

The purposes of this chapter are to describe each component used in the conventional and the partial ice-storage air-conditioning systems designed and analyzed in this work, to show the fundamental theory upon which the modeling of each of these components is based, and to demonstrate the important design and operating characteristics of each component. Before the components are discussed individually, the manner in which the various components are configured to form a system is addressed.

2.1 ICE-STORAGE SYSTEM CONFIGURATIONS

This brief section is designed to show the manner in which conventional air-conditioning systems and ice-storage air-conditioning systems are commonly configured.

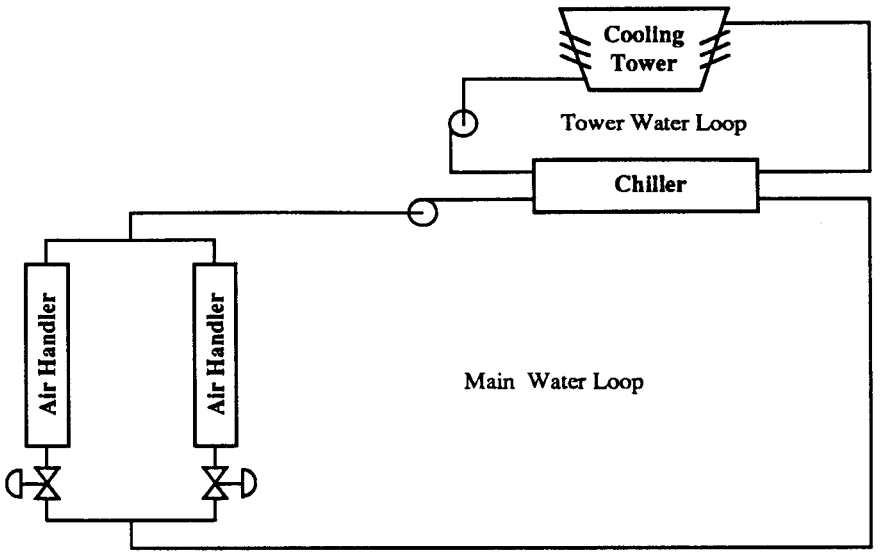

Figure 2.1 Conventional air-conditioning system.

The fundamental components of interest in a typical conventional air conditioning system are depicted schematically in Figure 2.1; they are the chiller, the air handling units, the cooling tower, the main water-loop pump, and the cooling tower water-loop pump. The air handling units are piped in parallel with each other and in series with the chiller. For systems with variables-speed main water-loop pumps, the flow of water through these units is typically modulated by *two-way valves* located upstream of each air handling unit, as shown in this figure. On the other hand, for systems with constant-speed main water-loop pumps, the flow of water through these units is typically modulated by *three-way bypass valves* in order to maintain a reasonable pressure difference across the air-handling units.

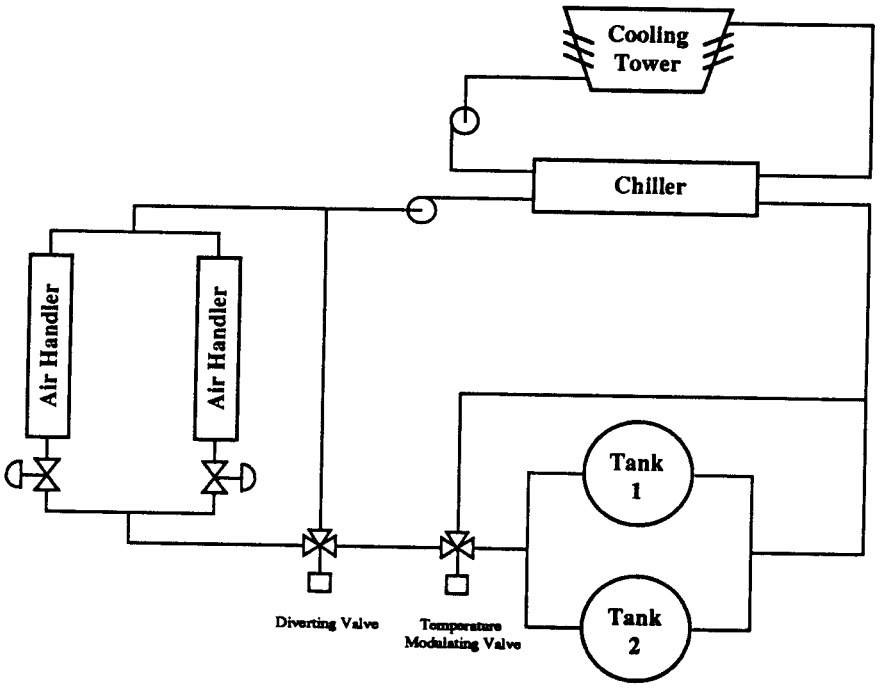

Figure 2.2 Ice-storage system configuration 1: series connection with chiller upstream.

An ice storage system which is a simple variation of the conventional system is shown in Figure 2.2. Storage tanks are piped in parallel with each other, piped in series with the chiller and the air handling units, and located such that the chiller is upstream; hence, the system is referred to as *a series connection with chiller upstream.* The flow of brine through these tanks is modulated by a three-way temperature-modulating valve located downstream of the tanks. For charging the tanks at night, a three-way diverting valve decouples the air handling units from the rest of the system.

A slight variation of this system is illustrated in Figure 2.3. This system employs the use of a *decoupler pipe* to establish two independent flow circuits: the *distribution circuit* which flows through the air handling units and the *main water-loop circuit*

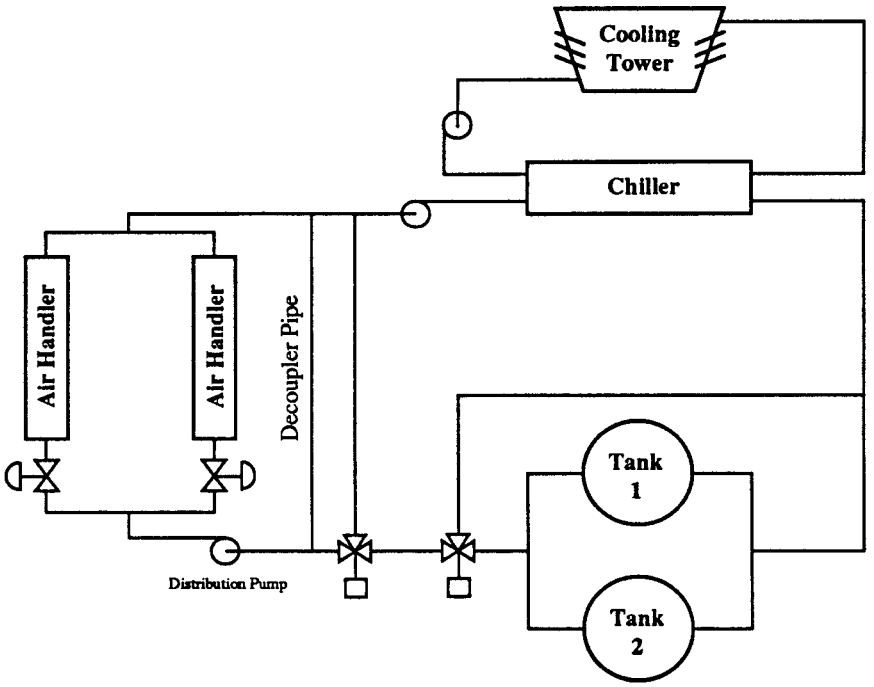

Figure 2.3 Ice-storage system configuration 2: series connection with chiller upstream, distribution pump, and decoupler pipe.

which flows through the chiller and the storage tanks. Two pumps are required. This configuration is particularly amenable to the use of variable-speed drives to control the flow of brine in the distribution circuit. Since manufacturer's typically prefer their chillers to operate at essentially constant flow, this configuration is preferred over that of Figure 2.2 for variable flow applications.

The disadvantage of both of the above ice-storage system configurations is that the transport fluid must be pumped through either the chiller or the chiller and the storage tanks; that is, it cannot pass through just the storage tanks. If the system is operated for a significant length of time using only the storage tanks to meet the load, substantial

pumping power consumption can be saved if the chiller is bypassed because the head loss through evaporator of the chiller is usually relatively large.

The ice-storage system shown in Figure 2.4 circumvents this problem. The chiller, storage tanks, and air handling units are connected in parallel; and a decoupler pipe, two pumps, and a number of two-way valves establish four independent flow circuits: one charging circuit and three discharging circuits. The charging circuit comprises the

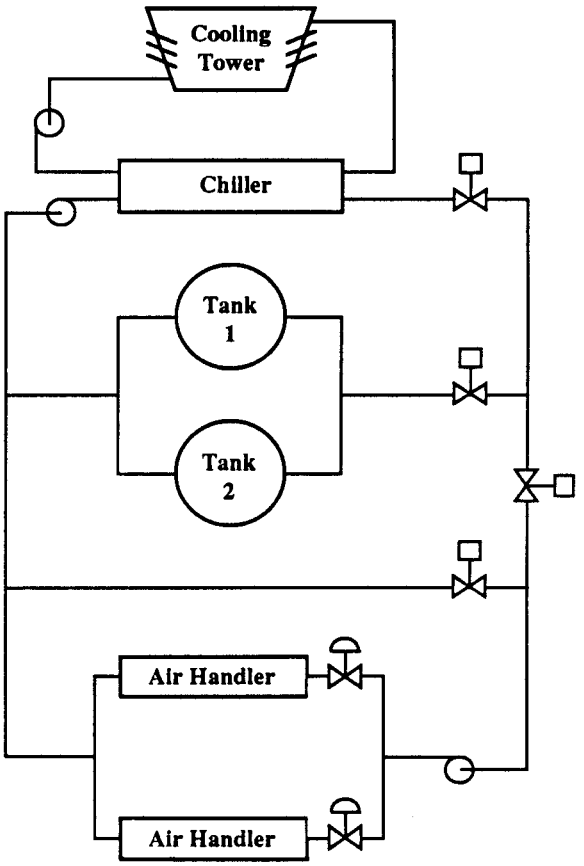

Figure 2.4 Ice-storage system configuration 3: parallel connection with distribution pump and decoupler pipe.

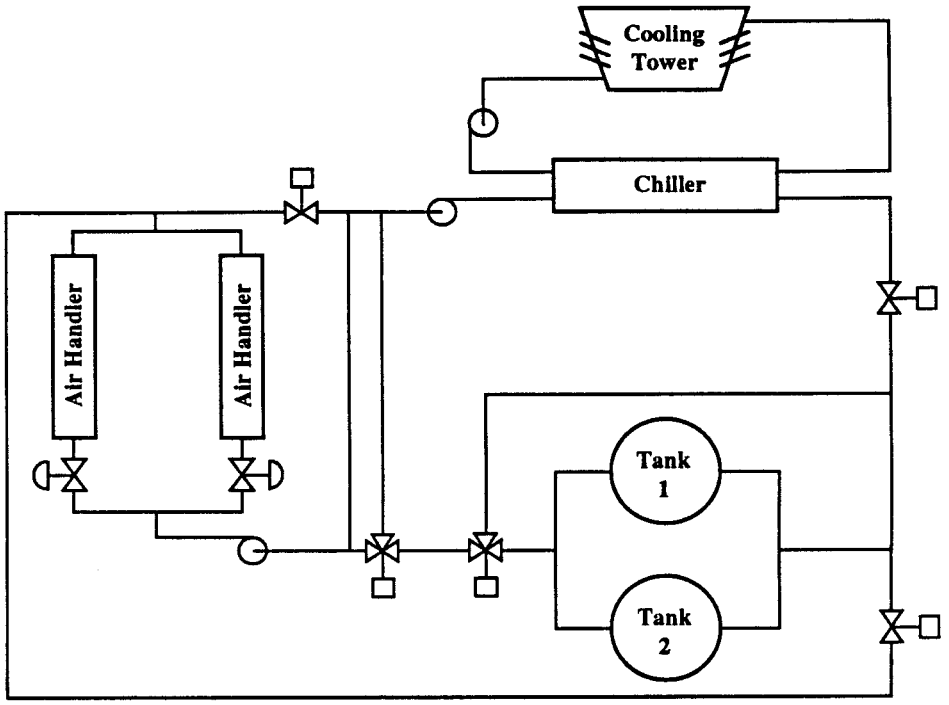

Figure 2.5 Ice-storage system configuration 4: independent series connection with chiller upstream, distribution pump, and decoupler pipes.

chiller and the storage tanks. The three discharging circuits are 1) a circuit comprising the chiller and the air handling units only, 2) a circuit comprising the storage tanks and the air handling units only, and 3) a circuit comprising the parallel connection of the chiller and the storage tanks piped in series with the air handling units. An additional advantage of this system configuration is that the storage tanks receive the benefit of operating at a higher inlet brine temperature (air-handler return temperature) which augments the rate at which these tanks can be discharged. On the other hand, a disadvantage is that the controls and piping arrangements are generally more complex than for the systems which have components connected in series.

Lastly, a modified version of the series connection with chiller upstream, distribution pump, and decoupler pipe (Figure 2.3) is shown in Figure 2.5. The modified system employs the use of a chiller bypass circuit which allows the storage tanks to supply cooling to the load without the aid of the chiller.

2.2 ICE-STORAGE SYSTEM COMPONENTS: OPERATION, THEORY AND CHARACTERISTICS

In this section each of the components used to model the performance of the partial ice-storage air-conditioning system is described; however, the description is general and may be applied to any air conditioning system. First, a physical description of each component and its manner of operation is given. Then the fundamental mathematical equations which govern the operation of each component are either summarized, for components developed outside this work, or developed in detail for all components developed as part of this work. Lastly, the important design and operational characteristics of each component are shown graphically. They serve as a reference for future discussions concerning design and control issues, and they also provide a clear understanding of the operational nature of each device.

2.2.1 Induced Draft, Crossflow Cooling Tower

By definition, a cooling tower is a device that transfers energy directly from a liquid to a gas by means of simultaneous heat and mass transfer. With regard to an air conditioning application, the primary purpose of the cooling tower is to reject the heat evolved in the air conditioning process to the surrounding atmosphere. This heat

comprises the cooling load of the building, the fan load, the ventilation load, and the heat evolved from the vapor compression process within the refrigeration plant.

Cooling Tower Operation Figures 2.6 and 2.7 show the outside and the inside of a induced draft, crossflow cooling tower along with the associated flow streams. The water stream is pumped from the outlet of the condenser to the *hot-water distribution basin* located on the top of the tower. Located within this basin are a series of nozzles which uniformly distribute the water stream over the packing material,

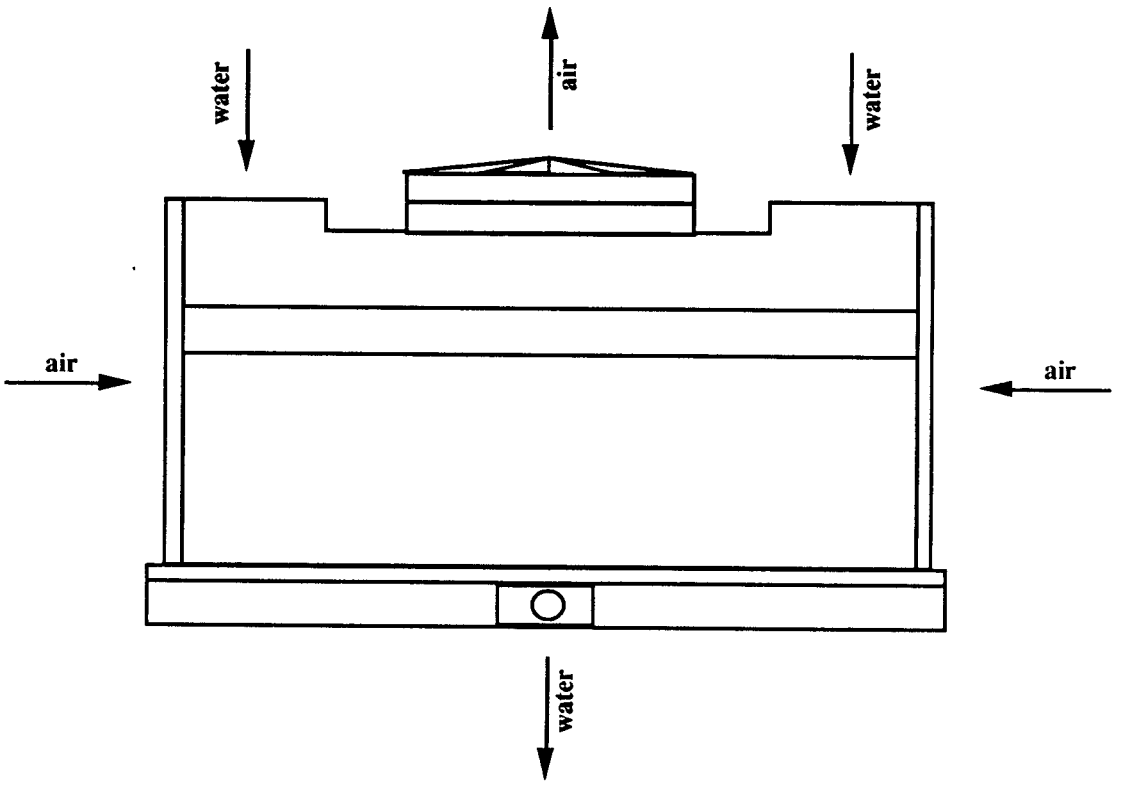

Figure 2.6 Cooling tower: outer view.

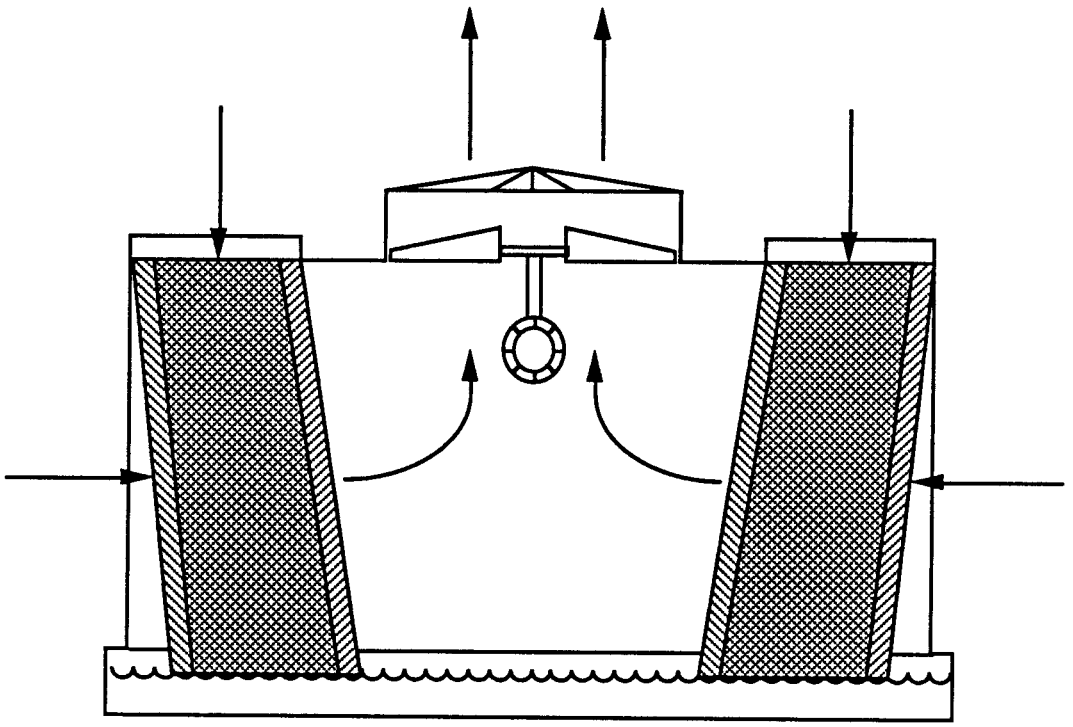

Figure 2.7 Cooling tower: inner view.

or *fill sheets*, located below. The water then cascades downward in the form of a thin film over the myriad of labyrinthine fill sheets, whose primary function is to enhance the surface area available for simultaneous heat and mass transfer between the air stream and water film. As the water continues to flow through the fill sheets, it *approaches* the wet-bulb temperature of the entering air stream. Finally, the water exits the fill sheets and is collected in the *cold-water basin,* or sump, located at the bottom of the cooling tower. The cold-water basin acts as a reservoir for chilled water used to supply the condenser of the refrigeration plant.

Meanwhile on the air side, the low pressure region within the tower created by the tower fan *induces* a flow of ambient air through a series of *louvers* which constitute the side of the tower. These louvers direct the air stream over the fill sheets where it intimately contacts the film of falling water in a perpendicular, or *crossflow*, orientation. After passing through the fill sheets, the air is drawn upward through the fan blades an exits the tower.

The Cooling Process Figure 2.8 shows a drop of liquid falling parallel to an air stream. The temperature of the water stream (droplet) and the air stream are T_L and T_G, respectively. Separating the two streams is the *phase interface*, the temperature of which is T_i. Energy is transferred across this interface from the adjacent gas-phase region (air) and the adjacent liquid-phase region (water).

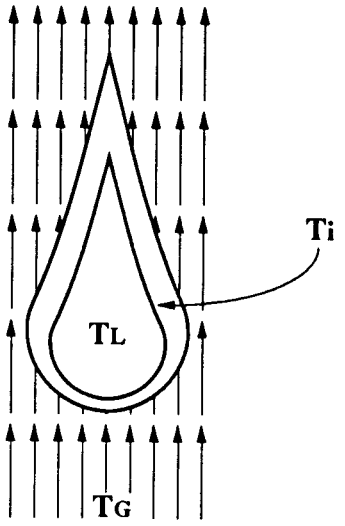

Figure 2.8 Gas-liquid interface between a falling water droplet and a rising stream of gas.

Most of the energy transferred from the phase interface to the air stream is a result of the diffusion of water vapor from the relatively highly concentrated region of the phase interface to the relatively sparsely concentrated region of the air stream. The water vapor, which acts as the primary mass-transfer agent, diffuses from the phase interface to the air stream and in doing so removes an amount of energy from the water film which is approximately equal to the product of the latent heat of vaporization at the temperature of the liquid phase and the mass flow rate of the vapor. Consequently, the air stream becomes laden with moisture as it progresses across the tower and usually reaches a nearly saturated condition as it exits the fill sheets. The remainder of the energy transferred between the air stream and the phase interface is in the form of heat which diffuses in accordance with the temperature gradient between these two phases.

Cooling Tower Definitions The difference between the inlet and the outlet water temperatures of the cooling tower is called the *range* of the cooling tower. The difference between the cooling-tower water-outlet temperature and the wet-bulb temperature of the entering air stream is called the *approach* of the cooling tower. The value of the wet-bulb temperature as it enters the louvers of the cooling tower is called the *entering wet-bulb temperature*, which may be significantly different than the ambient wet-bulb temperature because of the effects of *recirculation* (a condition in which a portion of air discharged from the tower outlet returns to the tower inlet primarily because of prevailing winds). *Make-up water* is the amount of water that must be added to the circulating system to compensate for the water lost primarily because of evaporation or *drift* (the entrainment of water droplet into the exhaust air stream). While operating under the *natural convection condition* the tower is capable of rejecting approximately 10 to 15 percent of its design load without the aid of a fan.

Fundamental Countercurrent Gas-Liquid Contact Equations Figure 2.9 shows the differential control-volume element that is used to derive the continuous countercurrent, adiabatic gas-liquid contact equations. The liquid and gas streams flow counter to each other and exchange both heat and matter across the phase interface. A temperature difference between the phase interface and the adjacent phases effects the heat transfer processes, whereas a concentration difference between the phase interface and the gas phase effects the mass transfer process. The gas is assumed to be essentially insoluble in the liquid phase; therefore, the matter transferred between the two phases is only the substance constituting the liquid phase, which diffuses in the form of a vapor and depending on the direction of mass transfer either vaporizes or

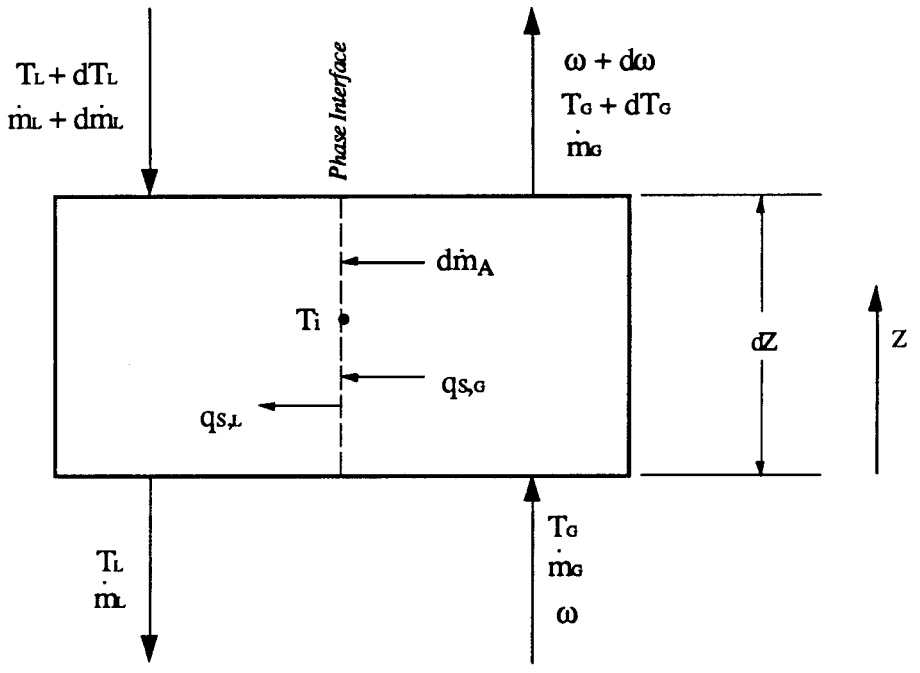

Figure 2.9 Differential cross section for a countercurrent adiabatic operation.

condenses. A rigorous derivation can be found in Reference 1. The resulting equations describing the simultaneous heat and mass transfer associated with these operations are summarized below.

From a mass balance on constituent A (the diffusing water vapor for a cooling-tower analysis) over the differential control volume,

$$d\dot{m}_L = \dot{m}_G \, d\omega \tag{2.1}$$

where $\dot{m}_L$ is the mass flow rate of liquid, $\dot{m}_G$ is the mass flow rate of pure, or dry, gas (which does not include the mass flow rate of the vapor which resides in the gas phase), and ω is the absolute humidity ratio (the quotient formed by dividing the mass of vapor contained within the gas phase by the mass of pure gas within that phase). Similarly, from a mass balance on constituent A over the gas cell,

$$d\dot{m}_A = - \dot{m}_G \, d\omega \tag{2.2}$$

where $\dot{m}_A$ is the mass transfer rate of constituent A across the phase interface. For steady-state turbulent diffusion, this transfer rate is given by

$$d\dot{m}_A = M_A \, F_G \ln\left(\frac{1 - P_{A,i}/P}{1 - P_{A,G}/P}\right) a_M \, dZ \tag{2.3}$$

where M_A is the molecular weight of constituent A; a_M is the surface area per unit *packed-height* available for mass transfer (which assumes a cooling tower with a uniform cross-sectional area); F_G is the gas phase mass-transfer coefficient; $P_{A,i}$ and $P_{A,G}$ are the partial pressure of constituent A at the phase interface and in the *bulk* gas

phase, respectively; P is the sum of the partial pressures of each of the two constituents A and B, or the total pressure; and Z is the packed-volume per unit cross-sectional area, or equivalently the coordinate along the height of the tower.

The sensible heat transferred from the gas to the phase interface is

$$\dot{q}_{s,G}\, a_H\, dZ = h_G^{'} (T_G - T_i)\, a_H\, dZ \tag{2.4}$$

where a_H = area per unit packed-height available for heat transfer,

$h_G^{'}$ = heat-transfer coefficient of the gas phase corrected to include the effects of mass transfer,

$$= \frac{N_A\, M_A\, C_{p,A}}{1 - e^{-N_A M_A C_{p,A} / h_G}}, \tag{2.5}$$

$C_{p,A}$ = specific heat of constituent A,

$N_A = \dfrac{d\dot{m}_A}{M_A\, a_M\, dZ}$

= absolute molecular flux of constituent A across the phase interface,

h_G = the convection coefficient of the gas phase in the absence of mass transfer effects,

T_G = temperature of the bulk gas phase,

T_i = temperature of the phase interface.

The corrected heat-transfer coefficient of the gas phase $h_G^{'}$ will be larger than the convention coefficient h_G if both mass and heat are transferred in the same direction, and $h_G^{'}$ will be smaller than h_G if mass and heat are transferred in opposite directions.

The sensible heat transferred to the liquid from the phase interface is

$$\dot{q}_{s,L}\, a_H\, dZ = h_L\, (T_i - T_L)\, a_H\, dZ \tag{2.6}$$

where h_L is the convection coefficient of the liquid phase and T_L is the liquid temperature.

An energy balance on the liquid cell of the differential element yields

$$\dot{m}_L\, C_{p,L}\, dT_L = (\dot{m}_G\, C_{p,L}\, d\omega - h_L\, a_H\, dZ)\, (T_i - T_L) \tag{2.7}$$

where $C_{p,L}$ is the specific heat of the liquid. Similarly, an energy balance on the gas cell of the differential element gives

$$\dot{m}_G\, C_S\, dT_G = h_G^{'}\, (T_i - T_G)\, a_H\, dZ \tag{2.8}$$

where Cs = specific heat of the gas-vapor mixture per unit mass of dry gas

$$= C_{p,G} + \omega\, C_{p,A}, \tag{2.9}$$

$C_{p,G}$ = specific heat of the pure gas.

Finally, an energy balance on the overall differential element results in

$$\dot{m}_L\, C_{p,L}\, dT_L = \dot{m}_G\, (C_S\, dT_G + [h_{fg,A} + C_{p,A}\, (T_G - T_o) - C_{p,L}\, (T_L - T_o)]\, d\omega) \tag{2.10}$$

where $h_{fg,A}$ is the latent heat of vaporization of constituent A at the reference temperature, T_o, where the enthalpy of constituent A in its liquid phase and at its equilibrium vapor pressure is zero.

The two mass balances (Equations 2.1 and 2.2), the mass-transfer rate equation (Equation 2.3), and the three energy balances (Equations 2.7, 2.8, 2.10) constitute a set of six fundamental equations which describe the process of simultaneous heat and mass transfer between a gas and a pure liquid which are in direct contact and are undergoing a continuous countercurrent adiabatic operation. The process which takes place within a cooling tower is well approximated by such an operation where the *gas* is air and the *liquid* is water. The thermodynamic and transport properties of these fluids aid in simplifying the fundamental equations.

Important Assumptions to Simplify the Fundamental Equations The following assumptions make the above equations more tractable.

1. The mass transfer is assumed to be small; in which case,

$$h_G' \approx h_G. \tag{2.11}$$

2. The product $h_L\, a_H$ is assumed to be very large; thus,

$$\dot{m}_G\, C_{p,L}\, d\omega << h_L\, a_H\, dZ. \tag{2.12}$$

3. The sensible heat of the transferred vapor is assumed to be negligible; that is,

$$\dot{m}_G\, [C_{p,A}\, (T_G - T_o) - C_{p,L}\, (T_L - T_o)]\, d\omega \approx 0. \tag{2.13}$$

4. The vapor pressure is assumed to be relatively low, or

$$M_A F_G \ln [(1 - P_{A,i}/P)/(1 - P_{A,G}/P)] \approx k_\omega (\omega - \omega_i) \tag{2.14}$$

where k_ω is the gas-phase mass-transfer coefficient and ω_i is the absolute humidity ratio at the phase interface.

5. The temperatures are assumed to be moderate compared to the reference temperature T_o and the specific heats are assumed to be constant for both the liquid and the gas phases; therefore, the differential of the enthalpy of the gas-vapor mixture dh_M is given by

$$\begin{aligned} dh_M &= d[C_S (T_G - T_o) + \omega h_{fg,A}] \\ &= C_S dT_G + (T_G - T_o) C_{p,A} d\omega + h_{fg,A} d\omega \\ &\approx C_S dT_G + h_{fg,A} d\omega. \end{aligned} \tag{2.15}$$

6. The packing surface is assumed to be fully wetted; thus, the surface area (per packed-volume) available for mass transfer is equal to that available for heat transfer, or

$$a_M = a_H. \tag{2.16}$$

7. The thermal diffusivity α and molecular diffusivity D, which govern the rate of heat transfer and mass transfer, respectively, are assumed to be approximately

equivalent; that is,

$$\begin{aligned} \text{Le} &= \frac{\alpha}{D_{AG}} \\ &\approx 1 \end{aligned} \tag{2.17}$$

where Le is the Lewis number and D_{AG} is the molecular diffusivity for a vapor A diffusing through a gas G. For cooling tower operations, assuming the Lewis number to be unity is appropriate since for turbulent flow past cylinders and single spheres [1]

$$h_G / k_\omega = C_S \, \text{Le}^{0.567} \tag{2.18}$$

and for an air water-vapor system h_G / k_ω has been measured to be approximately 950 J / kg-K [1] which is very close to the value of C_S for the mixture of air and its accompanying vapor (1024 J / kg-K at $\omega = .01$). Thus, under this assumption

$$C_S \approx h_G / k_\omega \tag{2.19}$$

8. Finally, the gas in the region of the phase interface is assumed to move very slowly, or be nearly stagnant, with respect to the liquid in this region; thus, the vapor residing in the region of the phase interface may be assumed to be saturated.

Simplified Set of Countercurrent Gas-Liquid Contact Equations Applying the above assumptions to the fundamental set of equations results in a set of five equations with five unknowns ($\dot{m}_L$, ω, h_M, T_L, T_i) which are now readily solvable.

The set of equations equations is divided into four groups:

Mass balance equation:

$$d\dot{m}_L = \dot{m}_G \, d\omega, \tag{2.20}$$

Mass-transfer rate equation:

$$\dot{m}_G \, d\omega = k_\omega \, (\omega_i - \omega) \, a_H \, dZ, \tag{2.21}$$

Heat-transfer rate equations:

$$\dot{m}_G \, dh_M = k_\omega \, (h_{M,i} - h_M) \, a_H \, dZ, \tag{2.22}$$

$$\dot{m}_G \, dh_M = h_L \, (T_L - T_i) \, a_H \, dZ, \tag{2.23}$$

Energy balance equation:

$$\dot{m}_L \, C_{p,L} \, dT_L = \dot{m}_G \, dh_M. \tag{2.24}$$

The mass balance, the three rate equations, and the energy balance constitute a set of five coupled differential equations which can be readily solved numerically if $\dot{m}_G$, k_ω, a_H, h_L, and $C_{p,L}$ are known; if ω_i and $h_{M,i}$ are known functions of the phase interface temperature T_i; and if the inlet air stream and water stream conditions are known.

The necessary intensive thermodynamic properties of the phase interface as a function of the phase interface temperature are

$$h_{M,i} = (C_{p,G} + \omega_i C_{p,A}) (T_i - T_o) + \omega_i h_{fg,A} \tag{2.25}$$

and

$$\omega_i = \frac{M_A P_A^{SAT}}{M_G (P - P_A^{SAT})} \tag{2.26}$$

where M_G is the molecular weight of the pure gas (dry air), and P_A^{SAT} is the partial pressure of constituent A (water vapor) at the temperature of the phase interface and in a saturated state (the saturation pressure of the water vapor at T_i). A correlation for P_A^{SAT} as a function of temperature may be found in Reference 2.

Two additional assumptions frequently made which greatly simplify the modeling of cooling towers are that the mass flow rate of water through the tower is approximately constant (the amount of water evaporated is small with respect to the water flow rate) and that the temperature of the phase interface is approximately that of the water. With these assumptions the number of equations necessary to model the cooling tower from an energy perspective is reduced to two; namely, the heat-transfer rate equation (Equation 2.22) and the energy balance equation (Equation 2.24). If necessary, the mass-transfer rate equation (Equation 2.21) may be numerically integrated to determine the absolute humidity distribution along the tower height, once the temperature distribution of the phase interface has been determined by solving the coupled heat-transfer rate equation and energy balance equations.

The Finite-Difference Model for a Crossflow Cooling Tower For a crossflow cooling tower, these two differential equations combined with the three algebraic equations which describe the intensive thermodynamic properties of the phase interface (Equations 2.25 and 2.26 and a correlation for P_A^{SAT}) constitute a set of five equations with five unknowns (h_M, $h_{M,i}$, T_L, ω_i, P_A^{SAT}). This set of equations is readily solved using a finite-difference scheme, as depicted in Figure 2.10.

Solution procedure for the finite-difference model The tower volume is discretized into a number of elements. The integration begins at the first element located at the top left section of the tower. With known inlet conditions to this first element, its outlet states are initially determined by integrating the two differential

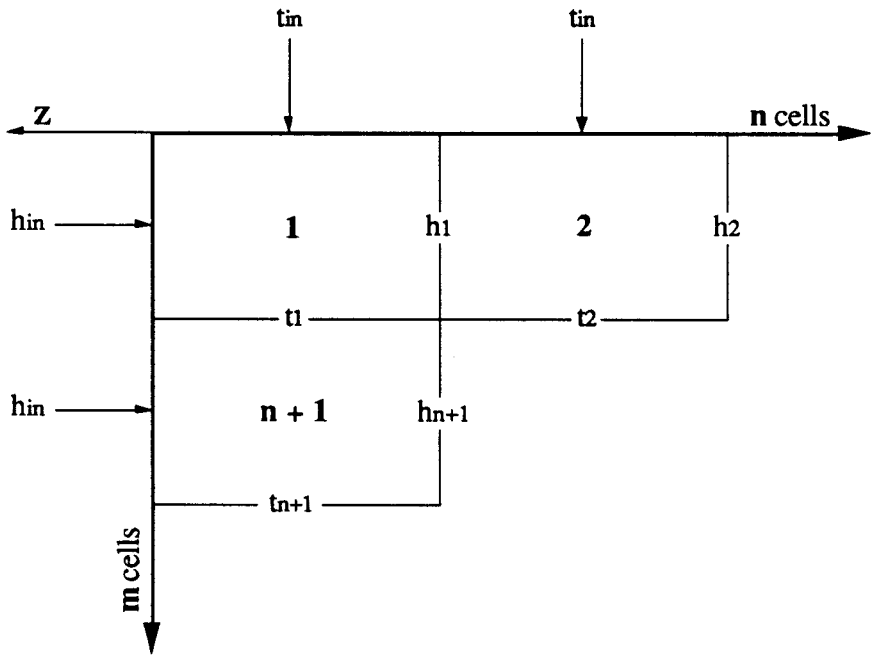

Figure 2.10 Finite-difference elements for a crossflow cooling tower.

equations using the known inlet conditions to solve the three algebraic equations for the properties of the phase interface. The inlet and outlet states are then averaged and used to compute a more accurate update of the properties of the phase interface. The iteration continues until satisfactory convergence has been attained with regard to the outlet conditions. These outlet conditions are then used as the inlet conditions for the adjacent elements, and the procedure is repeated for all elements of the cooling tower. Once this is complete, the outlet temperatures of the last row of elements are then averaged to determine the net outlet temperature of the water stream exiting the tower, and, similarly, the outlet enthalpies of the last column of elements are averaged to determine the net outlet enthalpy of the air stream exiting the tower.

This procedure was used to model the performance of the crossflow cooling tower shown in Figure 2.7. Since this tower is symmetrical, only the left half of the tower was analyzed. The packed-volume (fill sheets) was discretized into 30 elements. Manufacturer's performance data was then used to determine the product of the overall mass-transfer coefficient and the heat-transfer surface area per packed-volume, $k_\omega a_H$, for the cooling tower: the above solution procedure was conducted with a guessed value of $k_\omega a_H$, and the resulting water-outlet temperature predicted by the model was then be compared to the value given by the manufacturer's performance data; $k_\omega a_H$ was then updated accordingly and the procedure was repeated until agreement was achieved between the predicted value and the manufacturer's value. Since $k_\omega a_H$ is primarily a function of the mass flow rates of air and water through the cooling tower [1], a single value may be used to predict the tower's performance over a wide range of operating states if the mass flow rates are fixed.

Selected results from this procedure are compared with manufacturer's data in Table 2.1. The agreement is quite good. And is still good for a nine element model (3-by-3).

Also included in this table are the results for a one element model (1-by-1). The agreement is poor for this case; this is primarily caused by the nonlinear variation of the saturation enthalpy (the enthalpy of the gas-vapor mixture at the phase interface) with temperature, which in the one-element model is approximated as a straight line.

Within any particular element, the enthalpy of the air steam is a linear function of the water temperature as indicated by the energy balance equation (Equation 2.24); however, the enthalpy of the air-vapor mixture at the phase interface is a nonlinear function of temperature. The rate of heat transferred from one phase to the other within a particular element is directly proportional to the difference in these two enthalpies as

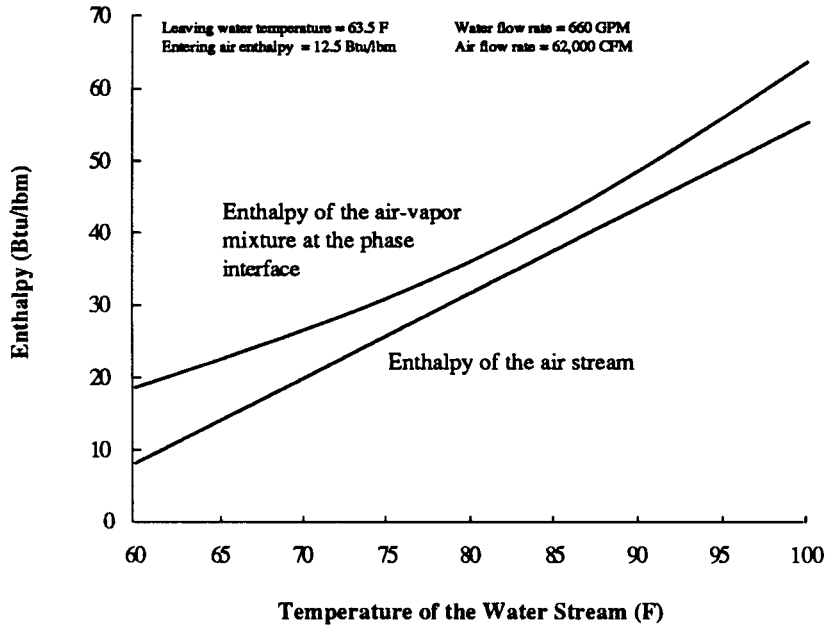

Figure 2.11 Operating diagram for a particular element within the crossflow cooling tower of Figure 2.17.

indicated by the heat-transfer rate equation (Equation 2.22); this difference is referred to as the *enthalpy driving force*. These two enthalpies are plotted for a single element in Figure 2.11.

Referring to this figure, if the temperature change of the liquid stream across a particular element is small, then using the average value of the driving force between the inlet and outlet states of the element is appropriate; conversely, if the temperature change is large, then an average value of the driving force will substantially over predict the actual value. This leads to predictions of the leaving water temperature that are consistently too low, as evidenced by the figures in Table 2.1.

Input Variables (F)		**Water Outlet Temperature (F)**			**Manufacturer's Data (F)**	
Entering Water Temperature	Wet-Bulb Temperature	Finite-Difference Model (5-by-6)	(1-by-1)	Manufacturer's Data	Approach	Range
73.5	50	63.5	62.5	63.5	13.5	10
88.7	75	80.5	79.7	80.7	5.7	8
92.6	65	77.3	75.5	77.6	12.6	15
66.6	55	61.7	61.2	61.6	6.6	5
Based on a tower water-flow rate of 660 GPM and a tower air-flow rate of 62,000 CFM.						

Table 2.1 Comparison of predicted values and manufacturer's values of the tower water-outlet temperature for the finite-difference model.

The cooling-tower model incorporated in the transient system simulation program, TRNSYS [3], used in this study is based on an effectiveness model [4, 5]. The important equations used in this model are given below.

The Effectiveness Model for a Crossflow Cooling Tower The *air-side effectiveness* is defined as the ratio of the actual energy transferred to the air stream divided by the maximum possible energy that could be transferred to the air stream, and it is given by

$$\varepsilon_a = \frac{h_{M,2} - h_{M,1}}{h_{M,i,2} - h_{M,1}} \tag{2.27}$$

where the subscript i designates the interface, and the subscripts 1 and 2 designate the air inlet and and air outlet conditions, respectively. The denominator represents the heat transfer per unit mass flow rate that could be achieved if the air stream left the tower fully saturated at the temperature of the entering water stream.

The *average saturation specific heat* at the phase interface is defined as

$$C'_{S,i} = \frac{h_{M,i,2} - h_{M,i,1}}{T_{L,1} - T_{L,2}} \tag{2.28}$$

where $h_{M,i,1}$ and $h_{M,i,2}$ are the enthalpies of the gas-vapor mixture at the phase interface at the air inlet and and outlet, respectively, and $T_{L,1}$ and $T_{L,2}$ are the temperatures of the water at its inlet and outlet, respectively. Additionally, the prime in the superscript position of $C'_{S,i}$ is used to distinguish the saturation specific heat from the specific heat of saturated air which is given by Equation 2.9 evaluated at the saturated condition of

the air stream; the saturation specific heat is greater than the specific heat of saturated air by the amount given by $[h_{fg,A} + C_{p,A} (T_i - T_o)]\, d\omega_i / dT_i$.

The *heat capacity rate* ratio is defined as

$$R = \frac{\dot{m}_G C'_{S,i}}{\dot{m}_L C_{p,L}}. \tag{2.29}$$

The ability of a cooling tower to effect simultaneous heat and mass transfer is measured by the *number of transfer units* Ntu, and it is equal to the number of times the mean enthalpy driving force Δh_{mean} divides into the overall change in the enthalpy of the air stream between its inlet and outlet states.

$$\text{Ntu} = \frac{(h_{M,2} - h_{M,1})}{\Delta h_{mean}} \tag{2.30}$$

where Δh_{mean} is found by integrating the enthalpy driving force between the inlet and outlet conditions. From the heat-transfer rate equation involving the enthalpy driving force (Equation 2.22), the number of transfer units is also given by

$$\text{Ntu} = \frac{k_\omega a_H H}{\dot{m}_G} \tag{2.31}$$

where H is the height of the fill sheets within the cooling tower.

In the TRNSYS model, the number of transfer units for a given cooling tower is assumed to be a function of only the ratio of mass flow rates through the tower and is

given by

$$\text{Ntu} = b\left(\frac{\dot{m}_L}{\dot{m}_G}\right)^a \tag{2.32}$$

where a and b are constants for a particular cooling tower, and they are determined from manufacturer's performance data using the method of least squares applied to the linear form of equation 2.30, which is obtained by taking the logarithm of both sides of that equation.

The air-side effectiveness of a cooling tower can be derived in a manner analogous to the derivation of the effectiveness of a heat exchanger. The steps are as follows: The differential form of the saturation specific heat, $C'_{s,i} = dh_{M,i} / dT_L$, is substituted into the energy balance equation (Equation 2.24). Next, $C'_{s,i}$ is assumed to be approximately constant at its average value between the inlet and outlet conditions, and the resulting energy balance equation is integrated analytically to obtain an expression for the enthalpy of the air steam, h_M, as a function of the enthalpy of the gas-vapor mixture at the phase interface, $h_{M,i}$. The resulting algebraic expression for h_M is then substituted into the remaining heat-transfer rate equation (Equation 2.22). The resulting first-order differential equation is then integrated over the entire height of the tower which results in a *log-mean enthalpy difference* that is directly analogous to the log-mean temperature difference used in heat exchanger theory: $\Delta h_{lm} = (\Delta h_2 - \Delta h_1) / \ln (\Delta h_2 / \Delta h_1)$ where Δh is the enthalpy driving force, $h_{M,i} - h_M$, and the subscripts 1 and 2 refer to the inlet and outlet conditions, respectively.

By performing appropriate algebraic manipulations on this expression and by noting that the log-mean enthalpy difference is in fact the mean enthalpy driving force

Δh_{mean} used in the definition of the number of transfer units (Equation 2.30), the effectiveness can be expressed as a function of the number of transfer units and the heat capacity rate ratio (such algebraic manipulations for a counterflow cooling tower are straightforward and can be found in their analogous form in many introductory heat transfer texts [6, 7], whereas for crossflow analogies, Reference 8 should be consulted). For a crossflow cooling tower, the result is

$$\varepsilon_a = \frac{1 - e^{-R(1-e^{-Nu})}}{R} . \tag{2.33}$$

An overall mass balance on the fill sheets of the tower allows the mass flow rate of water leaving the tower's fill sheets to be determined, which is expressed as

$$\dot{m}_{L,2} = \dot{m}_{L,1} - \dot{m}_G (\omega_2 - \omega_1) \tag{2.34}$$

where ω_1 and ω_2 are the absolute humidity ratios of the air stream at its inlet and outlet, respectively. A simple and reasonably accurate method of determining ω_2 is to assume that the air stream is fully saturated at the enthalpy of the air stream as it leaves the tower. On the other hand, the model incorporated in TRNSYS expresses the leaving humidity ratio as a function of the number of transfer units; these equations can be found in Reference 9.

The only unknown yet to be determined is the water temperature leaving the tower's fill sheets. The water outlet temperature is determined from an energy balance on the

fill sheets of the cooling tower; this yields

$$T_{L,2} = T_o + \frac{\dot{m}_{L,1}\, C_{p,L}\, (T_{L,1} - T_o) - \varepsilon_a\, \dot{m}_G\, (h_{M,i,2} - h_{M,1})}{\dot{m}_{L,2}\, C_{p,L}} \tag{2.35}$$

where $\dot{m}_{L,1}$ and $\dot{m}_{L,2}$ are the mass flow rates of the water stream at its inlet and outlet, respectively.

The advantage of the effectiveness model over the previously mentioned finite-difference method is that once the functional relationship between the number of transfer units and the ratio of mass flow rates has been ascertained, the procedure for predicting the performance of the cooling tower is straightforward.

Solution procedure for the effectiveness model A value for the leaving water temperature $T_{L,2}$ is guessed; the enthalpy of the air water-vapor mixture at the phase interface at the air inlet to the tower $h_{M,i,1}$ is calculated based on $T_{L,2}$; next, the saturation specific heat $C'_{S,i}$ and the heat capacity ratio R are computed; then, the number of transfer units Ntu are calculated based on the mass flow rate of water entering the tower—this is acceptable since the process is not highly sensitive to the value of Ntu; the air-side effectiveness ε_a is then computed and subsequently used to determine the enthalpy of the air stream leaving the tower $h_{M,2}$; this value of enthalpy is in turn used to determine $T_{G,2}$ which is then used to estimate the outlet absolute-humidity ratio ω_2; this value and the specified inlet humidity ratio are then used to compute the mass flow rate of water leaving the tower; finally, the temperature of the water stream leaving the tower $T_{L,2}$ is computed. The procedure is repeated using the updated values of $T_{L,2}$ until satisfactory convergence is achieved.

The procedure reveals the fundamental advantage of this method: it does not involve any numerical integration. This is highly advantageous when hourly simulations must be conducted over lengthy periods of time—that is, if it is sufficiently accurate.

Comparison of the Effectiveness and Finite-Difference Models for a Crossflow Cooling Tower Table 2.2 shows selected results over a variety of conditions which indicate that the effectiveness model is indeed quite accurate when the appropriate value of Ntu is ascertained. The third column of this table shows the number of transfer units determined for the finite-difference model by the procedure described previously; the fourth column shows the number of transfer units calculated from the effectiveness relationships using manufacturer's data under the conditions noted in columns 1, 2, and 5 of the table and assuming the water loss to be negligible.

Input Variables (F)		Number of Transfer Units		Water Outlet Temperature (F)		
Entering Water Temperature	Wet-Bulb Temperature	Finite-Difference Model (5-by-6)	Effectiveness Model	Manufacturer's Data	Effectiveness Model Ntu = 2.2	Ntu =3.4
73.5	50	2.2	3.4	63.5	64.1	63.5
88.7	75	2.2	2.8	80.7	81.0	80.6
92.6	65	2.2	3.2	77.6	78.3	77.5
66.6	55	2.2	2.6	61.6	61.8	61.4

Based on a tower water-flow rate of 660 GPM and a tower air-flow rate of 62,000 CFM.

Table 2.2 Comparison of predicted values and manufacturer's values of the tower water-outlet temperature for the effectiveness model.

For the effectiveness model, it is evident that the number of transfer units change considerably over the conditions listed, and that they are quite different (as much as 50 percent different) than those of the finite-difference model. Since both models are based on the same two governing equations (Equations 2.22 and 2.24) and only differ in their assumptions regarding the variation of saturation enthalpy with water temperature (the effectiveness model assuming a linear variation; the finite-difference model, a nonlinear variation), they should both determine approximately the same value of Ntu.

It should be pointed out here that with regard to determining the value of Ntu from manufacturer's performance data, an examination of the forgoing relationships indicates that the water loss which is accounted for in the effectiveness model (although it is assumed in the fundamental derivation of the effectiveness relationship—as in the finite-difference model—that the mass flow rate of liquid is constant) plays a role in determining the number of transfer units from manufacturer's performance data.

However, the performance data published by manufacturer's typically neglects water loss. Accordingly, when the effectiveness model is used to compute a value of Ntu based on this data and the forgoing relationships, frequently the logarithm of a negative argument halts the process. Since in manufacturer's performance data the inlet and outlet temperatures of water, the mass flow rate of water entering the tower, and the entering wet-bulb temperature of the air stream are specified, accounting for water loss (typically 1 percent) results in the air stream receiving significantly more energy than if the water loss was not accounted for (typically 4 percent; this 4-to-1 relationship is realized by the following relationship: $\dot{Q} / \dot{Q}_{const} = 1 + (\dot{m}_A / \dot{m}_L)\,(T_{L,2} - T_o) / R$ where $\dot{Q}$ and $\dot{Q}_{const}$ are the energies transferred to the air stream with and without water

accounted for, respectively, and R is the cooling-tower range). Because of this additional energy transfer and because the maximum possible energy transfer to the air stream is fixed by the manufacturer's performance data, the air-side effectiveness may exceed the thermodynamic limit, which can be determined by Equation 2.33 with Ntu taken as infinity. Thus, the manner in which manufacturer's performance data is correlated with the number of transfer units will depend on the nature of that data.

In short, for a cross-flow cooling tower, the effectiveness model is very accurate when it computes its own Ntu values; however, Ntu values supplied by the manufacturer, which are typically based on finite-difference methods, may not be suitable for use with the effectiveness model, as indicated in Table 2.2.

Crossflow Cooling Tower Characteristics This subsection presents several important operating characteristics of a particular induced draft, crossflow cooling tower. These characteristics will serve as a foundation for future discussions with regard to cooling tower selection and cooling tower control. The figures contained within this subsection are based on manufacturer's performance data [10].

In general, for a given cooling tower, its approach to the entering wet-bulb temperature is a moderately nonlinear function of applied fan power with diminishing returns as the fan power increases; Figure 2.12 indicates this trend at constant water flow rate, constant range, and various entering wet-bulb temperatures. A control strategy employing a fixed approach may result in high fan power consumption during periods of moderate weather; however, for a given entering wet-bulb temperature, these curves shift considerably with the load on the tower. This shift is indicated in Figure 2.13 which shows that the approach is strongly influenced by the total cooling load on the tower and also by the entering wet-bulb temperature.

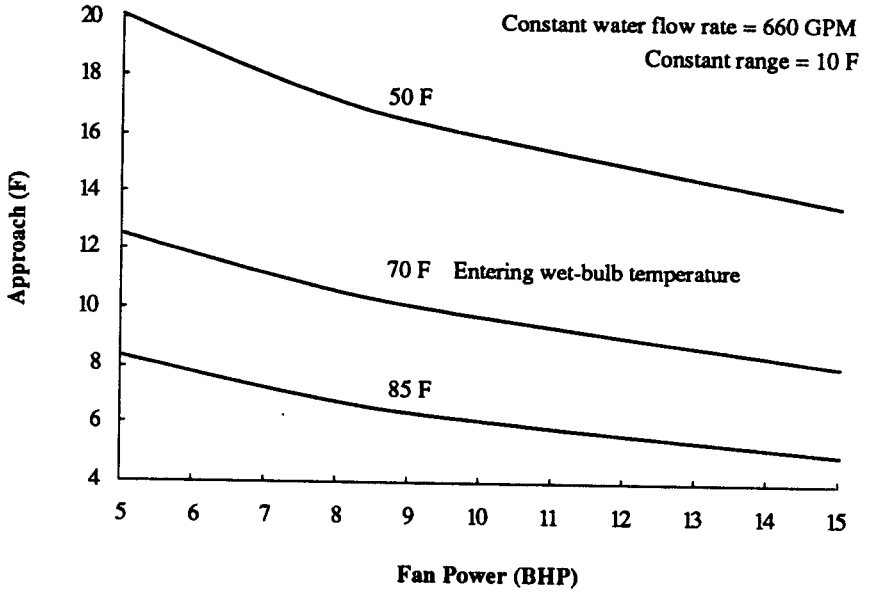

Figure 2.12 Variation in cooling-tower approach at constant water flow rate and constant range.

Tower operation under varying ambient conditions The most important point demonstrated by Figure 2.13 with respect to cool storage systems—particularly ice storage systems—is that under a fully loaded condition with a typical range of 10°F the temperature variation of the water leaving the cooling tower is some fraction, called the *damping coefficient,* of the variation in the ambient wet-bulb temperature. The damping coefficient is a function of the effectiveness of the cooling tower and approaches unity as the effectiveness approaches unity. For the cooling tower of Figure 2.13, the damping coefficient is approximately 0.75 for a range of 10°F and a mean ambient wet-bulb temperature of 74°F. In short, the cooling tower dampens the maximum thermal benefit achievable by operating the refrigeration plant during periods of lower ambient wet-bulb temperatures.

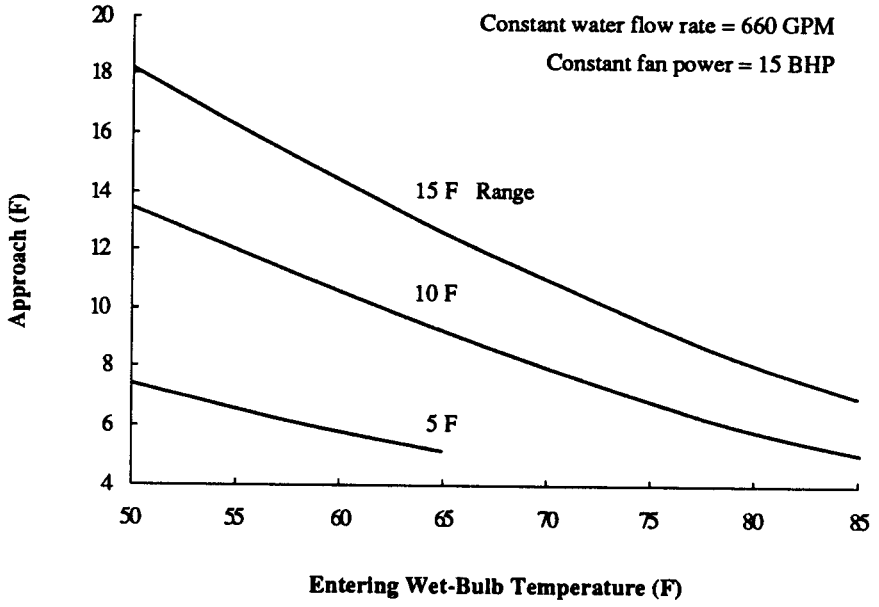

Figure 2.13 Variation in cooling-tower approach at constant water flow rate and constant fan power.

Tower fan control Cooling tower fans may be controlled to regulate the flow of air through the tower in response to changes in load or ambient conditions or both. The controlled variable is usually the temperature of the water leaving the cold-water basin of the cooling tower. Air flow control is achieved by one of four methods: fan cycling, two-speed fan motors, variable-speed drives, or automatic variable pitch fan blades [11]. Figure 2.14 demonstrates the progression of operating states for a cooling tower operating at full load under varying ambient conditions and controlled with a two-speed fan. The *switch point* occurs at a leaving water temperature of 80°F. Similar operating paths may be defined for each of the aforementioned control methods.

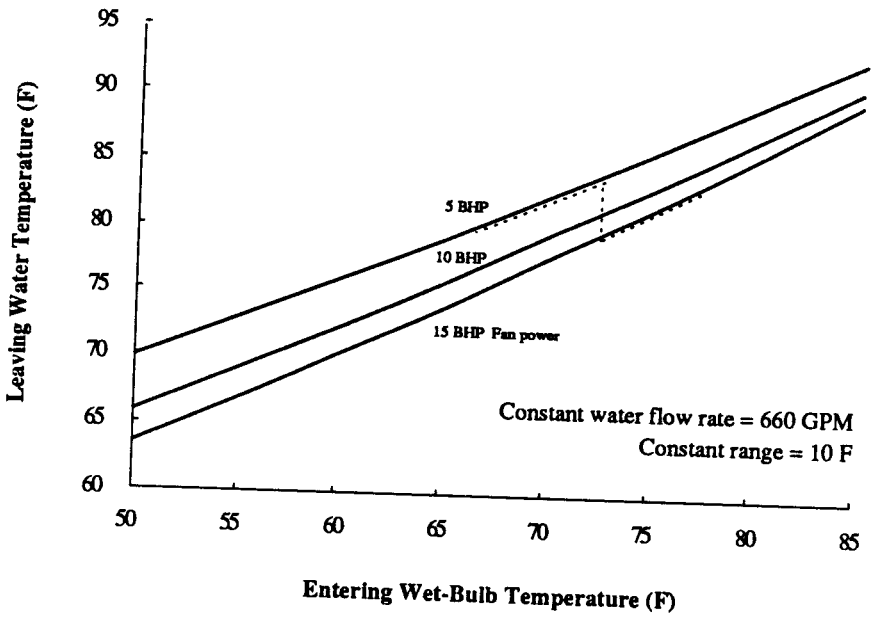

Figure 2.14 Variation in cooling-tower leaving-water temperature at constant water flow rate and constant range.

Optimizing the chiller and cooling-tower performance at part load In many air conditioning applications, since the chiller benefits from lower condensing temperatures and the power drawn by the chiller is typically 10 to 20 times as much as that drawn by the cooling tower fan the temperature of the water leaving the cold-water basin is allowed to float freely with the ambient wet-bulb temperature under full fan power (within certain operating limitations imposed by the particular refrigeration plant used in the system). Under these conditions, leaving water temperature is only a function of the range and the entering wet-bulb temperature. Figure 2.15 demonstrates this functional relationship. However, this is not necessarily the optimal control strategy.

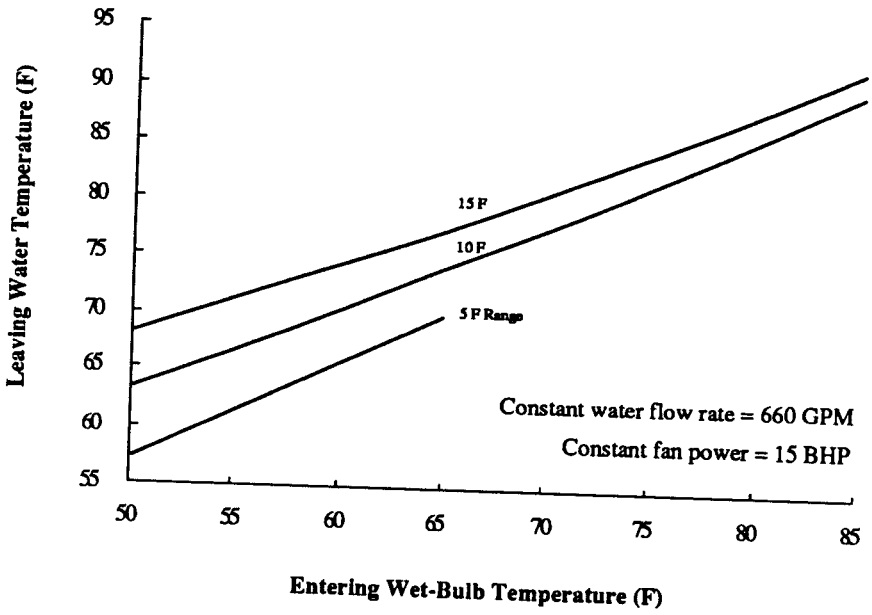

Figure 2.15 Variation in cooling-tower leaving-water temperature at constant water flow rate and constant fan power.

For a given load and ambient wet-bulb temperature, somewhere between zero and the maximum fan power lies the minimum collective power consumption of both the chiller and the cooling tower fan. Low fan powers result in high leaving water temperatures which adversely affects the performance of the chiller, whereas high fan powers result in low leaving water temperatures which enhance the performance of the chiller. Thus a trade-off exists, and the ultimate solution to this problem involves a one-dimensional search for the leaving water temperature at which the total power consumption is a minimum.

Figures 2.16 and 2.17 demonstrate a graphical solution to such a one dimensional search for a given load and ambient wet-bulb temperature. Referring to these figures it

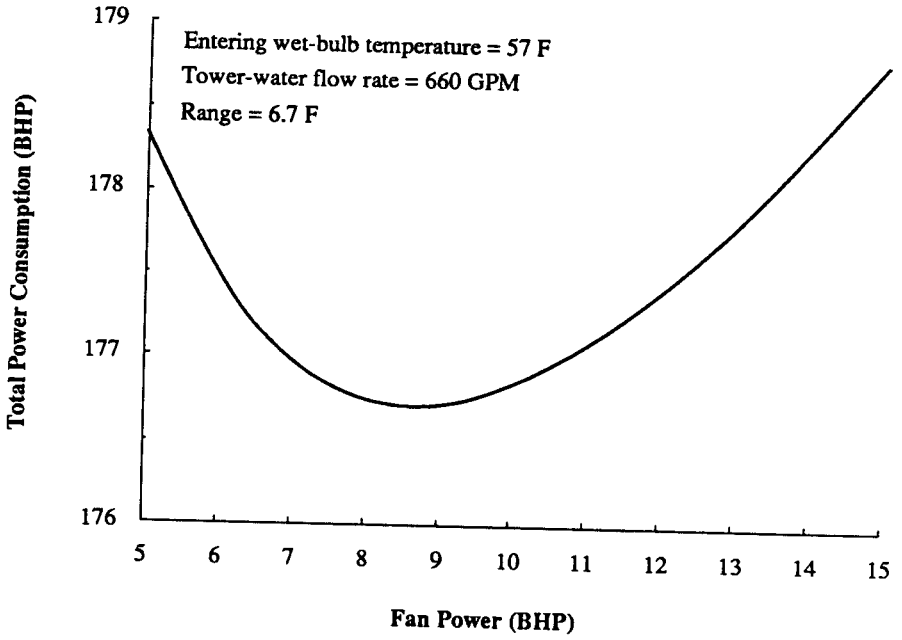

Figure 2.16 Fan power that minimizes the total power, which is the sum of the fan power and the chiller power.

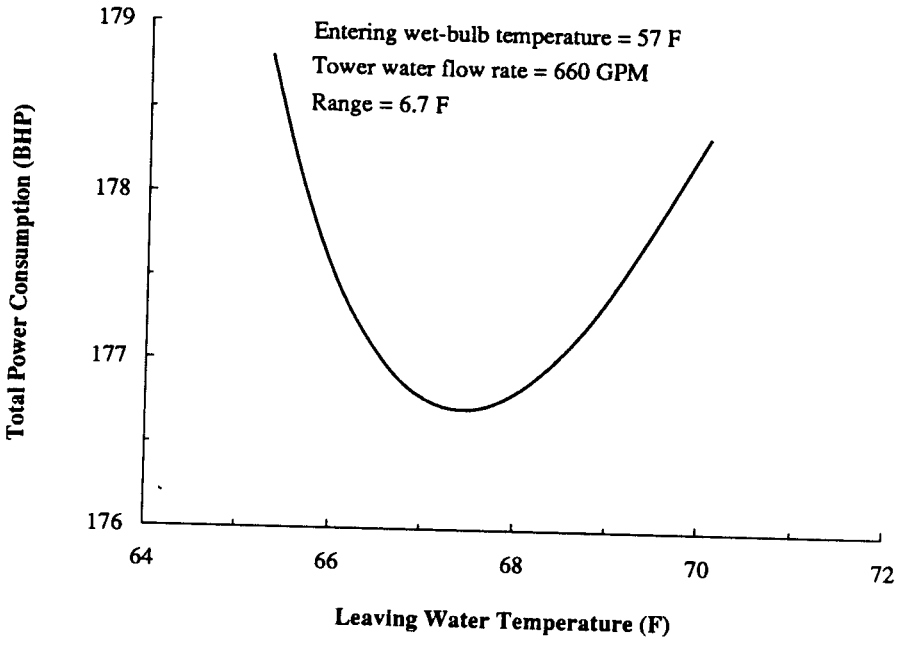

Figure 2.17 Leaving water temperature from the cooling tower that minimizes the total power, which is the sum of the fan power and the chiller power.

is evident that the total power consumed by the chiller and the fan collectively is minimized when the fan is controlled to operate at approximately $8\frac{1}{2}$ BHP which results in a leaving water temperature of approximately 67.4°F. The important aspect of this analysis is that although the total power consumed has indeed been reduced, the reduction is only about 2 BHP (Figure 2.16).

Tower pump control When the mass flow rate of water through the cooling tower is not constant then Figures 2.18 and 2.19 are useful for performance predictions. However, these figures are most useful for design purposes rather than part-load performance predictions during operational periods. Although there is a trade-off between pumping power and chiller power consumption, for common air

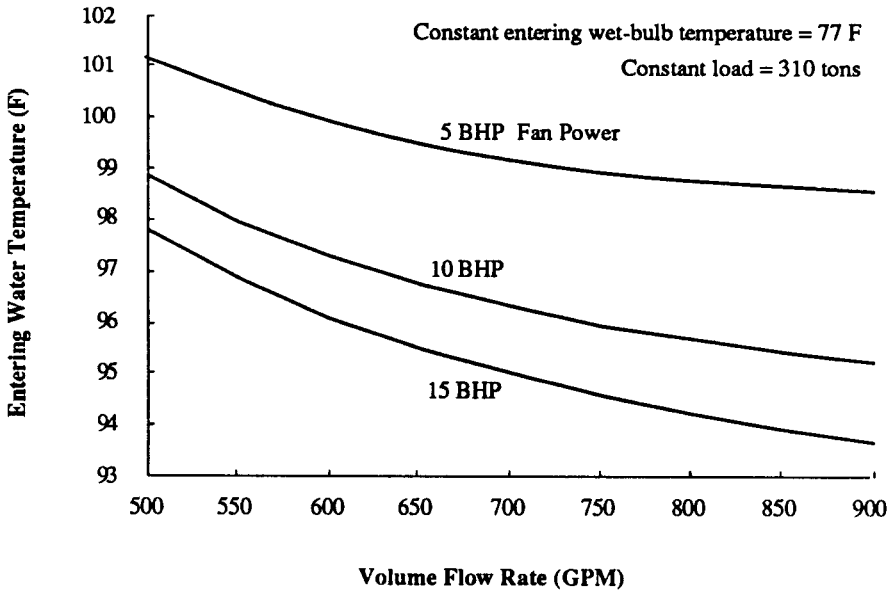

Figure 2.18 Variation in cooling-tower entering-water temperature at constant entering wet-bulb temperature and constant cooling tower load.

conditioning applications, once the cooling tower is installed, the flow rate of water through the tower is usually not altered for the purposes of energy conservation or capacity control [12].

The reason for this is that the thermal performance of a cooling tower depends on a uniform distribution of water to thoroughly cover the surface of the fill sheets. When the level of water in the hot-water basin becomes too low because of an inadequate water supply, the flow patterns which emerge from the nozzles located within the basin are irregular and do not effectively distribute water over the surface of the fill sheets. Because those sections which do not receive adequate water coverage offer the air stream a path of least resistance, the air stream concentrates its movement through fill

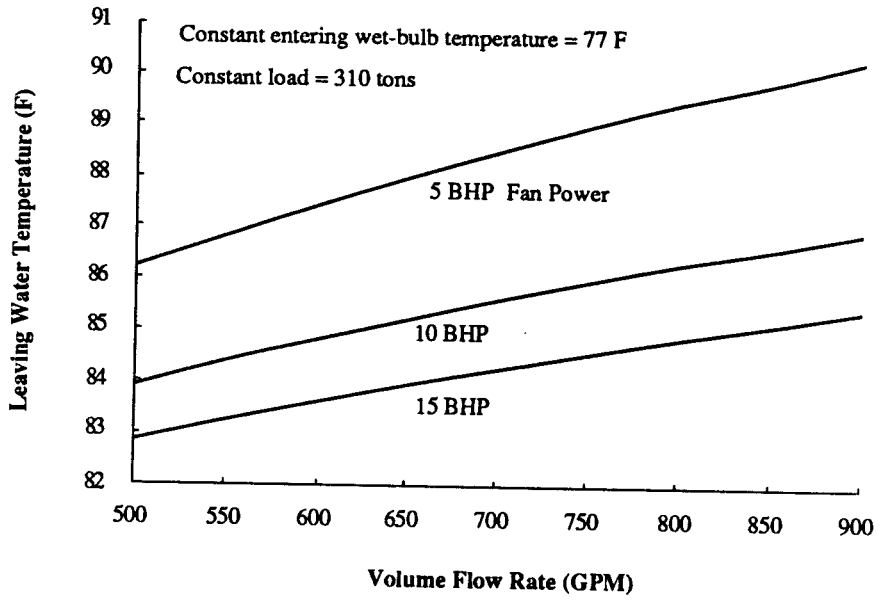

Figure 2.19 Variation in cooling-tower leaving-water temperature at constant entering wet-bulb temperature and constant cooling tower load.

sheets which are driest. This results in a significant reduction in the capacity of the cooling tower, since a portion of the air stream does not participate in the simultaneous exchange of heat and mass.

Optimizing the cooling tower selection procedure With regard to system design, when Figures 2.18 and 2.19 are used in conjunction with the operating characteristics of the refrigeration plant, they are very useful for optimizing the cooling tower selection procedure. The typical cooling tower range employed in air conditioning applications is approximately 10°F and the water flow rate which corresponds to this range is approximately 3 GPM per ton of refrigeration capacity. However, as illustrated in the following example, it is sometimes advantageous to specify a range which is higher than this typical value for three reasons: to decrease the cooling tower's size, to decrease its required fan power, and also to decrease its required pumping power [13].

EXAMPLE 2.1 For example, assume that a cooling tower is to be sized to meet a design-day chiller load of 250 tons with a design-day ambient wet-bulb temperature of 77°F. Figure 2.19 indicates that at the standard range of 10°F and the standard water flow rate of 750 GPM (250 tons × 3 GPM / ton), a tower equipped with a 15-BHP fan produces a leaving water temperature of 86.4°F. On the other hand, if the range is raised to 12°F, then the flow rate required to meet the same chiller load is 625 GPM and the same tower equipped with a just 10-BHP fan produces a leaving water temperature of 85°F. (The constant load specified in Figures 2.18 and 2.19 is greater than the chiller load by the amount of work—manifested as heat to be removed by the cooling tower—applied to the refrigerant during the vapor compression process and by the amount of heat generated in the tower water circuit by frictional dissipation.) The important question to be answered is does this save money?

For the case with the 10°F range, the temperature leaving the condenser is 94.6°F, whereas for the case with the 12°F range, the temperature is 97°F. Assuming a chiller coefficient of performance of 4.7 and a 1 percent power reduction per degree F decrease in the temperature of the water leaving the chiller, the chiller power is 250 BHP under the standard conditions, and is increased to 256 BHP (250 + (97 - 94.6) × .01 × 250) under the conditions with the 12°F range. Thus, the total power consumption is increased by 1 BHP by selecting a 12°F range; but, savings in the required pumping power have not yet been included.

Assume the required pumping head is 60 ft for this application; the pumping power

required is then 11.4 BHP ($(8.33 \times 750 \times 60) / 33{,}000$) and 9.5 BHP for the 10°F and 12°F range specifications, respectively.

Hence, the important result from this example is that approximately 1 BHP of power consumption is saved by selecting the cooling tower based on a range of 12°F and a water flow rate of 625 GPM. In addition, this selection would allow both the pump motor and the fan motor to be specified with a rated power of 10 BHP, whereas the alternative case with the 10°F range and a water flow rate of 750 GPM would necessitate the specification of two 15-BHP motors. Therefore, both first cost and operational costs are saved in this example by specifying a cooling tower range greater than the standard range.

Moreover, since additional power consumption savings are realized by reducing the fan power when the system operates at part load, this selection is beneficial during all days of system operation and not just the design day. Because additional capacity is required when the chiller operates at a higher condensing temperature, a potential drawback with this selection occurs when the chiller has been previously selected to just meet the design-day cooling load. On the other hand, an additional potential savings in first cost can be realized when the water flow rate is sufficiently reduced to enable the specification of a smaller diameter pipe (in this example, 6-inch and 5-inch outside-diameter schedule-40 steel pipes are required for the 10 and 12°F range cases, respectively, assuming a maximum water velocity of 10 ft/s).

2.2.2 Chilled-Water Cooling Coil

By definition, a cooling coil is a device that transfers heat from a gas to a liquid across a boundary which separates these two phases. With regard to an air conditioning application, its purpose is to transfer the heat evolved in the air conditioning process to

the transport fluid which links the cooling coil to the refrigeration plant; this heat comprises the building cooling load, the fan load, and the ventilation load.

Cooling Coil Operation Figure 2.20 and 2.21 show the various features of a spiral-fin chilled-water cooling coil along with the associated flow streams. The chilled-water stream is pumped from the refrigeration plant to the inlet distribution divided into several independent flow paths, or *circuits*. The water stream within each

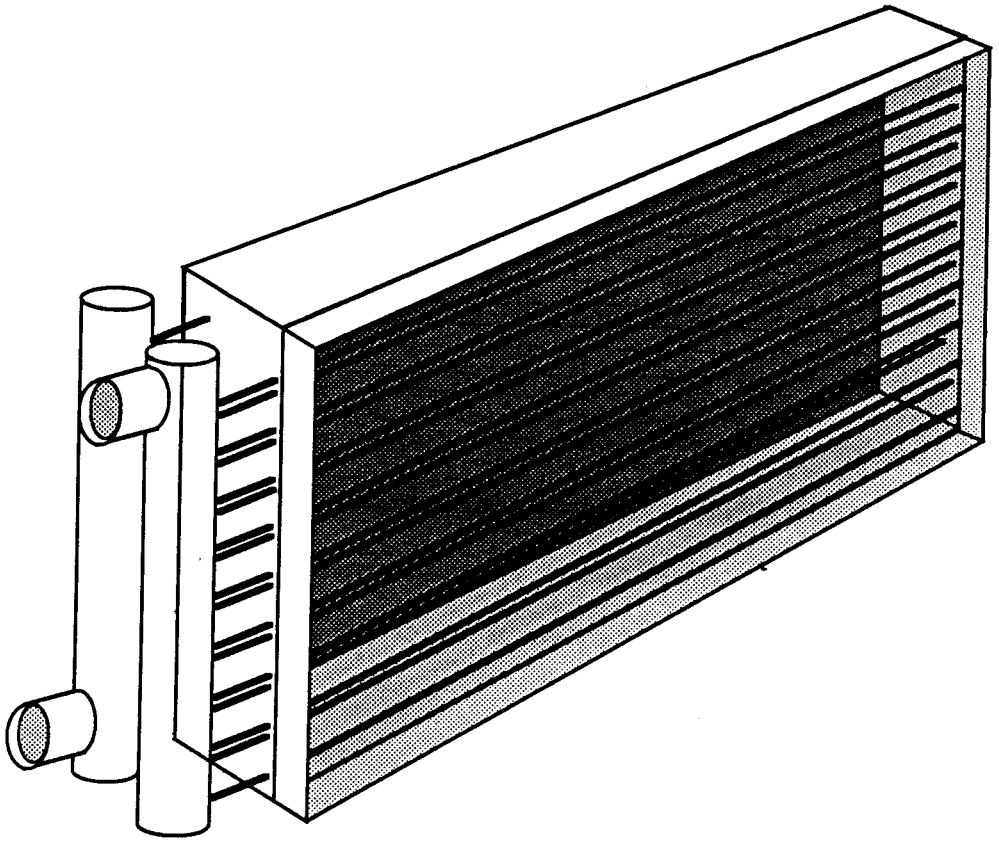

Figure 2.20 Chilled-water cooling coil.

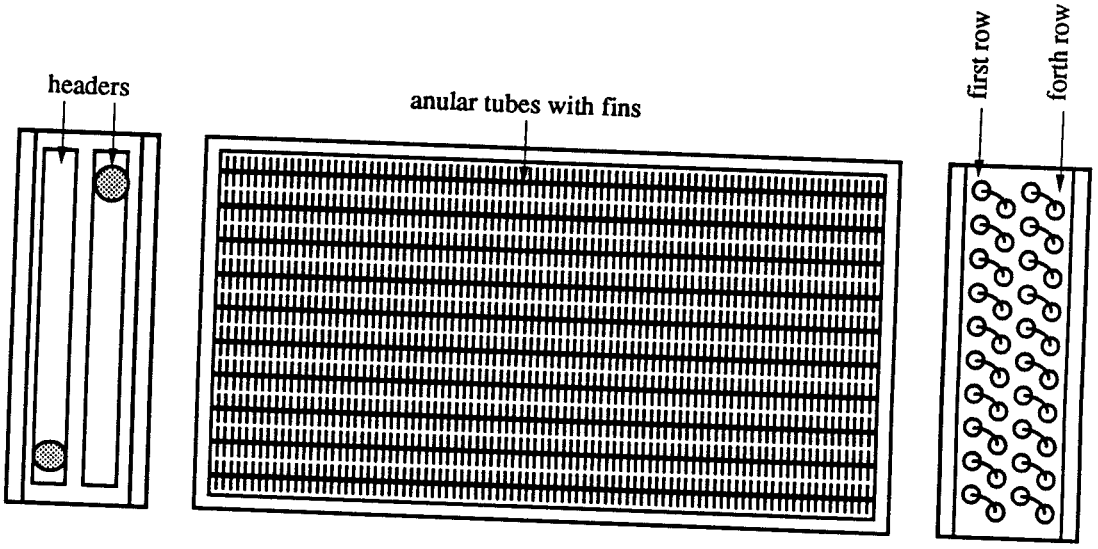

Figure 2.21 4-row, 10-tube face chilled water cooling coil with anular fins.

circuit passes first along the *face* of the coil and then in a serpentine fashion winds back-and-forth across the coil in a direction opposite to the flow of the air stream (Figure 2.21). The independent water streams finally recombine at the outlet header and the resulting hot-water stream is subsequently pumped back to the refrigeration plant for cooling.

Meanwhile on the air side, air is either blown or drawn through the rear face of the coil. As it passes across each successive plane of circuits, or *row* of tubes, it is cooled and if the surface temperature of the coil is lower than the dew point temperature of the entering air stream, it is also dehumidified. Because the air-side heat transfer coefficient is typically significantly less than that of the water-side, fins are commonly

attached to the surfaces of the tubes to enhance the air-side heat transfer (Figure 2.21). As the air progresses through the coil, it approaches the temperature of the entering chilled-water stream. Finally, the air stream exits the coil and is distributed to cool and dehumidify the rooms or zones of the building.

The Cooling Process The transfer of heat between the air stream and the water stream is similar to the energy transfer process that occurs within a cooling tower except that in the case of a cooling coil, the flow rate of water remains constant; that is, mass transfer between the two phases does not occur. However, mass transfer between the air stream and the surroundings does indeed occur if the air is dehumidified as it passes through the coil. (Section 2.2.1 contains a detailed discussion of the process of simultaneous heat and mass transfer.)

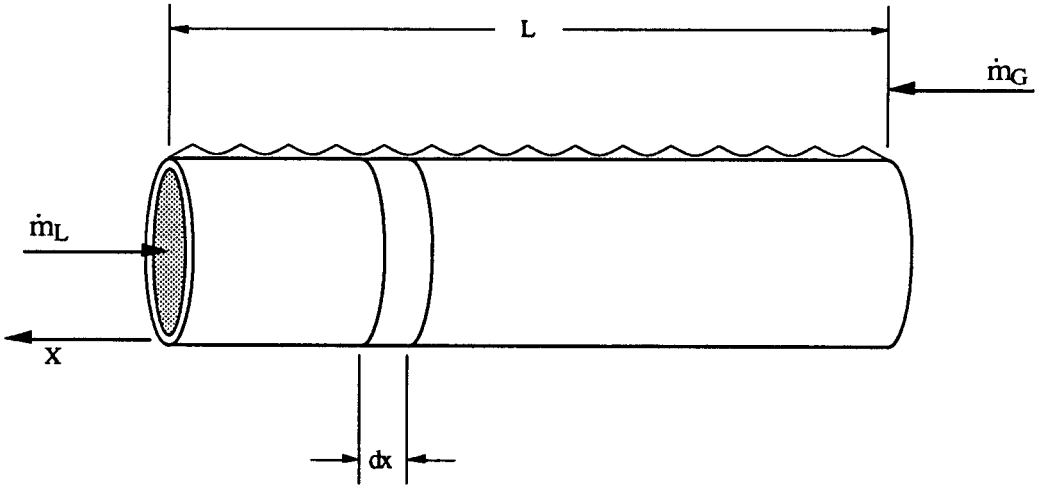

Figure 2.22 Couterflow cooling coil analysis assuming the entire coil to be wet.

CHAPTER
TWO

COMPONENT MODELING AND CHARACTERISTICS

The purposes of this chapter are to describe each component used in the conventional and the partial ice-storage air-conditioning systems designed and analyzed in this work, to show the fundamental theory upon which the modeling of each of these components is based, and to demonstrate the important design and operating characteristics of each component. Before the components are discussed individually, the manner in which the various components are configured to form a system is addressed.

2.1 ICE-STORAGE SYSTEM CONFIGURATIONS

This brief section is designed to show the manner in which conventional air-conditioning systems and ice-storage air-conditioning systems are commonly configured.

Figures 2.22 and 2.23 show the variables of interest for a counterflow cooling-coil analysis where the coil is assumed to be completely wet. It should be noted here that the counterflow cooling coil analysis is applicable to the chilled-water cooling coil previously described, which is of a crossflow nature, if the number of rows is approximately 4 or greater [14]. Like the energy transport process which occurs within a cooling tower, energy is transferred both to and from the phase interface of the cooling coil. The energy transfer between the liquid phase and the phase interface is only in the form of heat. On the other hand, since water vapor condenses on the surface of the coil during the dehumidification process, the energy transfer between the

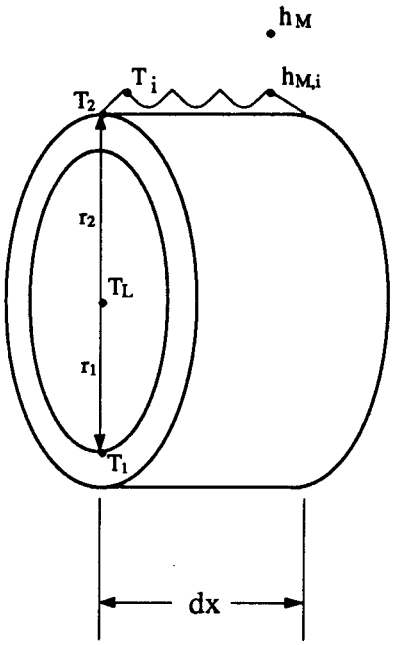

Figure 2.23 Thermodynamic variables and physical dimensions of interest for the couterflow cooling coil analysis.

gas phase and the phase interface comprises both heat and enthalpy. Unlike the simplifying assumption made in the cooling tower analysis where the temperature of the phase interface was assumed to be equal to that of the liquid phase, the temperature of the phase interface of the cooling coil is significantly different from that of the liquid phase (the liquid flowing through the tubes of the cooling coil) because of the convective resistance between the liquid phase and the inner tube surface, the small conductive resistance of the tube wall, and the convective resistance between the outer coil surface and the phase interface.

Cooling Coil Definitions An independent flow path through a cooling coil is called a *circuit.* A plane of tubes which are perpendicular to the flow of air constitute a *row.* The cross sectional area of the cooling coil at the air inlet or outlet is called the *coil face area.* The *coil face velocity* is the velocity of the air as it exits the coil. The *fin series,* or number of fins, is defined as the number of fins per inch of finned tube length. The total area available to the air stream for heat transfer is called the *surface area of the coil.*

Governing Equations for Cooling Coils Since the energy transport processes within the cooling tower are very similar to those within the cooling coil, a modified version of the reduced set of countercurrent gas-liquid contact equations is applicable. The appropriate groups of equations in their modified form are given below where the dimensional coordinate Z has been replaced by x and the convection coefficient of the liquid phase, h_L, has been replaced by an equivalent conductance, h_{eq}, which includes three constituents of thermal resistance between the liquid phase and the phase interface.

The set of equations is divided into three groups:

Mass-transfer rate equation:

$$\dot{m}_G \, d\omega = k_\omega \, (\omega_i - \omega) \, a_H \, dx, \tag{2.36}$$

Heat-transfer rate equations:

$$\dot{m}_G \, dh_M = k_\omega \, (h_{M,i} - h_M) \, a_H \, dx, \tag{2.37}$$

$$\dot{m}_G \, dh_M = h_{eq,2} \, (T_L - T_i) \, a_H \, dx, \tag{2.38}$$

Energy balance equation:

$$\dot{m}_L \, C_{p,L} \, dT_L = \dot{m}_G \, dh_M, \tag{2.39}$$

where a_H = air-side surface area per unit length of the coil: the sum of the finned surface area, a_f, and the prime (or unfinned) surface area,

$h_{eq,2}$ = equivalent overall conductance based on the air-side surface area

$$= \left[\frac{1}{h_2 \, \eta_o} + \frac{a_H}{2\pi \, k} \ln \frac{r_2}{r_1} + \frac{a_H}{2\pi \, r_1 \, h_1} \right]^{-1}, \tag{2.40}$$

η_o = temperature effectiveness of a fin

$$= 1 - \frac{a_f}{a_H} (1 - \eta_f),$$

a_f = finned surface area per unit length,

η_f = fin efficiency,

r_1 and r_2 are the inner and outer tube radii, respectively, and h_1 and h_2 are the

convection coefficients for the fluids in contact with the inner and outer tube surfaces, respectively.

Since mass is not exchanged between the two phases, the mass balance equation is no longer necessary and thus is not included in the above equations. Moreover, since the mass flow rate of the liquid phase and the gas phase are constant, the mass-transfer rate equation is decoupled from the remaining equations; thus, the absolute humidity of the exiting air stream may be determined—if necessary—by numerically integrating Equation 2.36 after the phase interface temperature distribution along the surface of the coil has been determined by solving the remaining heat-transfer rate equations and the energy balance equation.

Hence, the two rate equations, and the energy balance constitute a set of three coupled differential equations which can be readily solved numerically if $\dot{m}_G$, k_ω, a_H, $\dot{m}_L$, and $C_{p,L}$ are known; if $h_{M,i}$ is a known function of the phase interface temperature; if $h_{eq,2}$ is a known function of the temperatures and flow rates of the fluids in contact with the inner and outer tube surface; and if the inlet air stream and water stream conditions are known.

The Finite-Difference Model for Cooling Coils Like the equations which describe the processes within a cooling tower, the above equations which describe the processes within a cooling coil are readily solved using a finite-difference scheme.

Solution procedure for the finite-difference model The solution procedure for a counterflow cooling coil (which may also be adapted for a counterflow cooling tower, since the solution procedure for the cooling tower was given for a crossflow geometry) is as follows: The water-side and the air-side convection coefficients h_1 and h_2, respectively, are evaluated based on their respective flow rates

and inlet temperatures (h_2, the convection coefficient of the condensed water vapor, is assumed to be large); a value for the leaving water temperature $T_{L,2}$ is then guessed; next, the two heat-transfer rate equations (Equations 2.37 and 2.38) are equated and the resulting equation and the algebraic equation for the enthalpy of the gas-vapor mixture at the phase interface $h_{M,i}$ (Equation 2.25 and its ancillary equations) are then used to iteratively solve for the temperature at the phase interface at the air inlet; once T_i has been ascertained, the finite differential of air enthalpy and the finite differential of water temperature are computed; the position along the coil is then incremented by Δx; and the above procedure is subsequently repeated at the new position along the coil.

This procedure is continued until the end of the coil is reached at which point the computed water-inlet temperature is compared to the actual water-inlet temperature. Based on the difference between these values, a new value of the water-outlet temperature is guessed and the entire procedure is repeated until satisfactory convergence is attained. A third iteration may be required to determine the average temperature and enthalpy driving forces, which are used in the rate equations, within each incremental element; this procedure is outlined,with regard to cooling tower modeling, in Section 2.2.1.

This procedure was used to model the performance of a spiral-fin chilled-water cooling coil. The coil was discretized into 5 elements and a *crossflow analysis* was performed. In general, the water-side convection coefficient is readily determined from empirical correlations. However, since the air stream flows over a bank of tubes and through a myriad of fins located on the tube surface, the resulting flow is quite complex; therefore, an accurate air-side convection coefficient is significantly more

difficult to obtain from empirical correlations. In addition, since the tube surface is finned, the fin efficiency η_f and its temperature effectiveness η_o must be determined.

For these reasons, manufacturer's performance data [15] was used to iteratively determine both the effective air-side convection coefficient h_2 and the mass-transfer coefficient and area product $k_\omega a_H$ (as was done for $k_\omega a_H$ in the crossflow cooling-tower analysis). Briefly, this procedure was found to be adequate for coils with 6 rows or greater, but less adequate for coils with four rows—the air-side convection coefficient became unreasonably high (greater than 70 Btu/hr-ft^2-F). The results of this analysis are presented graphically in the Cooling Coil Characteristics subsection.

In summary, from an energy perspective, two of the three differential equations necessary to model the cooling coil are indeed very similar to the two differential equations necessary to model the cooling tower; the additional differential rate equation needed for modeling the cooling coil complicates the solution procedure and makes it iterative with respect to the phase interface temperature, the water outlet temperature from the coil, and the average driving forces within each incremental element. Like the cooling-tower model, the cooling-coil model incorporated in the transient simulation program, TRNSYS, used in this work is based on an effectiveness model.

The Effectiveness Model for Cooling Coils In the same manner that the set of coupled differential equations which describe the processes within a cooling tower are transformed into a set of algebraic equations, the same can be done for those equations which describe the processes within a cooling coil. The equations resulting from such a transformation may be found in Reference 4, 5, or 9. Furthermore, Reference 4 compares the effectiveness model to manufacturer's performance data for a spiral-

finned chilled water cooling coil with 6-rows and 8-fins per inch. These predictions are shown to agree well with the manufacturer's data over a wide range of operating conditions.

Cooling Coil Characteristics The primary variables used for selecting a coiling coil are the coil inlet conditions, the water and air flow velocities, the number of rows, the number of fins, and the water-temperature rise across the coil. Typically, the inlet conditions, the air flow rate, and the water temperature rise are specified; then, the number of rows, the number of circuits, and the water velocity are selected such that the coil load is met and the desired outlet conditions are obtained.

Since the water velocity and the air velocity through the coil directly influence the amount of power consumed by the chilled-water pump and the air-handling-unit fan, respectively, an economic analysis can be performed to determine the velocities, the number of rows, and the number of fins which would meet the specified load and desired outlet conditions with the minimum life cycle cost. Such an analysis can be found in Reference 16 or 17. The general conclusion of these works is that a larger, more expensive air-handling-unit which operates at lower face velocities can indeed have a lower life cycle cost under typical economic conditions. Because a general analysis cannot be conducted in this case—as was done for the cooling tower—without specific knowledge of first cost, a coil was selected to meet the load and the desired outlet conditions based on typical chilled-water and air velocities. The operating characteristics of the selected coil under the design-day load are shown in Figures 2.24, 2.25, and 2.26.

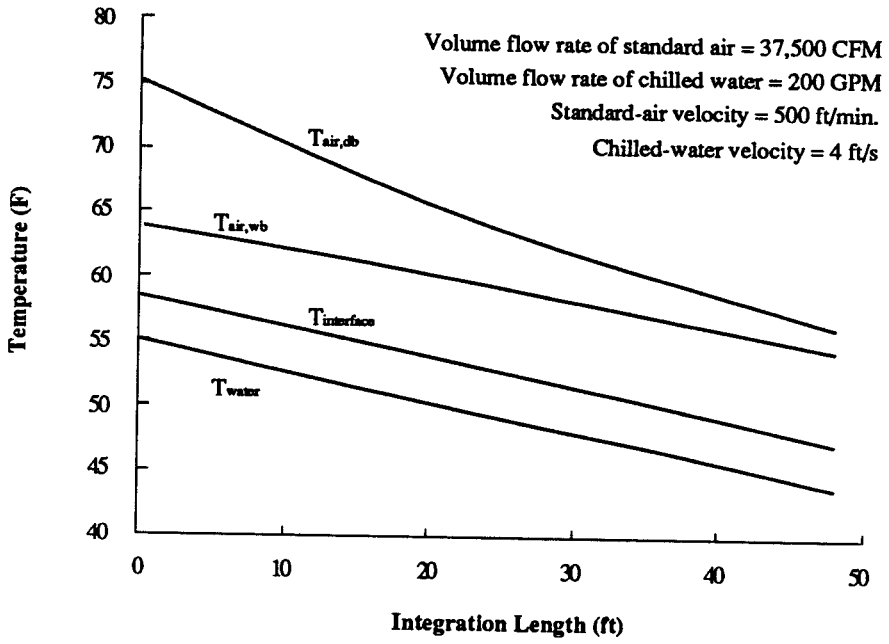

Figure 2.24 Temperature distribution along the length of the cooling coil. 4-row, 60-circuit, spiral-finned chilled-water cooling coil.

Temperature profiles Figure 2.24 shows the temperature profile of the air stream, the water stream, and the phase interface between the air inlet and outlet states. The significant point of interest is that the greatest fraction of sensible cooling takes place during the first two-fifths of the air stream's journey through the coil, as indicated by the steep temperature gradient between 0 and 20 ft. A second point of interest is that the temperature of the phase interface is indeed significantly greater than that of the water stream.

Enthalpy profiles Figure 2.25 demonstrates that the enthalpy driving force h_M - $h_{M,i}$, the driving force effecting the simultaneous transfer of heat and matter between the wetted coil surface and the adjacent air stream, is essentially constant between the

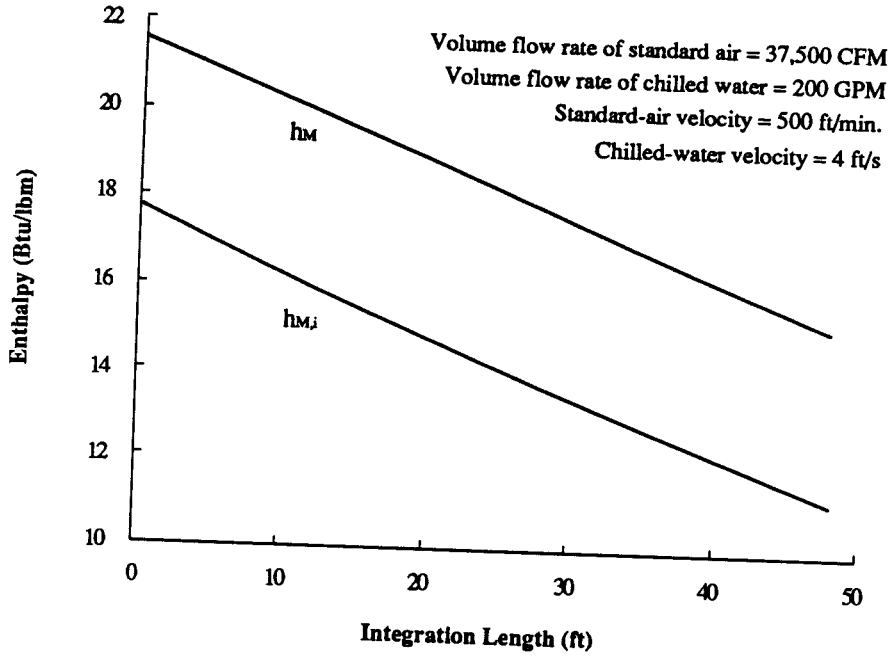

Figure 2.25 Enthalpy distribution along the length of the cooling coil. 4-row, 60-circuit, spiral-finned chilled-water cooling coil.

air inlet and outlet states. This indicates that the entire coil surface area is effectively utilized in the process of cooling the air stream; often, depending on the relative heat capacitance rates of the water and air stream, the driving force diminishes in the direction of the flow of air which results in less heat transferred from the air as it progresses through the coil.

Humidity profiles Figure 2.26 demonstrated the mass-transfer driving force $\omega - \omega_i$ between the wetted coil surface and the humid air-stream. When the absolute humidity ratio of the mixture at the phase interface ω_i is greater than that of the mixture in the air stream ω (Figure 2.26), then ω_i is fictitious since vapor does not yet reside

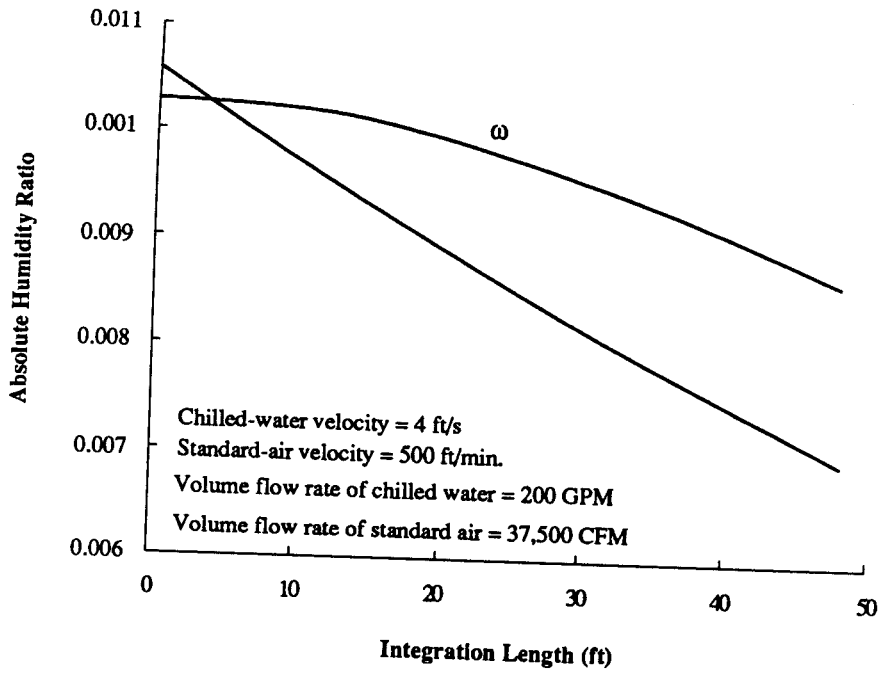

Figure 2.26 Absolute humidity distribution along the length of the cooling coil. 4-row, 60-circuit, spiral-finned chilled-water cooling coil.

on the surface of the coil; as a result, no mass transfer occurs until the driving force becomes positive at which time vapor begins to condense on the coil surface. The absolute-humidity profile of the mixture in the air stream is relatively flat for the first one-third of the air stream's journey through the coil; this indicates that sensible cooling of the air stream is predominant in this region. The profile then drops quite rapidly, which indicates that the air stream is undergoing dehumidification as well as sensible cooling.

2.2.3 Reciprocating and Centrifugal Liquid Chillers

A liquid chiller is a device that transfers heat from a low temperature source to a high temperature sink by means of work input. With regard to an air conditioning application, its purpose is to transfer the heat evolved in the air conditioning process to the transport fluid which links the chiller to the cooling tower; this heat comprises the building cooling load, the fan load, the ventilation load, the distribution pump load, and the main-water loop pump load.

Chiller Operation Figure 2.27 shows the various features of a water-cooled liquid chiller with a reciprocating compressor along with the associated flow streams. On the evaporator side, warm water, which is pumped from the load, enters the evaporator and is subsequently divided into a number of independent flow streams. A *tube sheet*

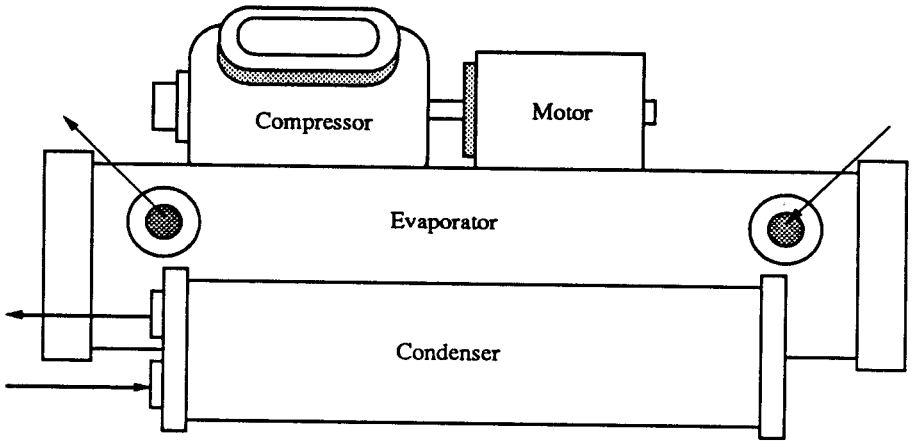

Figure 2.27 Liquid chiller with reciprocating compressor and associated flow streams.

located within the evaporator supports the evaporator *tube bundle* within the *shell* of the evaporator. As each stream makes its *single pass* through the tube bundle, it is cooled by liquid refrigerant evaporating from the outer surface of the evaporator tubes which are submerged in the liquid refrigerant. The streams recombine at the outlet tube sheet and the resulting chilled-water stream is pumped to the load. A similar process occurs in the condenser except that refrigerant vapors condense on the surface of the condenser tubes and warm the water stream as it makes its two passes through the condenser.

A pressure differential between the evaporator and condenser is maintained by the compressor and by an expansion valve which meters the flow of warm liquid refrigerant from the condenser to the evaporator. Liquid entering the low pressure region of the evaporator flashes to a two-phase mixture. The equilibrium temperature of this mixture is less than that of the liquid within the condenser. Since the net effect is the transfer of heat from a low temperature source—the conditioned space—to a high temperature sink—the surrounding atmosphere, work is required. The compressor transfers this work to the refrigerant during the vapor compression process (Figure 2.28).

Chiller Definitions The temperature of the water leaving the outlet of the evaporator is controlled to be equal to the *chilled-water set temperature*. The *rated power* and the *rated capacity* are the chiller power and capacity under standard conditions (45°F water temperature leaving the evaporator, 95°F water temperature leaving the evaporator, 10°F temperature change across the evaporator and the condenser, and .005 fouling factor on the inner surfaces of the tube bundles [18]). The *chiller coefficient of performance* is the ratio of heat transfer in the evaporator to the rate of work input to

the motor of the compressor. The *suction temperature* is the temperature of the refrigerant when it enters the suction port of the compressor, whereas the *discharge temperature* is that when it exits the discharge port of the compressor. The *thermal lift* of the chiller is defined as the difference between the temperature of the water stream leaving the condenser and that leaving the evaporator. A *ton* is a unit used to rate the capacity of chillers and is defined as the rate of heat transfer required to melt one ton of ice in one day (12,000 Btu/hr).

Governing Equations for Chillers Given the physical characteristics of the liquid chiller and the thermodynamic equations of state which represent the behavior of the refrigerant under the conditions it encounters within the vapor compression cycle, it is possible to accurately model the heat transfer processes that occur within the evaporator and the condenser and the vapor compression process. Such a model is presented in Reference 4. However, for the purposes of this study, such a detailed model of a liquid chiller is not warranted, since the results presented in Reference 4 indicate that the a single correlation accurately predicts the performance of this device.

The recommended equation correlates the chiller power as a *biquadratic* function of the chiller load and the thermal lift. Thus, the power required by the chiller to meet a specific load while operating under a specific thermal lift is given by

$$P_{ch} = a_0 + a_1 \dot{Q}_{ch} + a_2 \Delta T_{lw} + a_3 \dot{Q}_{ch}^2 + a_4 \Delta T_{lw}^2 + a_5 \dot{Q}_{ch} \Delta T_{lw} \qquad (2.41)$$

where $\dot{Q}_{ch}$ is the chiller load, ΔT_{lw} is the temperature difference between the two leaving water streams ($T_{w,o,c}$ - $T_{w,o,e}$), and a_0 through a_5 are constants for a specific chiller. The six constants are determined from either actual or manufacturer's performance data

using the method of least squares. Accordingly, the best linear regression model is obtained when many data points are selected which represent the range of operating conditions encountered by the chiller. With the chiller power expressed as a function of the leaving water temperatures, the effects of evaporator and condenser mass flow rate are not highly significant over reasonable chiller operating ranges [4]. The remaining equations necessary to complete the modeling of this component are straightforward.

The load on the chiller is given by

$$\dot{Q}_{ch} = \dot{m}_{w,e}\, C_{p,w,e}\, (T_{w,i,e} - T_{w,o,e}) \tag{2.42}$$

where $\dot{m}_{w,e}$ is the mass flow rate of water through the evaporator, $C_{p,w,e}$ is its specific heat, and $T_{w,i,e}$ and $T_{w,o,e}$ are its temperatures at the inlet and outlet of the evaporator, respectively.

The heat rejected by the condenser is equal to the heat absorbed by the evaporator plus the heat evolved from the vapor compression process which is numerically equivalent to the amount of work input into the refrigerant by the compressor. This equality is expressed as

$$\dot{m}_{w,c}\, C_{p,w,c}\, (T_{w,o,c} - T_{w,i,c}) = \dot{Q}_{ch} + \eta_m\, P_{ch} \tag{2.43}$$

where the subscript c denotes the condenser and η_m is the efficiency of the motor which powers the compressor.

Since the control strategy determines the leaving chilled-water temperature $T_{w,o,e}$ and the chiller load is determined from the sum of the building, fan, ventilation, and pump loads, the remaining unknowns are the chiller power and the temperature of the water

leaving the condenser. Thus, assuming known chiller inlet conditions, Equations 2.41 and 2.43 constitute a set of two equations and two unknowns, and they can be solved to determine the chiller power and the temperature of the water leaving the condenser.

In this analysis, like all that of the cooling tower and that of the cooling coil, the inlet conditions were assumed to be known. However, with regard to a system simulation, the inlet conditions are generally unknown and must, therefore, be determined by iteratively solving the complete set of equations which describe each component individually and collectively describe the operation of the system. For example, in the present case, the water inlet temperature to the condenser is a function the ambient conditions and the cooling tower load—which is the sum of the heat rejected by the condenser and the cooling-tower-pump load. Thus, if the chiller and the cooling tower are taken to be the system, the set of equations which describe both the chiller and the cooling tower must be iteratively solved to determine the unknown variables.

Capacity Limits Because ice-storage systems generally require the chiller to operate at maximum capacity over an extreme range of chilled-water set temperatures as well as a variety of ambient conditions, a mathematical relationship which describes the capacity limits of the chiller is crucial for effectively modeling the performance of these systems. A correlation which predicts the maximum capacity of a liquid chiller with a reciprocating compressor over the entire range of operational conditions is given by

$$\dot{Q}_{ch,max} = b_0 + b_1 T_{w,o,e} + b_2 T_{w,o,c} + b_3 T_{w,o,e}^2 + b_4 T_{w,o,c}^2 + b_5 T_{w,o,e} T_{w,o,c} \qquad (2.44)$$

where b_0 through b_5 are constants for a specific chiller. These six constants, like those

of the power equation, are determined from actual or manufacturer's performance data using the method of least squares.

The reciprocating compressor used in this study is capable of continuous operation while chilling water at loads as low as 10 percent of its rated capacity; below 10 percent, the compressor is cycled to meet the load. Therefore, the chiller can be modeled to effectively operate between zero load and its maximum capacity during conditions in which water is chilled. However, during ice-making conditions, reciprocating compressors may experience operating difficulties while functioning under part load [19]. And therefore, minimum capacity data should be obtained and correlated using Equation 2.44.

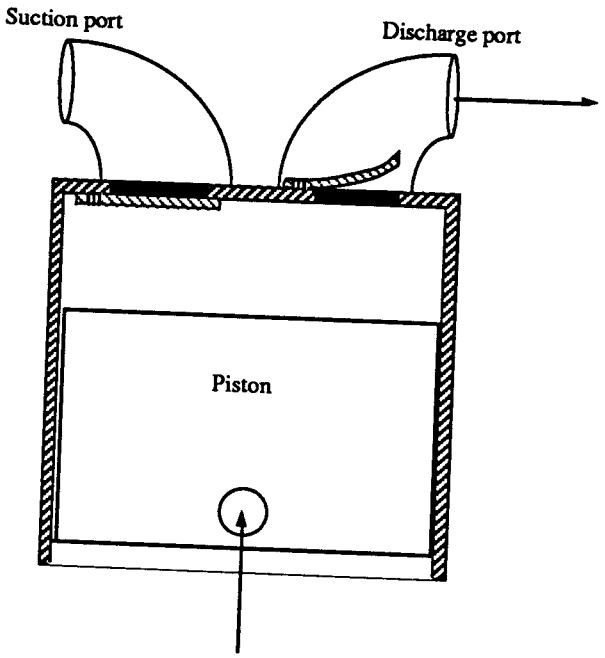

Figure 2.28 Piston of a reciprocating compressor. Discharge stroke.

Reciprocating Liquid-Chiller Characteristics This subsection presents the important operating characteristics of a particular liquid chiller employing a reciprocating compressor. These characteristics serve as a foundation for future discussions regarding chiller control. The figures contained within this subsection are based on manufacturer's performance data [18, 20, 21, or 22]. Figure 2.28, which schematically shows the innards of a reciprocating compressor, serves as a reference for the discussion to follow.

Part-load performance In general, the reciprocating liquid chiller has a linear part-load performance characteristic; that is, the chiller power is a linear function of chiller load as shown in Figure 2.29. This linear relationship arises primarily as a

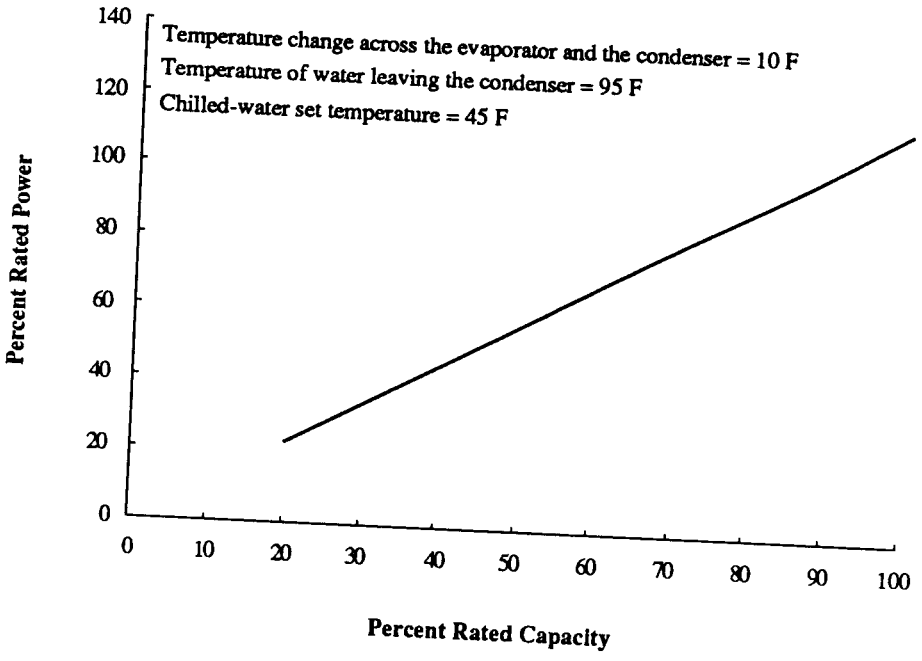

Figure 2.29 Part load performance. Reciprocating liquid chiller.

result of two opposing influences on the chiller performance. Since at part load the evaporator and condenser are effectively oversized with respect to the load, the temperature of the refrigerant in the evaporator and the temperature of the refrigerant in the condenser closely approach the temperature of the water in the evaporator and condenser, respectively; consequently, the thermal lift is effectively reduced. This benefits the compressor.

On the other hand, under this part-load operation, the chiller capacity control must act to match the chiller cooling rate to the required load. For the reciprocating compressor, this is done by *cylinder unloaders* which decrease the amount of refrigerant pumped by the compressor [23]. Cylinders are unloaded by maintaining an open suction port. Hence, the compressor piston draws refrigerant vapor from the evaporator into the cylinder through the suction port on the expansion stroke and discharges the same refrigerant vapor back into the evaporator through the same suction port on the compression stroke. Accordingly, the chiller capacity is reduced. However, this action penalizes the compressor, since it must supply the power required to move refrigerant into and out of the cylinder and to overcome the associated mechanical transmission losses.

Figure 2.30 shows the coefficient of performance of a reciprocating chiller rated at 200 tons based on the above part-load performance curve. Because this chiller comprises two individual compressors, the curve has two distinct regions which are similar: the region from 0 to 50 percent load and the region from 50 to 100 percent load. The coefficient of performance peaks at approximately 25 percent of the rated capacity since one compressor is off at this load and for the other reasons discussed above.

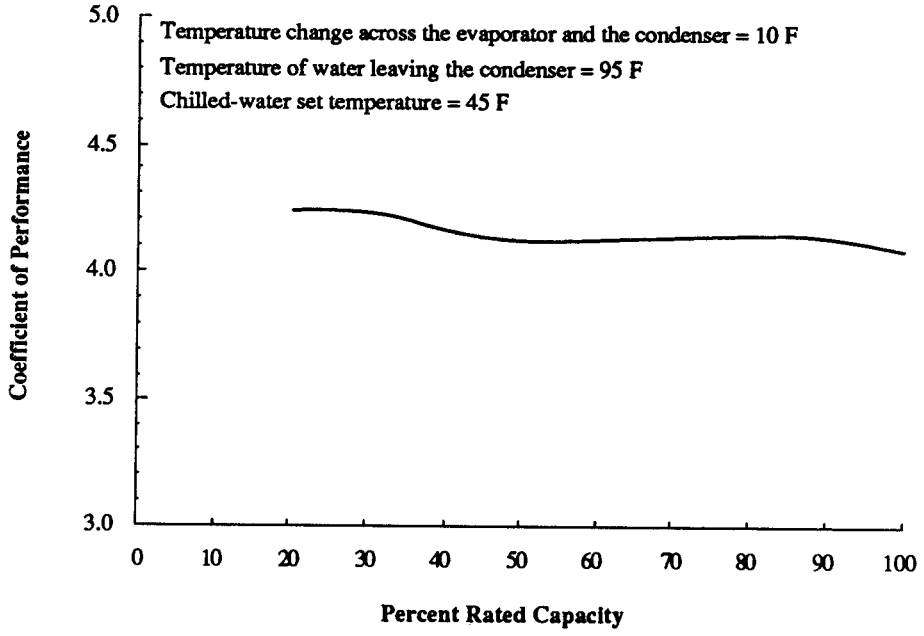

Figure 2.30 Chiller coefficient of performance at part load. Reciprocating liquid chiller rated at 200 tons.

Effect of chilled-water set temperature on chiller performance With respect to the modeling of ice-storage systems, a very important chiller characteristic is shown in Figure 2.31. For a constant leaving water temperature from the condenser, the coefficient of performance is a strong function of the chilled-water set temperature. During ice-making conditions where the chilled-water set temperature equals 25°F, the coefficient of performance of this machine is approximately 3.0. On the other hand, during water chilling conditions where the chilled water set temperature equals 45°F, it is 4.0. This 25 percent reduction in the chiller coefficient of performance is truly a significant thermal penalty due to making ice.

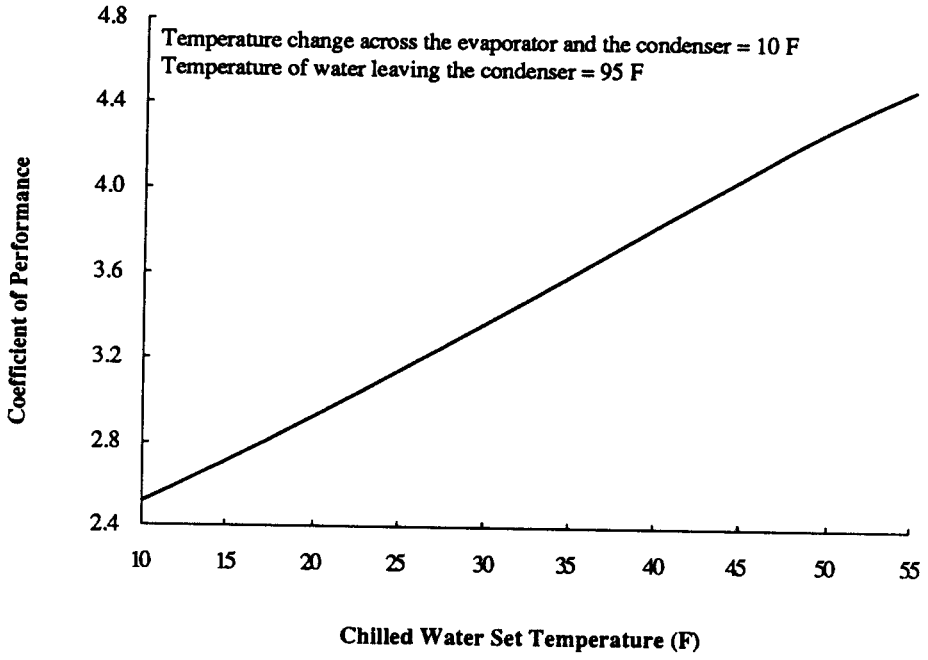

Figure 2.31 Chiller coefficient of performance at maximum capacity. Reciprocating liquid chiller rated at 200 tons.

Effect of chilled-water set temperature on chiller capacity The maximum capacity limits (given by Equation 2.44) of the 200 ton reciprocating compressor are depicted graphically in Figure 2.32 at several leaving water temperatures from the condenser. Under ice-making conditions (chilled-water set temperature = 25°F, leaving condenser water temperature = 95°F) this figure shows that the effective chiller capacity is only approximately 65 percent of its rated capacity.

In general, the chiller capacity is reduced as the chilled-water set temperature is decreased for two reasons: 1) the volumetric efficiency decreases significantly as the thermal lift increases, and 2) the density of the refrigerant vapor decreases as the

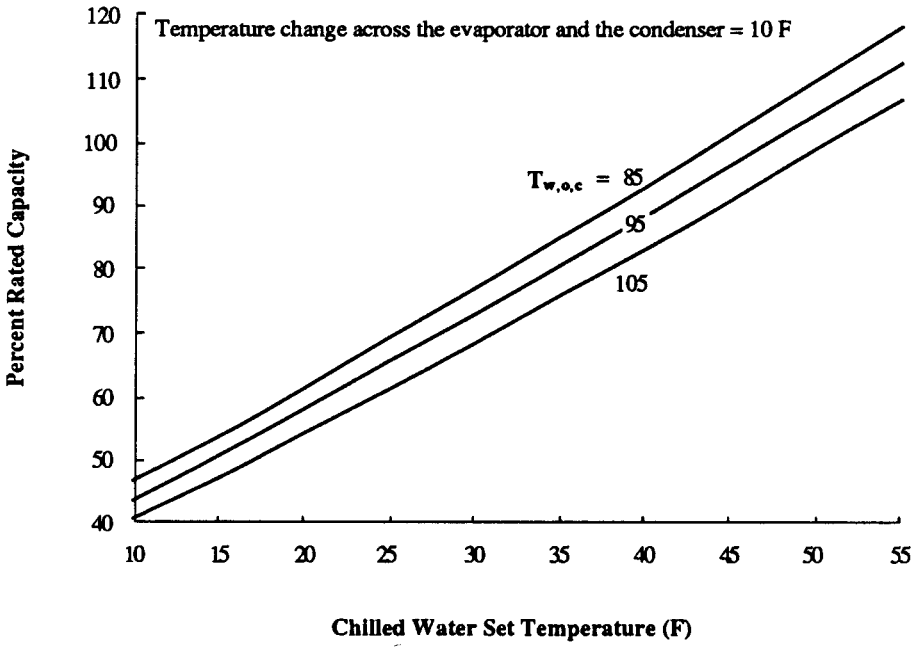

Figure 2.32 Maximum chiller capacity at three condenser-water outlet temperatures (F). Reciprocating liquid chiller rated at 200 tons.

evaporator temperature is lowered. Because at the end of each compression stroke a small volume, called the *clearance volume*, of refrigerant vapor remains within the cylinder, a portion of the cylinder is unavailable to refrigerant during the ensuing intake stroke. Naturally, this unavailable space increases as the pressure difference (thermal lift) between the condenser and the evaporator increases. Therefore, as the thermal lift increases, less refrigerant mass enters the cylinder during each intake stroke. In addition, since the intake stoke of a reciprocating compressor is essentially a constant volume process (for given conditions), as the density of the vapor decreases so does the amount of refrigerant mass issued into the cylinder on each intake stroke. For these reasons, the chiller capacity decreases considerably with an increase in thermal lift.

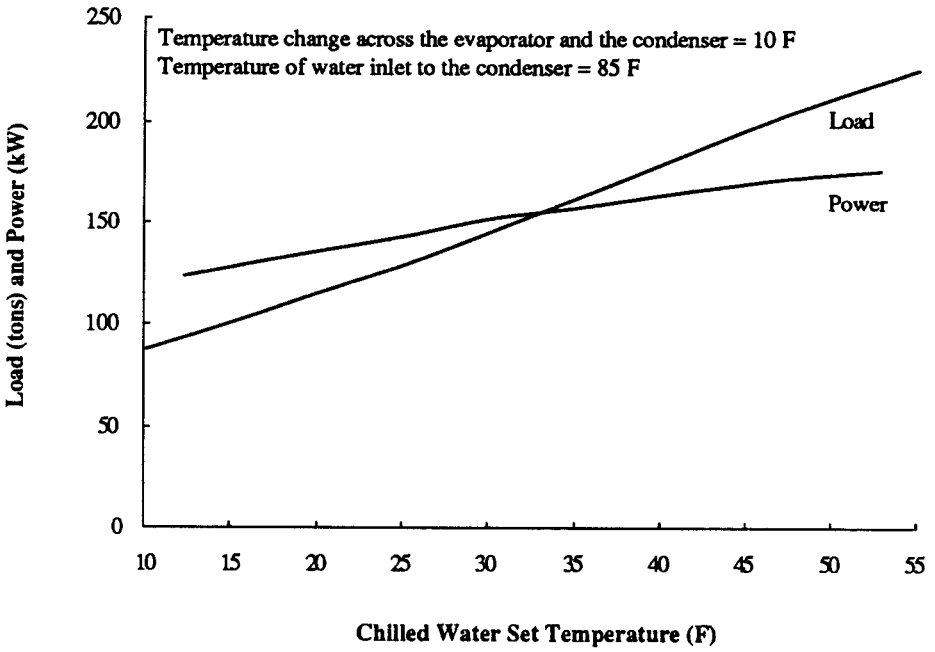

Figure 2.33 Chiller power and chiller load at maximum capacity. Reciprocating liquid chiller rated at 200 tons.

Effect of chilled-water set temperature on chiller power The power variation and the associated maximum chiller capacity are shown in Figure 2.33 for a 200 ton machine. The variation in chiller power with load is significantly less than that of the maximum chiller capacity. This is caused by the opposing effects of load and lift on the chiller power consumption. As the chilled-water set temperature decreases, the load (maximum chiller capacity) also decreases. Since the effect of load is more pronounced than that of lift for this particular machine, the power also decreases.

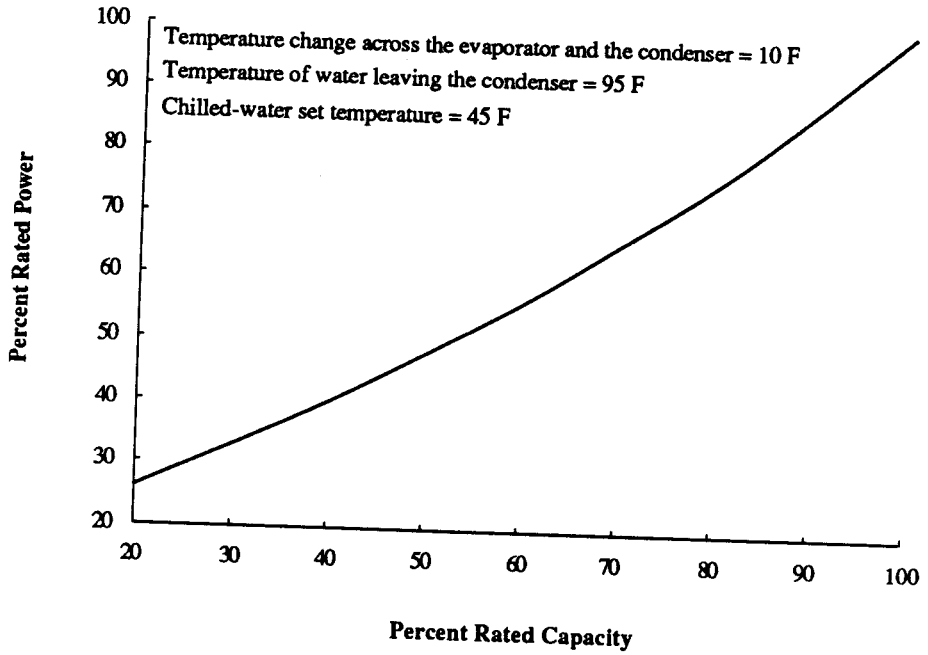

Figure 2.34 Part load performance. Centrifugal liquid chiller.

Centrifugal Liquid-Chiller Characteristics Figures 2.34 and 2.35 present the part-load characteristics of a three-stage centrifugal liquid chiller whose capacity is controlled with variable-pitch *inlet vanes*. In contrast to the reciprocating chiller, the centrifugal chiller has a nonlinear part-load characteristic (Figure 2.34). Figure 2.35 indicates that the chiller performance for a 500-ton unit is maximized when it operates between 60 and 80 percent of its rated capacity, and that performance decreases precipitously at loads below 40 percent of the rated load. However, the coefficient of performance of this centrifugal machine is at all loads substantially greater than that of the reciprocating machine.

The same comments made about the two opposing influences on chiller performance are valid with regard to the centrifugal machine except that the capacity

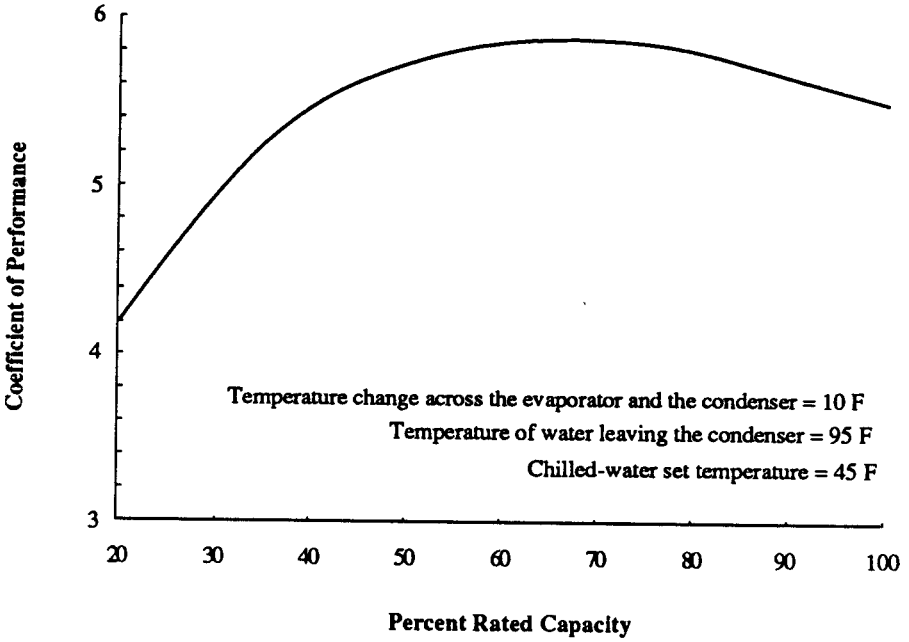

Figure 2.35 Chiller coefficient of performance at part load. Centrifugal liquid chiller rated at 500 tons.

control of this type of machine is typically effected either by the use of variable pitch inlet vanes or variable-speed drives which control the speed of the chiller motor in response to the chiller load. The vanes are used to pre-rotate the flow of refrigerant before it makes contact with the blades of the compressor. For relatively high loads or limited pre-rotation, this is a very efficient form of capacity control; on the contrary, for relatively low loads, the vanes begin to effectively throttle the flow of refrigerant. This is a very inefficient form of capacity control; as a result the chiller coefficient of performance decays significantly as the chiller load decreases below 40 percent of the rated load. In these cases of low load, the variable-speed drive is significantly more efficient than variable pitch inlet vanes [24].

2.2.4 Constrained-Area Ice-Storage Tank

The operation of the constrained-area ice-storage tank was previously discussed in Section 1.2.2. This section serves two purposes: 1) to present the fundamental mathematical equations which govern the charging process and the empirical equations which govern the discharging process of this component and 2) to show its important operating characteristics during both the charging and discharging periods. The fundamental methods presented for modeling the charging process can be extended to model the discharging process; however, since manufacturer's performance data for this period is easily correlated by using regression methods, such a model for the discharge period was deemed unnecessary for purposes of this work.

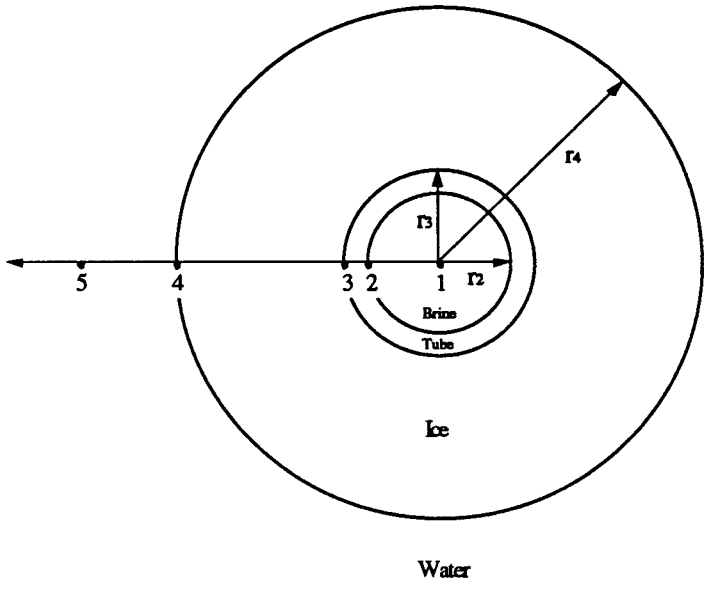

Figure 2.36 Cylindrical tube coverred by an ice formation.

Governing Equations for the Charging Process The constrained-area storage tank employs long lengths of tubing to effect the heat transfer process between the brine contained within these tubes and the surrounding water storage medium. An appropriate model of the heat transfer process during the charging period is that of a long, composite cylindrical tube with convective surface conditions. A cross-sectional view of such a tube along with the necessary physical dimensions and thermodynamic states are shown in Figure 2.36. The equations that describe the transfer of heat between the storage medium and the transport fluid during the charging period are given below.

The overall conductance between the transport fluid and the storage medium based on the outer surface area is given by

$$U_4 = \left[\frac{r_4}{h_{1,2}\, r_2} + \frac{r_4 \ln (r_3 / r_2)}{k_{2,3}} + \frac{r_4 \ln (r_4 / r_3)}{k_{3,4}} + \frac{1}{h_{4,5}} \right]^{-1} \tag{2.45}$$

where r_2 and r_3 are the inner and outer tube radii, respectively, r_4 is the radius of the ice formation, $h_{1,2}$ and $h_{4,5}$ are the convection coefficients of the brine and the water, respectively, and $k_{2,3}$ and $k_{3,4}$ are the thermal conductivities of the tube material (polyethylene) and the ice, respectively.

An energy balance on a differential element of tube length dx (Figure 2.37) results in the following differential equation:

$$\dot{m}_b\, C_{p,b}\, dT_b = U_4 \frac{A_4}{L} (T_w - T_b)\, dx \tag{2.46}$$

where $\dot{m}_b$ is the mass flow rate of brine through a single tube, $C_{p,b}$ is its specific heat, and $T_b = \overline{T}_1$ is its mean or bulk fluid temperature within the tube; $\frac{A_4}{L}$ is the tube surface

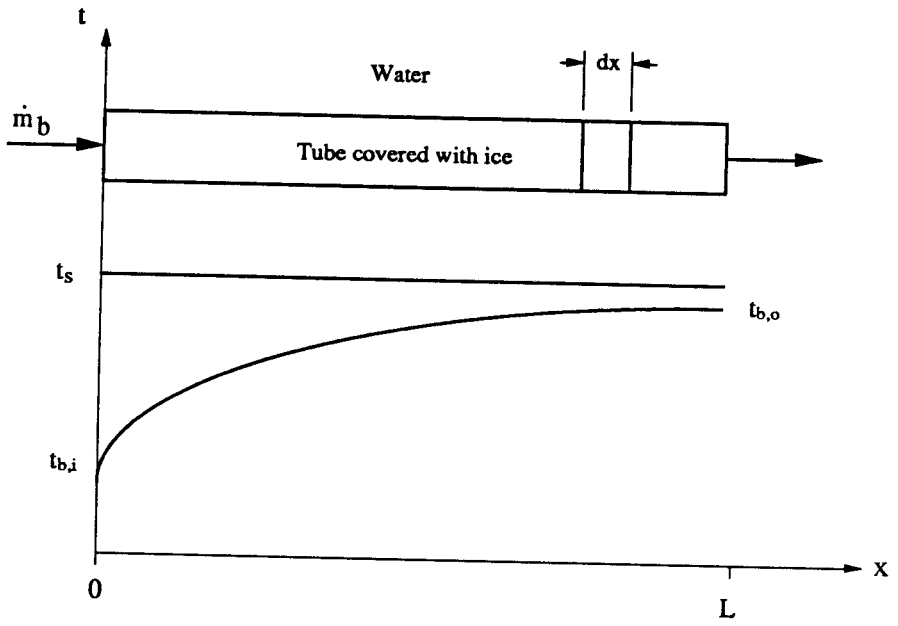

Figure 2.37 Mean temperature distribution of the brine solution.

area per tube length, $T_w = \overline{T}_5$ is the bulk temperature of the water storage medium. This expression may be integrated analytically over the length of the tube if the overall convection coefficient U_4 and the bulk temperature of the water T_5 are approximately constant over the length of the tube.

Under these assumptions, the bulk temperature of the transport fluid varies exponentially with distance along the tube; that is,

$$T_b = T_w + (T_{b,i} - T_w)\, e^{-U_4 A_4 x / L \dot{m}_b C_{p,b}} \quad . \tag{2.47}$$

where $T_{b,i}$ is the bulk temperature of the brine at the tank inlet.

The average driving force for heat transfer between the storage medium and the transport fluid $(T_w - T_b)_{mean}$ can be determined by integrating the second term on the right-hand side of Equation 2.47 over the length of the tube. The resulting mean driving force is referred to as the log-mean temperature difference and is given by

$$\Delta T_{lm} = \frac{(T_w - T_{b,i}) - (T_w - T_{b,o})}{\ln\left(\frac{T_w - T_{b,i}}{T_w - T_{b,o}}\right)} \tag{2.48}$$

where the subscripts i and o refer to the inlet and outlet conditions, respectively.

The integrated-average heat transfer rate over a single tube can then be expressed simply as

$$\dot{Q}_{tube} = U_4 A_4 \Delta T_{lm}. \tag{2.49}$$

The heat transferred to the tank from the surrounding atmosphere can be expressed in terms of the product of an overall conductance, the heat-transfer area, and the temperature difference between the ambient atmosphere and the storage medium:

$$\dot{Q}_{gain} = (UA)_{tank} (T_{amb} - T_w). \tag{2.50}$$

The above equations describe the heat transfer process that occurs within the tank at any given instant in time. In order to model the heat transfer process over a period of time, expressions for the mean water temperature within the tank, T_w; the surface area available for heat transfer per tube, A_4; and the ice thickness, t, as functions of time, θ, are needed. Since the variation in tank temperature and the variation in available surface

area are not continuous functions of time, the modeling procedure is divided into a number of discrete time periods such that a piecewise continuous solution can be realized.

Sensible charging During the sensible portion of the charging period, the bulk temperature of the water storage medium within the tank is progressively decreased toward its freezing point and little or no ice forms on the surface of the tubes. The additional necessary expressions are

$$\frac{dT_w}{d\theta} = - \frac{\dot{Q}_{\text{tube}} N_{\text{tube}} - \dot{Q}_{\text{gain}}}{m_w C_{v,w}}, \tag{2.51}$$

$$A_4 = 2\pi r_3 L, \tag{2.52}$$

$$\frac{dt}{d\theta} = 0, \tag{2.53}$$

where N_{tube} is the number of tubes, m_w is the mass of water within the tank, $C_{v,w}$ is its specific heat, θ is the independent variable which represents time, and t is the thickness of an *advancing* ice formation.

Latent charging During the latent portion of the charging period, the bulk temperature of the water storage medium remains essentially constant, and ice formations build in a cylindrical fashion on the surface of the tube. These advancing ice formations are shown in Figure 2.38 which depicts a cross-section of four adjacent tubes located within the storage tank. With respect to this figure, S is defined as one-half of the distance between the centerlines of adjacent tubes (this analysis assumes a

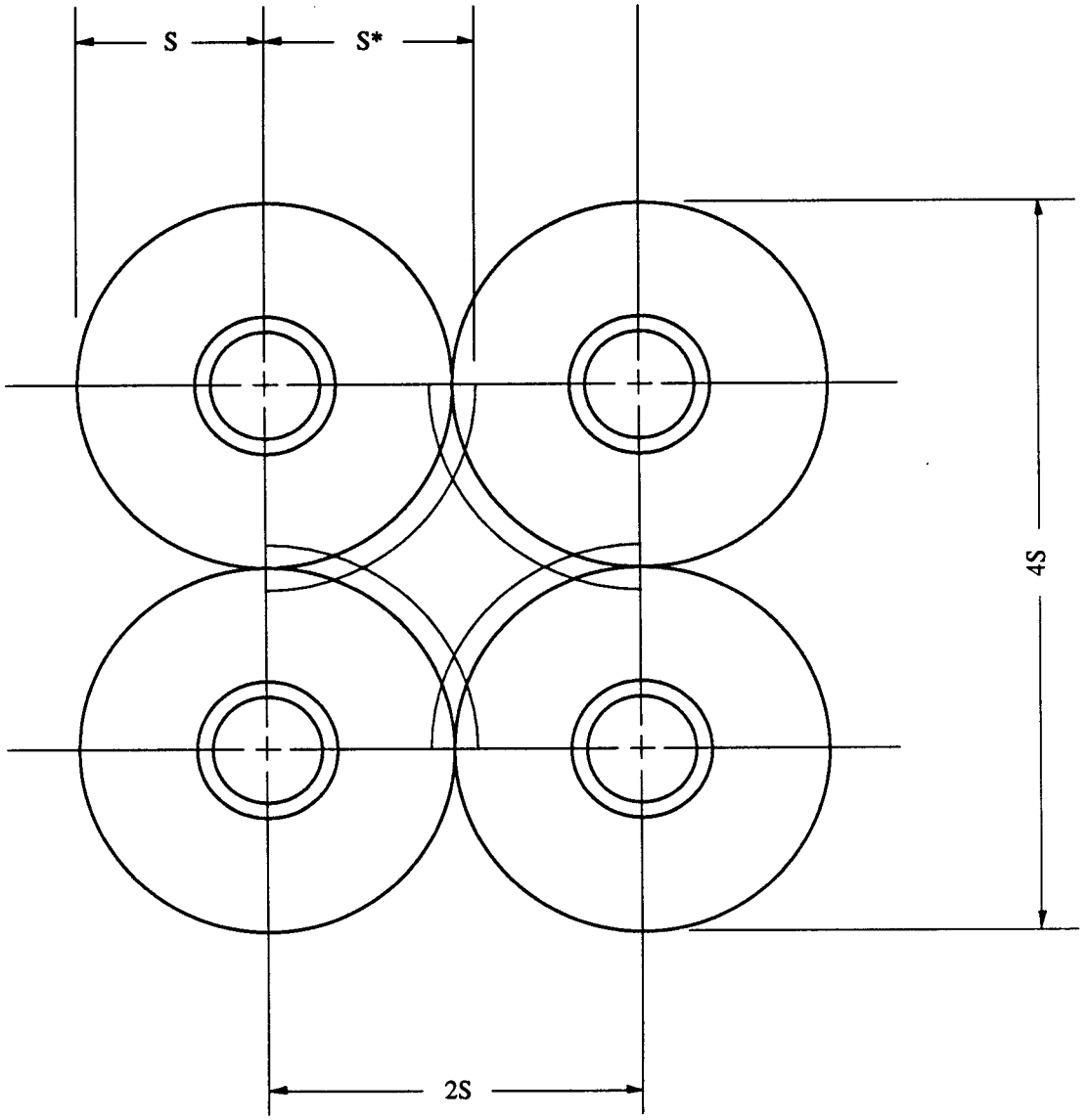

Figure 2.38 Advancing ice formations on the tubes of an ice-storage tank.

symmetrical distribution of tubes, but it can be extended to other geometries) or the *actual half-length* of the square volume element bounded by the centerlines of the four adjacent tubes, and S^* is defined as the *superficial half-length* of this volume-element.

The actual half-length and superficial half-length are given by

$$S = r_3 + t_{crit}, \tag{2.54}$$

$$S^* = r_3 + t, \tag{2.55}$$

respectively, where t_{crit} is the ice thickness when the advancing ice formations first intersect each other. Although the superficial half-length $S^* = r_4$ when $t < t_{crit}$, its use is only appropriate when $t \geq t_{crit}$, since its purpose is by definition to denote the superficial or imaginary half-length of a square volume element.

As ice forms on the surface of the tubes, the internal energy of the ice is progressively reduced as heat is transferred to the transport fluid. The water immediately adjacent to the surface of the ice freezes it transfers heat to the transport fluid. An energy balance on the storage medium results in a time dependent differential equation which may be solved numerically for the thickness of the ice.

With this in mind, if the ice thickness is less than t_{crit}, but greater than zero, the appropriate additional equations are

$$\frac{dT_w}{d\theta} = 0, \tag{2.56}$$

$$A_4 = 2\pi (r_3 + t) L, \tag{2.57}$$

$$\frac{dt}{d\theta} = \frac{\dot{Q}_{tube} N_{tube} - \dot{Q}_{gain} + m_{ice} C_{v,ice} \frac{d\bar{T}_{ice}}{d\theta}}{h_{if,w} \rho_{ice} 2\pi (r_3 + t) L N_{tube}}, \tag{2.58}$$

where m_{ice} is the total mass of ice within the tank, $C_{v,ice}$ and ρ_{ice} are its specific heat and

density, respectively, and $\overline{T}_{ice}$ is the bulk or integrated average temperature of the ice residing on the tubes of the tank; $h_{if,w}$ is the latent heat of fusion of water at its freezing point. The bulk temperature of ice $\overline{T}_{ice}$ is determined by first solving the general conduction equation with the proper boundary conditions for the temperature distribution in the ice as a function of the radial coordinate r; and second by integrating this result over the volume of ice and then dividing the result by the volume of ice. The resulting expression is

$$\overline{T}_{ice} = T_4 - (T_4 - T_3)\left[\frac{1}{2 \ln (r_4 / r_3)} - \frac{r_3^2}{r_4^2 - r_3^2}\right]. \tag{2.59}$$

On the other hand, if the ice thickness is greater than or equal to t_{crit}, the algebraic equation for the surface area A_4 and the differential equation for the ice thickness given above must be modified. From a geometrical analysis of the tube configuration depicted in Figure 2.42, an expression for the surface area available for heat transfer across a single tube can be obtained. The result is

$$A_4 = 2\pi S^* L - 8S^* L \cos^{-1} (S / S^*). \tag{2.60}$$

Based on this area, the corresponding time rate of change of ice thickness can be expressed as

$$\frac{dt}{d\theta} = \frac{\dot{Q}_{tube} N_{tube} - \dot{Q}_{gain} + m_{ice} C_{v,ice} \dfrac{d\overline{T}_{ice}}{d\theta}}{h_{if,w} \rho_{ice} N_{tube} \left[2\pi S^* L - 8S^* L \cos^{-1} (S / S^*)\right]}. \tag{2.61}$$

Since the ice formations are no longer cylindrical when the ice thickness is greater than

t_{touch}, the overall heat transfer coefficient must be modified; that is,

$$U_4 = \left[\frac{A_4}{h_{1,2}\, 2\pi\, r_2\, L} + \frac{A_4 \ln (r_3 / r_2)}{2\pi\, k_{2,3}\, L} + \frac{A_4 \ln (r_4 / r_3)}{2\pi\, F_{3,4}\, k_{3,4}\, L} + \frac{1}{h_{4,5}}\right]^{-1} \tag{2.62}$$

where $F_{3,4}$ is a correction factor which accounts for the fact that the heat transfer from the outer surface of the ice formation to the outer surface of the tube is not a one-dimensional process. (A similar term could be included for the second term in the above expression; however, this term is relatively small, since the resistance associated with the ice is now the dominant term.) If the heat transfer process were one-dimensional, then $F_{3,4}$ would take on its minimum value:

$$F_{3,4,\min} = \frac{A_4}{2\pi\, r_4\, L}.$$

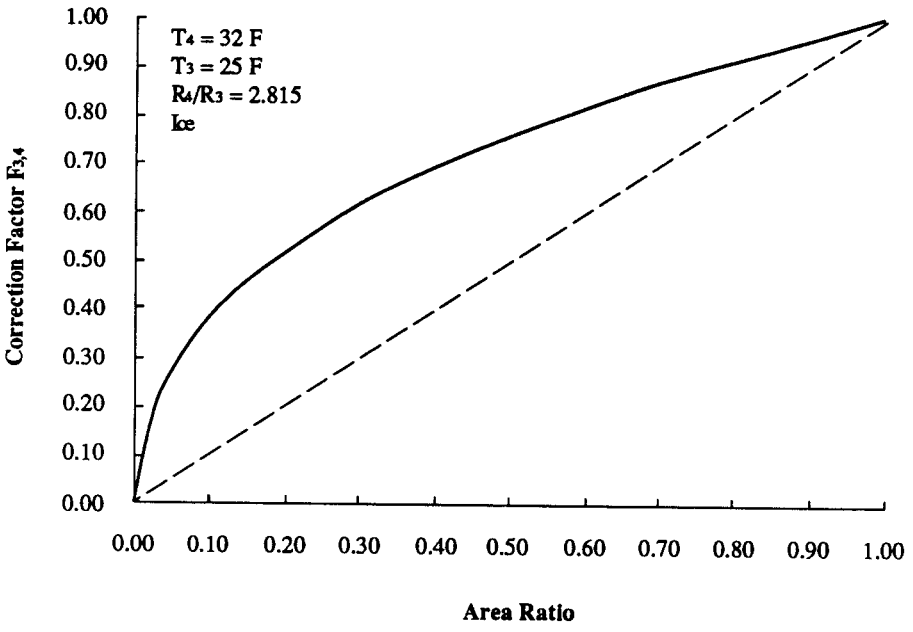

Figure 2.39 Two-dimensional heat-transfer correction factor of the ice storage tanks for ice thicknesses greater than the critical ice thickness.

The actual value of the correction factor $F_{3,4}$ is by definition equal to the minimum value $F_{3,4,\min}$ when the outer surface of the ice formation A_4 is equal to its maximum value ($2\pi r_4 L$) or its minimum value (0). Figure 2.39 shows this correction factor as a function of the area ratio $A_4 / 2\pi r_4 L$. This figure was generated by performing a two-dimensional finite-element heat-transfer analysis on one-forth of a tube cross-section covered with various thicknesses of ice [25].

In addition, the bulk ice temperature should be evaluated by some other means besides that given by Equation 2.59, although this equation can be used to estimate the bulk ice temperature if r_4 is replaced by the superficial half-length S^*. This is a conservative estimate since it tends to over predict the rate at which the ice formations advance. For the ice storage tanks used in this study the effects associated with the sensible heat stored by the ice were small (approximately 1%) and therefore were neglected; however, for storage systems which rely on greater ice thicknesses, these effects may be highly significant.

Solution Procedure for the Charging Period The solution procedure for the sensible portion of the charging period comprises two iterative loops: the first loop, which is nested within the second loop, iteratively determines the proper overall heat transfer coefficient, whereas the second loop iteratively determines the rate of heat transfer from the tank.

FIRST LOOP The procedure for the first loop is as follows: For given inlet conditions and a given initial tank temperature, the bulk temperature of the brine outlet from the tank is guessed. Based on this guess, the average bulk brine temperature

between the inlet and outlet conditions is computed and then used to estimate an average tube surface temperature. Next, fluid property correlations are used to evaluate the two convection coefficients $h_{1,2}$ and $h_{4,5}$ based on the average bulk brine temperature and the average tube surface temperature and the temperature of the water in the tank, respectively. The overall heat transfer coefficient, U_4, is then computed and subsequently used to compute the bulk brine outlet temperature (Equation 2.47) and also to ascertain a more accurate value of the mean surface temperature. The above procedure is repeated until satisfactory convergence is obtained, whereupon the resulting bulk brine outlet temperature is used in the ensuing loop.

SECOND LOOP The procedure for the second loop is as follows: For a given time step, once the bulk temperature of the brine outlet from the tank has been ascertained, the heat transferred from the tank and the change in water temperature within the tank are calculated using Equations 2.49 and 2.51, respectively. Next, an average tank temperature over the time step is computed. The first loop of the solution procedure is then repeated based on this average tank temperature. The entire solution procedure is repeated until satisfactory convergence is obtained and a new tank temperature is ascertained.

The solution procedure for both phases of the latent charging period is the same as the procedure listed above except that instead of iteratively converging upon a new tank temperature, the solution procedure for the latent charging period iteratively converges upon a new ice thickness. Furthermore, the appropriate equations must be implemented in accordance with the thickness at which the ice formations touch.